NASA CONTRACTOR REPORT

NASA CR-1821

TURBULENCE AND LONGITUDINAL FLYING QUALITIES

by James A. Franklin

Prepared by
PRINCETON UNIVERSITY
Princeton, N. J. 08540
for

NATIONAL AERONAUTICS AND SPACE ADMINISTRATION • WASHINGTON, D. C. • JULY 1971

1. Report No.	2. Government Accession No.	3. Recipient's Catalog No.
NASA CR-1821		

4. Title and Subtitle	5. Report Date
TURBULENCE AND LONGITUDINAL FLYING QUALITIES	July 1971
	6. Performing Organization Code

7. Author(s)	8. Performing Organization Report No.
James A. Franklin	

9. Performing Organization Name and Address	10. Work Unit No.
Princeton University Princeton, New Jersey 08540	126-62-10-00-10
	11. Contract or Grant No. W-12,994
	13. Type of Report and Period Covered: Contractor Report

12. Sponsoring Agency Name and Address	14. Sponsoring Agency Code
National Aeronautics and Space Administration Washington, D. C. 20546	

15. Supplementary Notes

Prepared under Naval Air Systems Command Contract No. N00019-70-C-0156 with partial funding under NASA Purchase Order W-12,994

16. Abstract

This report presents the results of an experimental investigation into the influences of atmospheric turbulence on longitudinal flying qualities. In-flight evaluations of various combinations of simulated turbulence disturbances and open loop airplane dynamics were made for the ILS approach task. Test configurations were chosen to permit an independent study of the effects of turbulence to be made for a set of satisfactory longitudinal dynamics. Further testing was performed for a selective combination of turbulence and dynamics characteristics to assess their interacting influences on flying qualities for the ILS task. The turbulence disturbances were defined in terms of rms magnitudes of the pitch and heave components, the bandwidth or frequency content of the turbulence power spectrum, and the correlation between pitch and heave disturbances. Variations of longitudinal dynamics were made in the short period natural frequency (or angle of attach stability), short period damping, and lift curve slope. Data in the form of pilot opinion ratings and commentary, and time histories of airplane response, control inputs, and simulated turbulence disturbances were obtained. The time histories were digitally processed for rms measures of the precision of task performance and the pilot's control workload.

17. Key Words (Suggested by Author(s))	18. Distribution Statement
Turbulence, Flying Qualities, Aircraft Dynamics	Unclassified - Unlimited

19. Security Classif. (of this report)	20. Security Classif. (of this page)	21. No. of Pages	22. Price*
Unclassified	Unclassified	188	$3.00

*For sale by the National Technical Information Service, Springfield, Virginia 22151

FOREWORD

This research program was sponsored by Headquarters, National Aeronautics and Space Administration. It was conducted by the Flight Research Laboratory of Princeton University under Contract No. N00019-70-C-0156. Mr. R. J. Wasicko was the Project Monitor for NASA. Professor Edward Seckel was the Principal Investigator, and Dr. James A. Franklin was the Project Engineer for Princeton.

The author particularly wishes to acknowledge the forebearance of the project evaluation pilots and the safety pilots throughout the flight test program. The evaluation pilots were Mr. W. B. Nixon of Princeton University, Mr. R. E. Smith of the Cornell Aeronautical Laboratory, and Mr. L. H. Person, Jr. of the Langley Research Center and Mr. A. E. Faye, Jr. of the Ames Research Center of NASA. Mr. D. R. Ellis and Mr. T. E. Wallis of Princeton University were the project safety pilots.

ABSTRACT

This report presents the results of an experimental investigation into the influences of atmospheric turbulence on longitudinal flying qualities. In-flight evaluations of various combinations of simulated turbulence disturbances and open loop airplane dynamics were made for the ILS approach task. Test configurations were chosen to permit an independent study of the effects of turbulence to be made for a set of satisfactory longitudinal dynamics. Further testing was performed for a selective combination of turbulence and dynamics characteristics to assess their interacting influences on flying qualities for the ILS task. The turbulence disturbances were defined in terms of rms magnitudes of the pitch and heave components, the bandwidth or frequency content of the turbulence power spectrum, and the correlation between pitch and heave disturbances. Variations of longitudinal dynamics were made in the short period natural frequency (or angle of attack stability), short period damping, and lift curve slope. Data in the form of pilot opinion ratings and commentary, and time histories of airplane response, control inputs, and simulated turbulence disturbances were obtained. The time histories were digitally processed for rms measures of the precision of task performance and the pilot's control workload.

The dominant influences on longitudinal flying qualities are the pilot's control workload required to fly the ILS approach and the precision of performance of the task. Turbulence disturbances and airplane dynamics are found to be important insofar as they influence these two factors. Closed loop pilot-airplane systems analyses substantially support the pilots' ratings and flight test performance-workload data.

The dominant influence of turbulence is the rms disturbance magnitude. Pitch disturbances have a more adverse effect than heave disturbances on the ILS task. Spectral bandwidth has a mildly degrading effect on flying qualities for increases in the dominant corner frequency of the spectrum up to 2.0 radians/second. This influence is not altered appreciably by the variations

in longitudinal dynamics considered in this program. Correlation between pitch and heave disturbances is of no importance to the task.

Short period frequency (or angle of attack stability) affects longitudinal flying qualities through its primary influence on pitch attitude control and on airspeed and glide slope or altitude control. Reducing the short period frequency adversely affects flying qualities, particularly when frequencies corresponding to the boundary for static angle of attack stability are reached. Furthermore, the effect of pitch disturbances is more pronounced when the frequency is low. Short period damping has only a modest influence on flying qualities for the range of damping tested in this program. A minor deterioration of pitch attitude control accompanies a reduction in damping from a value typical of a light general aviation airplane to neutral pitch damping. Changes in the slope of the lift curve did not affect the ILS task to any significant extent. Glide slope or altitude tracking performance suffered somewhat with a reduction in lift curve slope. Combined influences of the lift curve slope and heave disturbances are such that there is no net effect on flying qualities for the approach when changes in lift curve slope are accompanied by appropriate changes in the magnitude of heave disturbances.

TABLE OF CONTENTS

LIST OF FIGURES

LIST OF TABLES

NOTATION AND SYMBOLS

Capital Letters

AR	Aspect ratio
A/S	Airspeed
A_h	Gain factor for the h/δ_e transfer function
A_θ	Gain factor for the θ/δ_e transfer function
C.L.	Closed loop
C_{L_α}	Lift curve slope $\frac{1}{qS}\frac{\partial L}{\partial \alpha}$ (1/rad, 1/deg)
$C_{m_{\alpha_w}}$	Dimensionless angle of attack stability derivative of the wing $\frac{1}{qS\bar{c}}\frac{\partial M_w}{\partial \alpha}$
$C_{m_{\alpha_t}}$	Dimensionless angle of attack stability derivative for the tail $\frac{1}{qS\bar{c}}\frac{\partial M_t}{\partial \alpha}$
D	Drag force (lbs); Drag acceleration (ft/sec^2)
D_α	Drag force derivative due to angle of attack $\frac{1}{m}\frac{\partial D}{\partial \alpha}$ (ft/sec^2 per rad)
G/S	Glideslope
$H_{M_{g_w}}$	Fourier transform of $h_{M_{g_w}}$; Transfer function in the frequency domain defining pitching moment of the wing due to vertical gusts
$H_{M_{g_t}}$	Fourier transform of $h_{M_{g_t}}$; Transfer function defining pitching moment of the tail due to vertical gusts
$H_{Z_{w_g}}$	Fourier transform of $h_{Z_{wg}}$; Transfer function in the frequency domain defining vertical force due to vertical gusts
IFR	Instrument flight rules
ILS	Instrument landing system
K_h	Pilot gain in the $h \rightarrow \delta_e$ loop (deg/ft)
K_T	Pilot gain in the $u \rightarrow \delta_T$ loop (inch per ft/sec)
K_θ	Pilot gain in the $\theta \rightarrow \delta_e$ loop (inch/deg)

L	Turbulence integral scale length (ft); Lift force (lbs); Lift acceleration (ft/ sec^2); Roll acceleration (rad/ sec^2)
L_α	Lift curve slope $\frac{1}{m}\frac{\partial L}{\partial \alpha}$ (ft/ sec^2 per rad)
L_β	Dihedral effect derivative $\frac{1}{I_x}\frac{\partial L}{\partial \beta}$ (rad/ sec^2 per rad)
L_{δ_a}	Aileron effectiveness $\frac{1}{I_x}\frac{\partial L}{\partial \delta_a}$ (rad/ sec^2 per inch)
M_u	Pitching moment derivative due to forward speed $\frac{1}{I_y}\frac{\partial M}{\partial u}$ (rad/ sec^2 per ft/ sec)
M_{u_g}	Pitch angular acceleration due to longitudinal gusts (rad/ sec^2)
M_{w_g}	Pitching moment due to vertical gusts (ft-lbs); Pitch angular acceleration due to vertical gusts (rad/ sec^2)
M_α	Pitching moment derivative due to angle of attack, angle of attack stability, $\frac{1}{I_y}\frac{\partial M}{\partial \alpha}$ (rad/ sec^2 per rad)
M_{α_w}, $M_{\alpha_{g_w}}$	Angle of attack stability contribution of the wing; Pitching moment derivative of the wing due to α gust (rad/ sec^2 per rad)
M_{g_w}	Pitching moment contribution of the wing due to vertical gusts (ft-lbs)
M_{α_t}, $M_{\alpha_{g_t}}$	Angle of attack stability contribution of the tail; Pitching moment derivative of the tail due to α gust (rad/ sec^2 per rad)
M_{g_t}	Pitching moment contribution of the tail due to vertical gusts (ft-lbs)
$M_{\dot\alpha}$	Pitching moment derivative due to rate of change of angle of attack, angle of attack damping, $\frac{1}{I_y}\frac{\partial M}{\partial \dot\alpha}$ (rad/ sec^2 per rad/ sec)
$M_{\dot\theta}$	Pitching moment derivative due to pitch rate, pitch damping, $\frac{1}{I_y}\frac{\partial M}{\partial \dot\theta}$ (rad/ sec^2 per rad/ sec)

M_δ	Pitching moment derivative due to control deflection, longitudinal control effectiveness, $\frac{1}{I_y}\frac{\partial M}{\partial \delta}$ (rad/ sec^2 per in)
N	Yaw acceleration (rad/ sec^2)
N_{δ_r}	Rudder effectiveness $\frac{1}{I_z}\frac{\partial N}{\partial \delta_r}$ (rad/ sec^2 per inch)
N_i^r	Transfer function numerator relating the response r to an input i
$N_{w_g}^{h\ \theta}{}_{\delta_e}$	Coupling numerator for altitude response to vertical gusts with the $\theta \rightarrow \delta_e$ loop closed
O. L.	Open loop (uncontrolled)
POR	Pilot opinion rating
R_e	Real part of a complex variable
Rms	Root mean square
R_{MZ}	Cross-correlation function for pitch and heave disturbances
$R_{ww}(r), R_{ww}(\tau)$	Autocorrelation function for vertical gusts in spatial or time domain
S	Wing area (ft^2)
$T_{h_1}, T_{h_2}, T_{h_3}$	Time constants of the first order roots of the $h \rightarrow \delta_e$ numerator (sec)
T_{h_1}''	Time constant of the first order characteristic root for $\theta \rightarrow \delta_e$ and $h \rightarrow \delta_e$ loops closed which is associated with h/δ_e zero at $1/T_{h_1}$ (sec)
T_{L_θ}	Pilot lead time constant in the $\theta \rightarrow \delta_e$ loop (sec)
T_{ph_1}, T_{ph_2}	Time constants of the first order factors of the characteristic equation nominally associated with the phugoid mode (sec)
T_R	Roll mode time constant (sec)
T_{sp_1}, T_{sp_2}	Time constants of the first order factors of the characteristic equation nominally associated with the short period mode (sec)

T_{w_1}, T_{w_2}	Time constants of the power spectral approximation for vertical force and pitching moment due to vertical gusts (sec)
$T_{\theta_1}, T_{\theta_2}$	Time constants of the first order roots of the $\theta \rightarrow \delta_e$ numerator (sec)
$T_{\theta_1}', T_{\theta_2}'$	Time constants of the first order characteristic roots with the $\theta \rightarrow \delta_e$ loop closed associated with the open loop zeros at $1/T_{\theta_1}$ and $1/T_{\theta_2}$ (sec)
VFR	Visual flight rules
V_o	True airspeed (mi/hr, ft/sec)
X_u	Longitudinal force derivative due to forward speed $\frac{1}{m}\frac{\partial X}{\partial u}$ (1/sec)
X_{u_g}	Longitudinal acceleration due to longitudinal gusts (ft/sec^2)
X_{w_g}	Longitudinal acceleration due to vertical gusts (ft/sec^2)
X_α	Longitudinal force derivative due to angle of attack $\frac{1}{m}\frac{\partial X}{\partial \alpha}$ (ft/sec^2 per rad)
X_δ	Longitudinal force derivative due to control deflection $\frac{1}{m}\frac{\partial X}{\partial \delta}$ (ft/sec^2 per inch)
Y_A	Generalized transfer function of airplane response to control inputs
Y_G	Generalized transfer function of airplane response to turbulence disturbances
Y_p	Generalized pilot describing function
Y_{p_h}	Pilot describing function in the $h \rightarrow \delta_e$ loop
Y_{p_u}	Pilot describing function in the $u \rightarrow \delta_T$ loop

Y_{p_θ}	Pilot describing function in the $\theta \rightarrow \delta_e$ loop
ΔZ	Incremental normal acceleration due to simulated heave disturbance (g's)
Z_u	Vertical force derivative due to forward speed $\frac{1}{m}\frac{\partial Z}{\partial u}$ (1/ sec)
Z_{u_g}	Vertical acceleration due to longitudinal gusts (ft/ sec^2)
Z_{w_g}	Vertical force due to vertical gusts (lbs); Vertical acceleration due to vertical gusts (ft/ sec^2)
Z_α, Z_{α_g}	Vertical force derivative due to angle of attack $\frac{1}{m}\frac{\partial Z}{\partial \alpha}$; Vertical force derivative due to α gust $\frac{1}{m}\frac{\partial Z}{\partial \alpha_g}$ (ft/ sec^2 per rad)
Z_δ	Vertical force derivative due to control deflection $\frac{1}{m}\frac{\partial Z}{\partial \delta}$ (ft/ sec^2 per inch)

Lower Case

b	Wing span (ft)
$\bar{c}$	Mean aerodynamic chord; mean chord $\frac{S}{b}$ (ft)
c(y)	Wing chord at spanwise location y (ft)
$c_\ell(y)$	Section lift coefficient at spanwise location y
db	Decibels, $20 \log_{10}$ ( )
e	Exponential function
g	Acceleration due to gravity (ft/ sec^2)
h	Altitude perturbations (ft)
h_c	Altitude command (ft)
h_ϵ	Altitude tracking error (ft)
$h_{M_{g_w}}$	Indicial (step) response influence function in the time domain of pitching moment of the wing due to vertical gusts

$h_{M_{g_t}}$	Indicial (step) response influence function in the time domain of pitching moments of the tail due to vertical gusts
$h_{Z_{w_g}}$	Indicial (step) response influence function in the time domain of vertical force due to vertical gusts
i	Generalized variable
j	Imaginary number $\sqrt{-1}$
$k(t_1)$	Transient lift response function to a step gust input
ℓ_t	Tail (horizontal stabilizer) moment arm from the c.g. (ft)
mph	Miles per hour
q	Dynamic pressure (lbs/ ft^2)
r	Incremental spatial separation
s	Laplace operator $\sigma \pm j\omega$
t, t_o, t_1	Time, initial time, dummy time variable (sec)
u, w	Longitudinal and vertical perturbation velocities (ft/ sec)
u_g, w_g	Longitudinal and vertical gust velocities (ft/ sec)
u_c	Airspeed command (ft/ sec)
u_ϵ	Airspeed tracking error (ft/ sec)
x, x_o	Distance along the longitudinal axis (typically associated with the airplane's flight path); initial longitudinal position (ft)
y	Distance along the lateral (spanwise) axis (ft)
Δy	Incremental spanwise separation (ft)

Greek Symbols

α	Angle of attack (rad, deg)
$\gamma_{M_{g_w}}$	Dimensionless spanwise pitching moment distribution of the wing due to vertical gusts
$\gamma_{Z_{w_g}}$	Dimensionless spanwise lift distribution for vertical gusts
Δ	Open loop longitudinal characteristic equation or matrix

Δ'	Longitudinal characteristic equation or matrix with $\theta \rightarrow \delta_e$ loop closed
δ_e, δ_s	Elevator deflection (rad, deg); Longitudinal stick deflection or force (inch, lbs)
δ_f	Flap deflection (rad)
δ_T	Throttle deflection (inch)
ϵ	Generalized closed loop tracking error
ζ_d, ω_d	Dutch roll damping ratio and natural frequency
ζ_h'', ω_h''	Damping ratio and frequency of the low frequency oscillatory roots of the $h \rightarrow \delta_e$ loop closure ($\theta \rightarrow \delta_e$ also closed)
ζ_{ph}, ω_{ph}	Phugoid damping ratio and natural frequency
ζ_{sp}, ω_{sp}	Short period damping ratio and natural frequency
$\zeta_{sp}', \omega_{sp}'$	Short period damping ratio and frequency as modified by the $\theta \rightarrow \delta_e$ loop
$\zeta_{sp}'', \omega_{sp}''$	Short period damping ratio and frequency as modified by the $h \rightarrow \delta_e$ loop closure ($\theta \rightarrow \delta_e$ also closed)
ρ_{MZ}	Normalized cross-correlation between pitch and heave disturbances $\rho_{MZ} = \dfrac{R_{MZ}(0)}{\sigma_M \sigma_Z}$
σ	Real part of a complex variable
σ_i	Root mean square of the variable i (same units as i)
σ_M	Root mean square pitch angular acceleration due to pitch disturbances (rad/ sec^2)
σ_{n_z}	Root mean square incremental normal acceleration (g's)
σ_Z	Root mean square normal acceleration due to heave disturbance (g's)
σ_{α_g}	Root mean square angle of attack disturbance (rad, deg)

τ	Incremental time delay
τ_e	Effective pilot time delay (sec)
τ_e'	Time constant associated with the closed loop root originating at $\sigma = -2/\tau_e$ in the $\theta \rightarrow \delta_e$ loop (sec)
τ_e''	Time constant of the first order characteristic root for $\theta \rightarrow \delta_e$ and $h \rightarrow \delta_e$ loops closed which is associated with the open loop root at $\sigma = -2/\tau_e$ (sec)
θ	Pitch attitude (rad, deg)
θ_c	Pitch attitude command (deg)
θ_ϵ	Pitch attitude tracking error (deg)
Φ_{uw}	Cross-power spectral density of longitudinal and vertical gusts (ft^2/sec^2 per rad/sec)
$\Phi_{\theta_{u_g}}$, $\Phi_{\theta_{w_g}}$	Power spectral densities of pitch attitude due to longitudinal and vertical gusts (deg^2 per rad/sec)
Φ_θ	Power spectral density of pitch attitude (deg^2 per rad/sec)
Φ_{uu}, Φ_{ww}	Power spectral density of longitudinal and vertical gusts (ft^2/sec^2 per rad/sec)
Φ_{ff}	Power spectral density of generalized turbulence disturbances
Φ_{rr}	Power spectral density of the airplane's response
Φ_{w_e}	Power spectral density of vertical gusts weighted to give average vertical gust velocity
$\Phi_{Z_{w_g}}$	Power spectral density of vertical force due to vertical gusts (lbs^2 per rad/sec)
$\Phi_{M_{g_w}}$	Power spectral density of pitching moment of the wing due to vertical gusts (ft^2-lb^2 per rad/sec)
$\Phi_{M_{g_t}}$	Power spectral density of pitching moment of the tail due to vertical gusts (ft^2-lb^2 per rad/sec)
Φ_{θ_ϵ}	Power spectral density of pitch attitude tracking error (deg^2 per rad/sec)

Φ_{h_ϵ}	Power spectral density of altitude tracking error (ft^2 per rad/ sec)
φ_k	Sears function for unsteady lift during gust penetration
φ_m	Phase margin (deg)
ω	Angular frequency (rad/ sec)
ω_c, ω_{co}	Crossover frequency, frequency where transfer function amplitude ratio is unity (rad/ sec)
ω_{w_1}, ω_{w_2}	Corner frequencies of the power spectral approximation for vertical force and pitching moment due to vertical gusts (rad/ sec)

Miscellaneous

$[\ ]^*$	Complex conjugate of [ ]
$\lvert(\ )\rvert$	Absolute value of ( )
$\sphericalangle(\ )$	Angle of ( )
$\doteq$	Approximately equal to

SECTION 1

INTRODUCTION

In mid-1968 a study of the influence of atmospheric turbulence on flying qualities of piloted airplanes was undertaken at Princeton University with the support of NASA Headquarters. The first effort in this program involved an analytical and experimental investigation of lateral-directional flying qualities and the turbulence induced aerodynamic disturbances appropriate to the lateral-directional degrees of freedom of the airplane. A detailed discussion of the program and the results of the lateral-directional flight test program and analysis are presented in Reference 1. Under the continuing sponsorship of the NASA, this research program has been extended to the consideration of longitudinal flying qualities in turbulence. The results of this effort are presented in this report.

As was the case with the lateral-directional investigation, the longitudinal program involves a generalized study of the problems of longitudinal flying qualities in turbulence. It is directed toward the general aviation category of airplane and to an instrument landing approach task whenever such distinction is necessary and appropriate. Otherwise it is unrestricted as to type of airplane or flight task for the sake of broad application.

It was stated in Reference 1 that a suitable statistical description of the airplane's response to turbulence is provided by the power spectral density of the appropriate motion variable. In general this form of the response is related to atmospheric disturbances by

$$\Phi_{rr} = \left|\frac{Y_G}{1 + Y_p Y_A}\right|^2 \Phi_{ff} \tag{1}$$

where Φ_{rr} is the power spectral density of the airplane's turbulence response, Φ_{ff} is the turbulence spectral density, and $\left|\frac{Y_G}{1 + Y_p Y_A}\right|$ is the closed loop transfer function (pilot in the loop) relating turbulence response to the gust disturbance.

Section 2 of this report describes the turbulence induced aerodynamic disturbances associated with the power spectral density function Φ_{ff} which are appropriate to the longitudinal equations of motion. An experimental program for obtaining in-flight data on the effects of turbulence on longitudinal flying qualities is discussed in Section 3. Finally, Section 4 contains the results of that flight test program supplemented by a detailed pilot-airplane systems analysis which was undertaken to provide a more complete and unified understanding of the flight test results.

SECTION 2

TURBULENCE INDUCED AERODYNAMIC DISTURBANCES

Summary of the Description of Turbulence

Section 2 of Reference 1 contains a thorough review of the characteristics of atmospheric turbulence and the statistical description of turbulence appropriate to the study of airplane flying qualities. It is sufficient here to summarize the turbulence model discussed in Reference 1 and then proceed to consider its application to the definition of longitudinal disturbances due to turbulence.

The turbulence model of Reference 1 has the following characteristics.

- It is time stationary, homogeneous, and isotropic.
- It complies with Taylor's hypothesis for the flight speeds associated with conventional fixed wing aircraft operation.
- Its power spectral density may be adequately represented by the Dryden model.
- It may be described in terms of the mean square gust intensity and scale length.

The spectral densities for the gust velocities of interest, the longitudinal and vertical components u_g and w_g, may be expressed mathematically by the one-dimensional Dryden model

$$\Phi_{uu}(\omega) = \frac{2L}{\pi}\sigma_u^2 \frac{1}{(\frac{\omega L}{V_o})^2 + 1} \tag{2}$$

$$\Phi_{ww}(\omega) = \frac{L}{\pi}\sigma_w^2 \frac{3(\frac{\omega L}{V_o})^2 + 1}{[(\frac{\omega L}{V_o})^2 + 1]^2} \tag{3}$$

Given this turbulence model, it is now necessary to define the perturbations in longitudinal and vertical force and pitching moment imposed on the airplane by these gust velocities.

General Approach

The longitudinal equations of motion which define the airplane's response to control inputs and turbulence disturbance are

$$\begin{bmatrix} s - X_u & -X_\alpha & g \\ -Z_u & V_o s - Z_\alpha & -V_o s \\ -M_u & -(M_{\dot{\alpha}} s + M_\alpha) & s(s - M_{\dot{\theta}}) \end{bmatrix} \begin{Bmatrix} u \\ \alpha \\ \theta \end{Bmatrix} = \begin{Bmatrix} X_\delta \\ Z_\delta \\ M_\delta \end{Bmatrix} \{\delta\}$$

$$+ \begin{Bmatrix} X_{u_g} \\ Z_{u_g} \\ M_{u_g} \end{Bmatrix} + \begin{Bmatrix} X_{w_g} \\ Z_{w_g} \\ M_{w_g} \end{Bmatrix} \qquad (4)$$

One simplification made in these equations for the simulation of turbulence in the flight test program was the elimination of forces and moments due to the longitudinal gust component. The consequence of this simplification is shown in Figure 1 for an example of a single engine light airplane in a one foot/second rms gust environment. Power spectra of the airplane's open loop (uncontrolled) pitch attitude, altitude, and airspeed response to turbulence are presented for three conditions: for combined longitudinal and vertical gust disturbances, for vertical gust disturbances alone, and for vertical gust disturbances neglecting the longitudinal force contribution, X_{w_g}. In the case where both longitudinal and vertical gusts are imposed on the airplane, the power spectra of the total response is the sum of the power spectra of the response to longitudinal and vertical gusts separately, e.g., $\Phi_\theta = \Phi_{\theta_{u_g}} + \Phi_{\theta_{w_g}}$ for pitch attitude spectrum. No cross-spectral contribution exists since the longitudinal and vertical components are uncorrelated, i.e., $\Phi_{uw} = 0$. It is apparent that elimination of the aerodynamic disturbances due to longitudinal gust reduces pitch attitude and altitude response considerably in the low frequency range ($\omega < 1.0$ rad/sec)

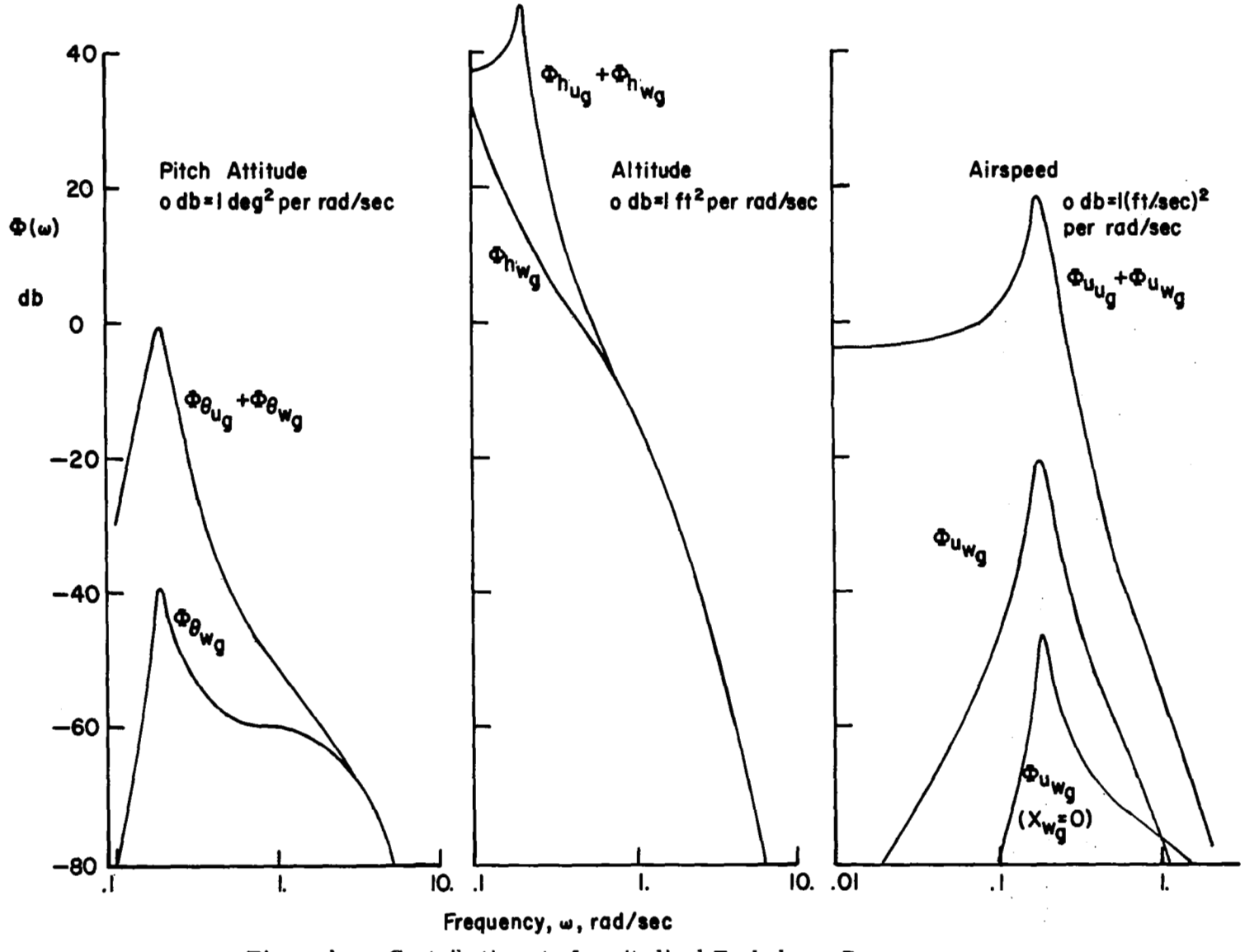

Figure 1. Contributions to Longitudinal Turbulence Response Spectra

and reduces airspeed response by a great deal all across the frequency spectrum. The consequences of this simplification of the simulated turbulence for the longitudinal flying qualities evaluation are not as severe as might be expected from the comparisons shown in Figure 1. The predominant difference between the airplane's response, longitudinal gusts included or excluded, occurs at frequencies in the region of the phugoid mode. As will be seen in the closed loop systems analysis of Section 4, the pilot can quite effectively suppress the airplane's phugoid response by controlling pitch attitude excursions with the elevator, a primary control technique used by the pilot in either VFR or IFR flight. As a result of this control technique, the dominant response to turbulence, so far as the pilot is aware, is shifted to the higher frequency ranges of the spectrum. In this high frequency region ($\omega > 1.0$ rad/sec) neither pitch attitude nor altitude response are particularly influenced by the longitudinal gust component. Although a considerable difference remains between airspeed response spectra for $\omega > 1.0$ rad/sec, u_g included or absent, the magnitude of airspeed response at these higher frequencies is sufficiently attenuated to be of little consequence to the problem.

A further simplification of the turbulence simulation was made by eliminating the longitudinal force disturbance due to vertical gusts ($X_{w_g} \sim (D_\alpha - g)\ w_g / V_o$). This simplification has no effect on pitch attitude or altitude response for the example shown (D_α for the light airplane of the analysis is 26.2 ft/sec^2 per rad). Airspeed response again is affected at low frequency; however, errors in this range of the spectrum have been discounted previously. It is also well to note at this point that the variable stability airplane used for the flight simulation is incapable of producing longitudinal force disturbances at high frequencies. Longitudinal force control is achieved through servo actuation of the airplane's throttle. The equivalent first order time constant representing the thrust lag to throttle commands is on the order of .25 to .5 seconds. Hence, longitudinal forces are limited to a frequency range less than one to two radians/second.

With the contribution of longitudinal gusts and longitudinal force excluded the remaining disturbances to be considered are the vertical (heave) force and pitching moment due to vertical gusts. Contributions to these disturbances arise due to forces and moments generated by the wing, fuselage, horizontal stabilizer, and their mutual interference effects. Specific contributions of these airplane components to the heave force and pitching moment disturbances are listed in Table 1. From this table it is apparent that the lifting surfaces such as the wing and horizontal stabilizer produce the dominant disturbances imposed on the airplane. By comparison, the fuselage's effects are of secondary importance, with the exception of the instance of aft c.g. locations where the airplane is balanced so that the fuselage contribution to pitching moment is of the same magnitude as the total pitching moment itself. However, in this instance, the total pitching moment disturbance is unlikely to be of sufficient magnitude to degrade the pilot's task performance. Therefore, the fuselage contribution is neglected for the definition of longitudinal turbulence disturbances. The horizontal stabilizer's contribution to vertical force is also ignored for the sake of simplifying the vertical force disturbance.

Vertical Force Disturbance

The turbulence induced aerodynamic forces of the wing and horizontal tail are defined based on the work of Diederich and others at NASA (References 2 and 3), which applies a modified strip theory to the prediction of the spanwise airload distribution of an airfoil with an arbitrary spanwise variation in angle of attack. Use of this modified strip theory in predicting the lift force of the wing in turbulence is demonstrated by the expression

$$Z_{w_g}(t) = \frac{1}{b} \int_{-\infty}^{\infty} \int_{-b/2}^{b/2} h_{Z_{w_g}}(t_1)\, \gamma_{Z_{w_g}}(y)\, w[V_o(t-t_1), y]\, dy\, dt_1 \qquad (5)$$

where the influence function $h_{Z_{w_g}}$ which accounts for the streamwise penetration of the gust field may be written

TABLE 1

CONTRIBUTIONS TO PITCH AND HEAVE DISTURBANCE

Disturbance	Airplane Component	Contribution
Pitching Moment	Wing	Significant. Depends on c.g. location
	Fuselage	Generally small compared to wing - tail contribution
	Horizontal Stabilizer	Dominant
Vertical Force	Wing	Dominant
	Fuselage	Small compared to wing contribution
	Horizontal Stabilizer	Generally small compared to wing contribution

$$h_{Z_{w_g}}(t_1) = \frac{C_{L_\alpha}\, q\, S}{V_o}\, k(t_1) \tag{6}$$

and $\gamma_{Z_{w_g}}$, the normalized spanwise lift distribution may be expressed as

$$\gamma_{Z_{w_g}} = \left[\frac{c_\ell(y)\, c(y)}{C_{L_\alpha}\, \bar{c}}\right]_{\alpha=1} \tag{7}$$

The gust velocity $w[V_o(t-t_1), y]$ represents a two-dimensional gust field where according to Taylor's hypothesis the streamwise spatial dimension and the time variable are related by $x - x_o = V_o(t-t_o)$.

The vertical force may be transformed to spectral form and written as

$$\Phi_{Z_{w_g}}(\omega) = |H_{Z_{w_g}}(\omega)|^2\, \Phi_{w_e}(\omega) \tag{8}$$

where $H_{Z_{w_g}}(\omega)$ is the Fourier transform of $h_{Z_{w_g}}(t)$

$$H_{Z_{w_g}}(\omega) = \frac{C_{L_\alpha}\, q\, S}{V_o}\, \varphi_k(\omega) \tag{9}$$

and $\varphi_k(\omega)$ is the transform of $k(t_1)$ and is the Sears function for transient lift discussed in Reference 4. For the airfoil planforms of interest and for the range of frequency, ω, significant to the analysis of flying qualities, the function φ_k for infinite aspect ratio suffices. This form of the Sears function as noted in Reference 4 is

$$|\varphi_k(\omega)|^2 = \frac{1}{\frac{\pi c}{V_o}\,\omega + 1} \tag{10}$$

Only for low aspect ratio (AR < 3) does this function depart significantly from its value for infinite aspect ratio over the frequency range of interest.

The function $\Phi_{w_e}(\omega)$ is related to the spanwise lift distribution $\gamma_{Z_{w_g}}(\omega)$ and the cross-spectral density function for vertical gusts, Φ_{ww}, noted in Reference 1 on page 18. $\Phi_{w_e}(\omega)$ may be considered as the power spectral density of a so-called average of all the spanwise vertical gusts as seen by the wing. This spectral function according to Reference 2 is

$$\Phi_{w_e}(\omega) = \frac{2}{b^2} \int_0^b \left[\int_{-b/2}^{b/2-\Delta y} \gamma_{Z_{w_g}}(y)\, \gamma_{Z_{w_g}}(y+\Delta y)\, \Phi_{ww}(\omega, \Delta y)\, dy \right] d\Delta y \qquad (11)$$

and is given in fully expanded analytical form on page 21 of Reference 2. A plot of this spectral density function is shown in Figure 2, reflecting the influence of the frequency parameter V_o / L and the wing span to turbulence scale, b/L, on its magnitude and frequency content. Another interesting feature of Φ_{w_e} is its insensitivity to the character of the spanwise lift distribution. Plots of Φ_{w_e} for uniform, parabolic, and triangular load distribution are reproduced from Reference 3 in the inset diagram of Figure 2. Differences between the three spectra would be of no consequence to this investigation. The form of the spectrum used in the subsequent analyses will be for the uniform load distribution.

The complete vertical force spectrum given by equation (8) is shown in Figure 3. Both the rms level of the vertical gust field and the magnitude of the slope of the lift curve determine the magnitude of the vertical force disturbance. Wing geometry has an influence on the high frequency attenuation of the spectrum due to the averaging effect of the wing which spans gust wave lengths in the spanwise direction (where V_o / b is the relevant parameter) and due to the attenuating influence of transient lift development associated with streamwise penetration of turbulence (where V_o / c is the relevant parameter). Planform influences such as aspect ratio and taper are, of course, inherent in the lift curve slope derivative. The dominant corner frequency of the spectrum which effectively characterizes the bandwidth of the turbulence is related to the equivalent angular frequency of a gust wavelength of dimension, L, traversed by an airplane at a trim speed, V_o (i.e. $\omega = V_o / L$).

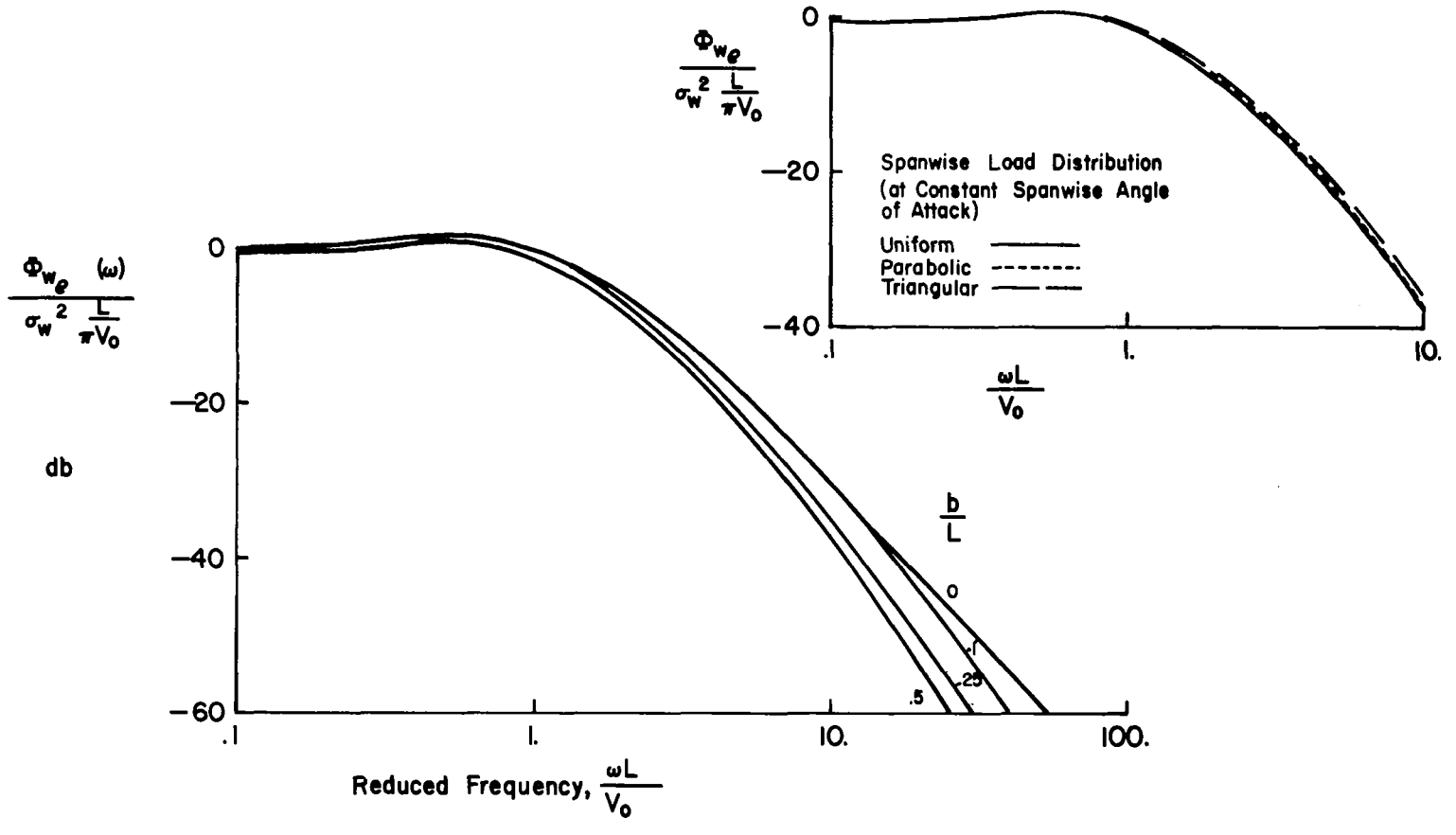

Figure 2. Effect of Frequency and Span on Spanwise Averaging of the Vertical Gust Spectrum

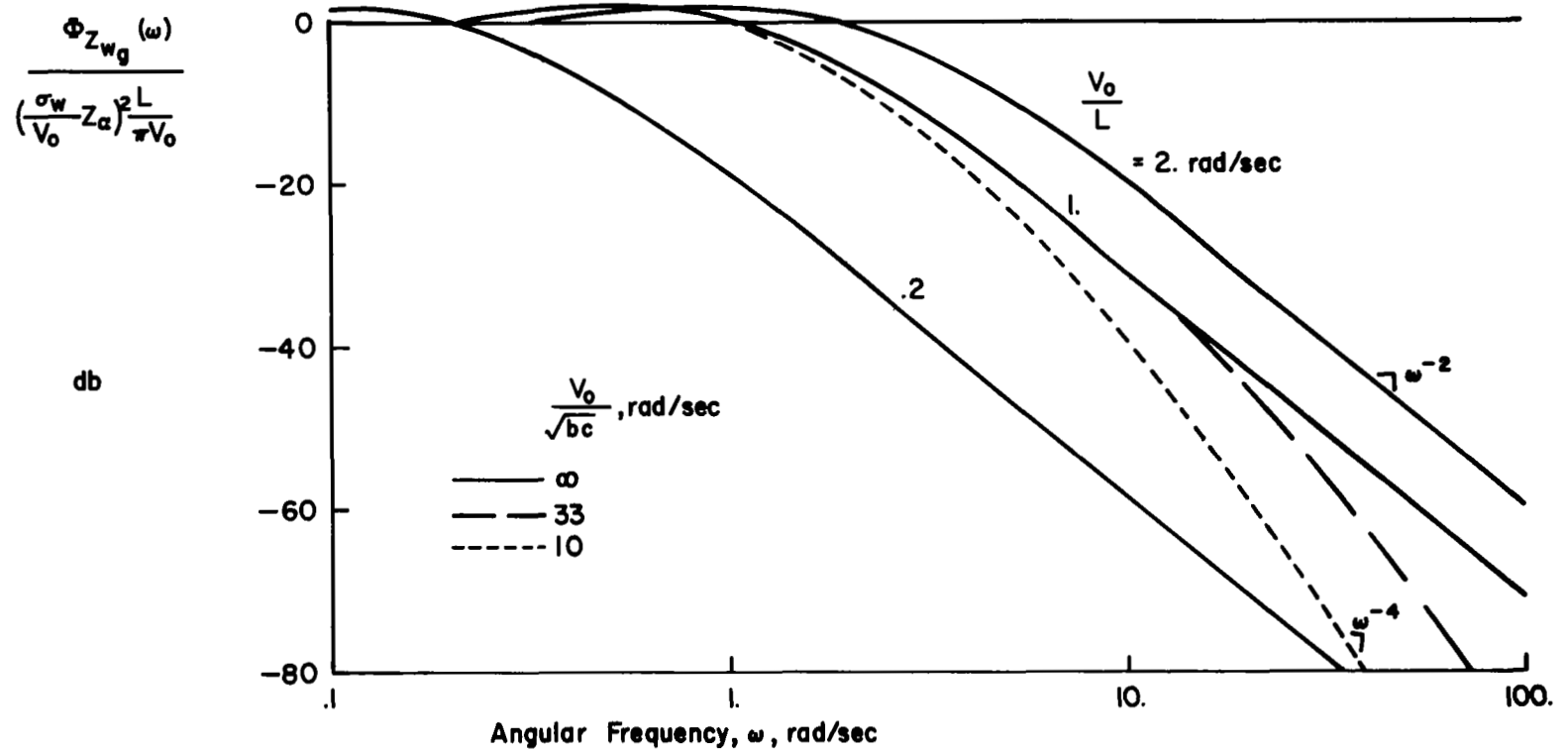

Figure 3. Vertical Force Spectra due to Vertical Gusts

Pitching Moment Disturbance

First, to consider the pitching moment contribution of the wing, the modified strip theory which was used for the prediction of vertical force produces the expression

$$M_{g_w}(t) = \frac{1}{b} \int_{-\infty}^{\infty} \int_{-b/2}^{b/2} h_{M_{g_w}}(t_1)\, \gamma_{M_{g_w}}(y)\, w[V_o(t-t_1), y]\, dy\, dt_1 \tag{12}$$

which is quite similar to equation (5) for vertical force. In this case the influence function $h_{M_{g_w}}$ may be written

$$h_{M_{g_w}}(t_1) = \frac{C_{m_{\alpha_w}}\, q\, S\, \bar{c}}{V_o}\, k(t_1) \tag{13}$$

and the spanwise lift distribution $\gamma_{M_{g_w}}$ is the same as that shown in equation (7).

Transformation of equation (12) into the frequency domain produces the pitching moment spectrum

$$\Phi_{M_{g_w}}(\omega) = |H_{M_{g_w}}(\omega)|^2\, \Phi_{w_e}(\omega) \tag{14}$$

where

$$H_{M_{g_w}}(\omega) = \frac{C_{m_{\alpha_w}}\, q\, S\, \bar{c}}{V_o}\, \varphi_k(\omega) \tag{15}$$

and $\varphi_k(\omega)$ is the Sears function for infinite aspect ratio. $\Phi_{w_e}(\omega)$ is the spectrum of the "average" vertical gust velocity given previously in equation (11) and shown in Figure 2. The power spectrum of pitching moment will have precisely the same character as the lift spectrum of Figure 3 with the exception that the normalized spectrum plotted on the ordinate is

$$\Phi_{M_{g_w}} \Big/ \left(\frac{\sigma_w}{V_o}\, M_{\alpha_w}\right)^2 \frac{L}{\pi V_o}$$

Both the rms vertical gust velocity and the angle of attack stability contributed by the wing determine the magnitude of the pitching moment disturbance of the wing. Planform influences are the same as those noted for the vertical force.

The pitching moment contribution of the horizontal stabilizer may be expressed by making only minor revision to equation (12), i.e.,

$$M_{g_t}(t) = \frac{1}{b} \int_{-\infty}^{\infty} \int_{-b/2}^{b/2} h_{M_{g_t}}(t)\, \gamma_{M_{g_t}}(y)\, w\left[V_o\left(t - t_1 - \frac{\ell_t}{V_o}\right), y\right] dy\, dt_1 \qquad (16)$$

The influence function $h_{M_{g_t}}$ is identical to its counterpart for the wing except the angle of attack stability coefficient now applies to the tail ($C_{m_{\alpha_t}}$). The spanwise lift distribution is again identical in form to equation (7). Note that the vertical gust velocity, $w[V_o(t-t_1 - \ell_t/V_o), y]$ contains a term, ℓ_t/V_o, to account for the delay in the time of the wing and then the tail encountering the same vertical gust.

Transformation of equation (16) to get the power spectrum of pitching moment due to the horizontal stabilizer gives

$$\Phi_{M_{g_t}}(\omega) = |H_{M_{g_t}}(\omega)|^2\, \Phi_{w_e}(\omega) \qquad (17)$$

This spectrum will, in general, have the same appearance as ΦZ_{w_g} and $\Phi_{M_{g_w}}$. However, the spectral attenuation associated with planform effects for a horizontal stabilizer of small span and chord occur at such high frequencies that the energy levels are low enough to be of no consequence to the pitching moment spectrum. Hence, the stabilizer's power spectrum could as well be written

$$\Phi_{M_{g_t}}(\omega) = |H_{M_{g_t}}|^2\, \Phi_{ww}(\omega) \qquad (18)$$

where

$$H_{M_{g_t}} = \frac{C_{m_{\alpha_t}}\, q\, S\, \bar{c}}{V_o}$$

and Φ_{ww} is the one-dimensional power spectrum of vertical gusts given in equation (3).

Finally, the complete expression for pitching moment, including wing and tail terms is

$$M_{w_g}(t) = M_{g_w}(t) + M_{g_t}(t) \tag{19}$$

which leads to the power spectrum of pitching moment

$$\Phi_{M_{w_g}}(\omega) = |H_{M_{g_w}}(\omega)|^2 \Phi_{w_e}(\omega) + |H_{M_{g_t}}|^2 \Phi_{ww}(\omega) + 2 R_e [H_{M_{g_t}}][H_{M_{g_w}}]^* \Phi_{w_e}(\omega) e^{-j \frac{\ell_t}{V_o}(\omega)} \tag{20}$$

A final simplification, which is in order if the high frequency attenuation of the wing spectrum is at low enough amplitudes to be ignored, replaces $\Phi_{w_e}(\omega)$ with $\Phi_{ww}(\omega)$ thereby eliminating the spanwise averaging or filtering effect, and removes the Sears function from $H_{M_{g_w}}$ thus eliminating the chordwise filter for transient aerodynamic effects. Thus, equation (20) may be rewritten

$$\Phi_{M_{w_g}}(\omega) = [\,|H_{M_{g_w}}|^2 + |H_{M_{g_t}}|^2 + 2 R_e (H_{M_{g_w}} H_{M_{g_t}}) e^{-j \frac{\ell_t}{V_o} \omega}\,] \Phi_{ww}(\omega) \tag{21}$$

Approximation of the Disturbance Spectra

Following the technique used in Reference 1 for the approximation of the disturbance spectra, and noting that the heave and pitching moment spectra at high frequency are proportional to ω^{-4}, the following spectral approximation will be applied

$$\Phi(\omega) = \frac{\Phi(0)}{(T_1^2\omega^2 + 1)(T_2^2\omega^2 + 1)} \tag{22}$$

First, consider the heave disturbance spectrum of Figure 3. This spectrum is replotted in Figure 4 for one condition of V_o / L and $V_o/\sqrt{bc}$, and with the asymptotes of equation (22) superimposed. The lowest corner frequency associated with the time constant T_1 is related to the turbulence bandwidth parameter V_o / L by

$$\omega_{w_1} = \frac{1}{T_{w_1}} = \sqrt{3}\ \frac{V_o}{L} \tag{23}$$

If the heave spectrum and its asymptotic approximation are to coincide at high frequency as shown in Figure 4, then the following relationship must hold

$$\frac{\Phi_{Z_{w_g}}(0)}{T_{w_1}^2 T_{w_2}^2 \omega^4} = \Phi_{Z_{w_g}}(0)\left[3\pi\left(\frac{L}{b}\right)\left(\frac{V_o}{L}\right)^3\left(\frac{V_o}{\pi c}\right)\right]\frac{1}{\omega^4} \tag{24}$$

where the right side of this equation is an approximation to the spectrum of equation (8) using the form of Φ_{w_e} given in Reference 2. Thus, from equation (24)

$$T_{w_1}^2 T_{w_2}^2 = \frac{1}{3}\left(\frac{L}{V_o}\right)^2\left(\frac{bc}{V_o^2}\right) \tag{25}$$

and finally solving for T_{w_2}

$$T_{w_2} = \frac{\sqrt{bc}}{V_o} \tag{26}$$

or

$$\omega_{w_2} = \frac{1}{T_{w_2}} = \frac{V_o}{\sqrt{bc}}$$

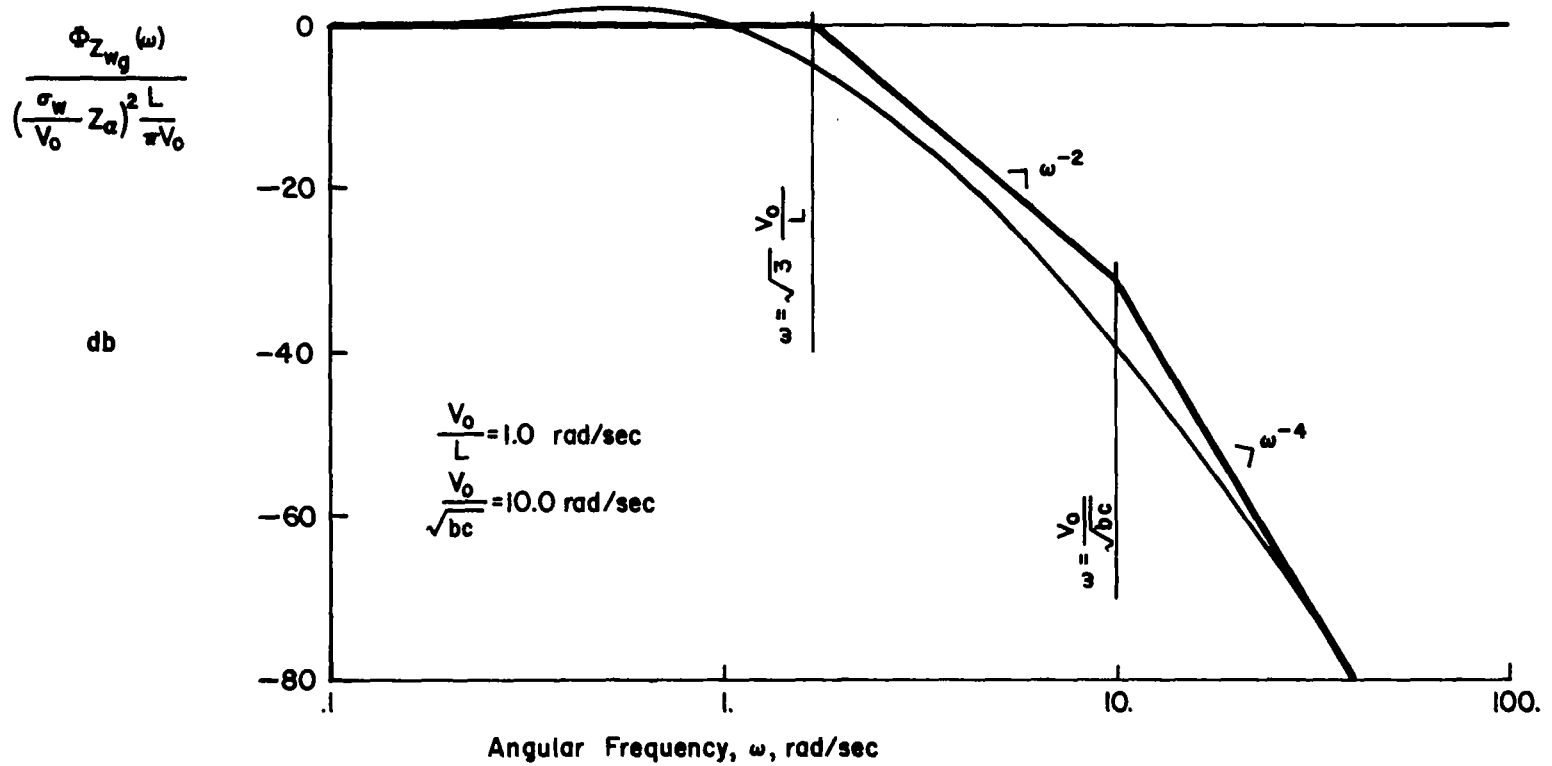

Figure 4. Approximation of Vertical Force Spectrum due to Vertical Gusts

At low frequency, the spectrum becomes

$$\Phi_{Z_{w_g}}(\omega) = \Phi_{Z_{w_g}}(0)$$

$$= \left(\frac{\sigma_w}{V_o} Z_\alpha\right)^2 \frac{L}{\pi V_o} \tag{27}$$

Thus, the complete form of the spectral approximation is

$$\Phi_{Z_{w_g}}(\omega) \doteq \frac{\left(\frac{\sigma_w}{V_o} Z_\alpha\right)^2 \frac{L}{\pi V_o}}{\left[\left(\frac{\omega L}{\sqrt{3} V_o}\right)^2 + 1\right]\left[\frac{bc}{V_o^2} \omega^2 + 1\right]} \tag{28}$$

A comparison of the true heave disturbance spectrum with the approximation of equation (28) is made in Figure 5 for a typical value of the parameters V_o/L, V_o/b, and V_o/c. The approximation can be expected to represent the true spectrum to an rms level within eight percent of the actual rms heave magnitude.

Since the pitching moment spectrum for the wing is identical in form to the heave spectrum, their approximations differ only in their steady state values, i.e., their low frequency asymptotes. For pitching moment $\Phi(0)$ is

$$\Phi_{M_{g_w}}(0) = \left(\frac{\sigma_w}{V_o} M_{\alpha_w}\right)^2 \frac{L}{\pi V_o} \tag{29}$$

and the spectral approximation is

$$\Phi_{M_{g_w}}(\omega) \doteq \frac{\left(\frac{\sigma_w}{V_o} M_{\alpha_w}\right)^2 \frac{L}{\pi V_o}}{\left[\left(\frac{\omega L}{\sqrt{3} V_o}\right)^2 + 1\right]\left[\frac{bc}{V_o^2} \omega^2 + 1\right]} \tag{30}$$

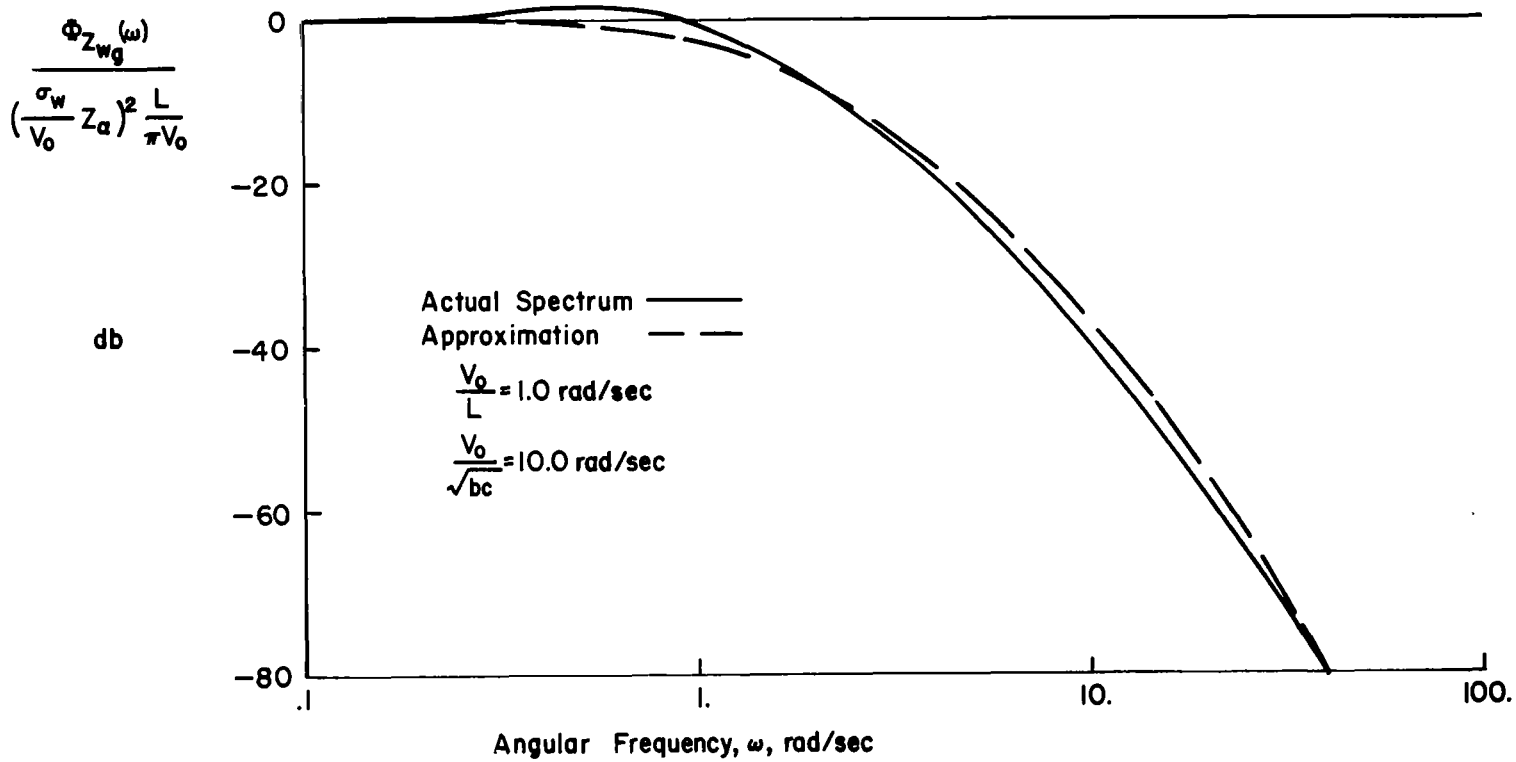

Figure 5. Comparison of Actual Vertical Force Spectrum with Asymptotic Approximation

Comparison of the approximate and true spectra are identical to the heave spectra of Figure 5.

If the horizontal stabilizer pitching moment contribution is to include the highest frequency attenuation associated with spanwise averaging and chordwise gust penetration filtering, then the appropriate spectral approximation will be identical to equation (30) with M_{α_w} replaced by M_{α_t}. If the highest frequency attenuation is ignored, then only the low frequency and the ω^{-2} asymptotes remain and the approximate spectra becomes

$$\Phi_{M_{g_t}}(\omega) \doteq \frac{\left(\frac{\sigma_w}{V_o} M_{\alpha_t}\right)^2 \frac{L}{\pi V_o}}{\left(\frac{\omega L}{\sqrt{3} V_o}\right)^2 + 1} \tag{31}$$

SECTION 3

DEFINITION OF THE TEST PROGRAM

Variations of the Turbulence Disturbances

The characteristics of turbulence incorporated in the test program represent the disturbances as they are recognized by the pilot. These characteristics are the magnitude of the heave and pitch disturbances, the correlation between pitch and heave, and the frequency content or bandwidth of the disturbance spectra. They are defined analytically in Appendix B and may be summarized here as follows:

- heave disturbance magnitude represented by the rms incremental normal acceleration due to turbulence

$$\sigma_Z = \left[\frac{\sqrt{3}}{2}\left(\frac{\sigma_w}{V_o} Z_\alpha\right)^2\right]^{\frac{1}{2}} \tag{32}$$

  which is a function of the rms vertical gust magnitude and the airplane's lift curve slope,

- pitching moment disturbance represented by the rms angular acceleration in pitch

$$\sigma_M = \left[\frac{\sqrt{3}}{2}\left(\frac{\sigma_w}{V_o}\right)^2 \left(M^2_{\alpha_{g_w}} + M^2_{\alpha_{g_t}} + 2 M_{\alpha_{g_w}} M_{\alpha_{g_t}} e^{-\sqrt{3}\frac{\ell_t}{L}}\right)\right]^{\frac{1}{2}} \tag{33}$$

  which is predominantly a function of the rms vertical gust magnitude and the static angle of attack stability derivatives of the wing and horizontal stabilizer,

- correlation between the pitch and heave disturbances represented by the normalized cross correlation

$$\rho_{MZ} = \frac{R_{MZ}(0)}{\sigma_M \sigma_Z}$$

$$= \left(\frac{\sqrt{3}}{2}\right)^{\frac{1}{2}} \left(\frac{\sigma_w}{V_o}\right) \left[\frac{M_{\alpha_{g_w}} + M_{\alpha_{g_t}} e^{-\sqrt{3}\frac{\ell_t}{L}}}{\sigma_M}\right] \tag{34}$$

which is determined by the relative contributions of the wing and stabilizer to static longitudinal stability and the normalized tail length,

- frequency content of the disturbance spectra determined by the two corner frequencies of the turbulence model

$$\omega_{w_1} = \sqrt{3}\,\frac{V_o}{L} \tag{35}$$

$$\omega_{w_2} = \frac{V_o}{\sqrt{bc}} \tag{36}$$

defined in the previous section.

The role played by these descriptors of the turbulence induced disturbances may be better appreciated if their contribution to the airplane's response is considered. Using pitch attitude as an example, the power spectrum of pitch excursions due to pitch and heave turbulence may be written

$$\Phi_\theta = \left|\frac{N^\theta_{M_g}}{\Delta'}\right|^2 \Phi_{M_g} + \left|\frac{N^\theta_{Z_g}}{\Delta'}\right|^2 \Phi_{Z_g}$$

$$+ 2\,R_e \left[\frac{N^\theta_{M_g}}{\Delta'}\right]\left[\frac{N^\theta_{Z_g}}{\Delta'}\right]^* \Phi_{M_g Z_g} \tag{37}$$

It should be clear from the definition of the turbulence disturbances in the preceding section that the characterizations of turbulence by rms magnitude, correlation, and bandwidth have their counterparts in the pitch response to turbulence, equation (37), i.e.,

- the rms heave disturbance, σ_Z, and the corner frequencies, ω_{w_1} and ω_{w_2}, are sufficient to specify Φ_{Z_g},
- the rms pitch disturbance, σ_M, and the same corner frequencies, ω_{w_1} and ω_{w_2}, define Φ_{M_g},
- the pitch-heave correlation determines the magnitude of the cross-spectrum Φ_{MZ}.

Contributions of rms vertical gust intensity and the airplane's lift curve and static angle of attack stability derivatives to the magnitudes of the vertical force and pitching moment disturbances are shown in Figure 6. Also included are the influences of the relative magnitudes of pitching moment due to wing and tail and the normalized tail length on the correlation between pitch and heave disturbances.

The tradeoff between the rms gust magnitude and the slope of the lift curve in determining the vertical force disturbance is shown in Figure 6a for the three levels of heave disturbance used in the flight test program. Rms gust magnitude is given either as an rms angle of attack disturbance or an rms vertical gust velocity, where the two are related by the trim airspeed ($\sigma_\alpha = \sigma_w / V_o$, V_o = 120 mph or 176 ft/ sec). As a point of information, the lift curve slope of the basic Navion at this flight speed is Z_α = 352 ft/ sec^2/ rad.

Similarly, the tradeoff between rms vertical gust magnitude and angle of attack stability in pitch which determines the pitch disturbance magnitude is shown in 6b. At the airspeed listed previously and for a nominal c.g. position, the pitching moment derivatives of the Navion are M_α = -5.2 rad/ sec^2/ rad, $M_{\dot\theta}$ = -1.9 rad/ sec^2 per rad/ sec, $M_{\dot\alpha}$ = -.9 rad/ sec^2 per rad/ sec, $M_{\alpha_w} \doteq$ +6.4 rad/ sec^2/ rad, $M_{\alpha_t} \doteq$ -11.6 rad/ sec^2/ rad.

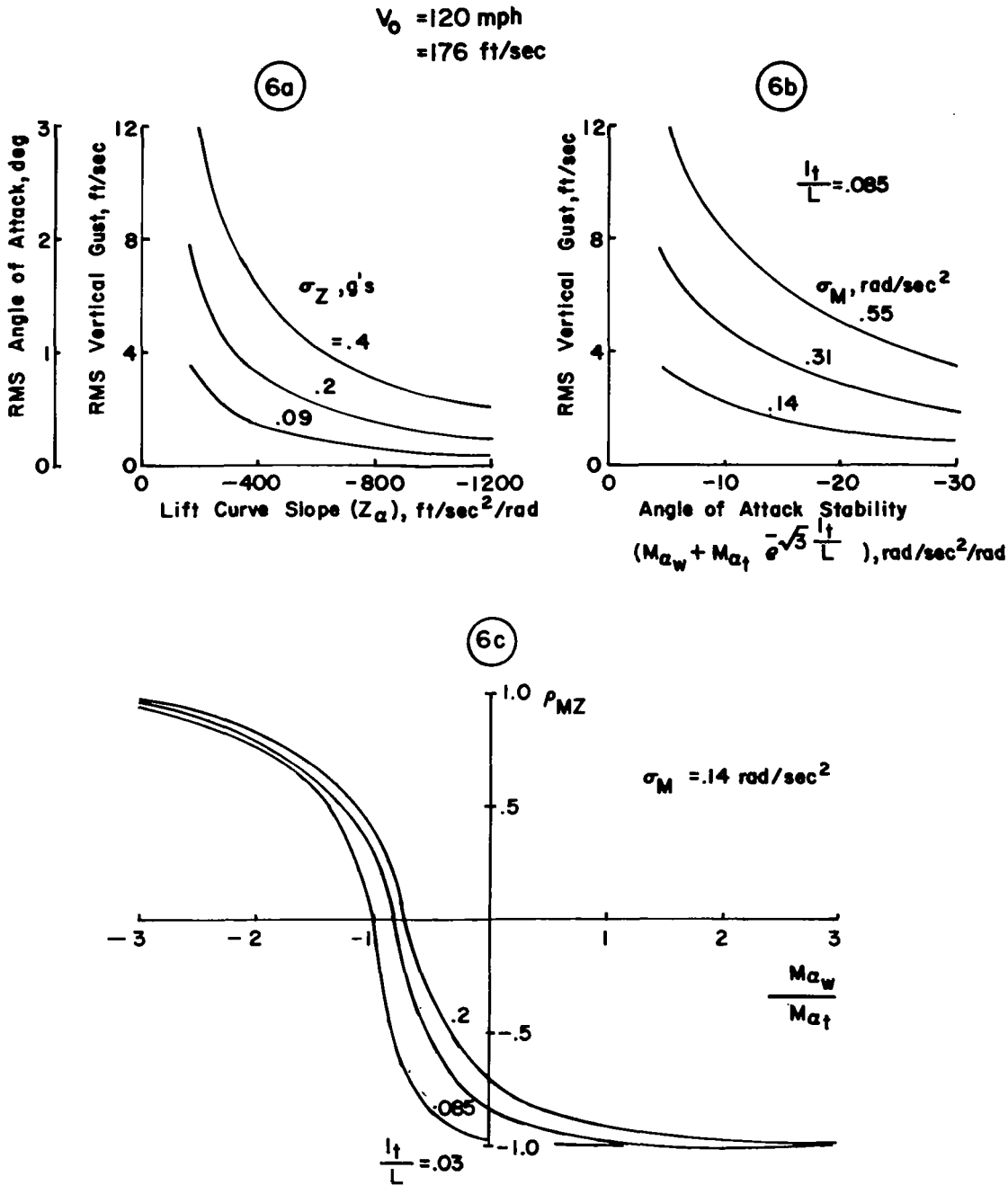

Figure 6. Contributions to the Turbulence Model Parameters

Contributions to the pitch-heave correlation coefficient are shown in 6c. The ratio of the wing and tail contributions to static angle of attack stability can conceivably cover a wide range, therefore this parameter has a larger influence on the normalized correlation than does the tail length. Figure 6c shows a range of normalized tail length appropriate to the general aviation class of airplane.

Dynamics Configurations

The airplane's dynamic characteristics in pitch and heave are also of interest in the study of problems relating to longitudinal control of the airplane in turbulence. While the illustration of pitch response to turbulence given in equation (37) is written in terms of the airplane's closed loop dynamics, these closed loop characteristics are influenced to a considerable extent by the open loop or uncontrolled longitudinal dynamics of the airplane. These open loop dynamics and their eventual effect on closed loop longitudinal control have been given a good deal of attention in previous analytical studies, simulator and variable stability airplane experiments. The purpose of this program is to attempt to evaluate the combined influences of open loop dynamics and turbulence disturbances on the pilot's ability to perform a specified flight task.

The characteristic motion of the airplane related to the three longitudinal degrees of freedom (forward and vertical velocity and rotation in pitch) are typically two second order oscillatory responses, the phugoid and short period modes. While there are exceptions to this description, where either of these modes may degenerate into two real roots, in general the so-called short period mode is a relatively high frequency and moderate to well damped motion while the phugoid is a very low frequency response frequently of light to neutral or sometimes negative damping.

Perhaps the most important single requirement for satisfactory longitudinal flying qualities is precise control of pitch attitude. Many tasks performed by the pilot require pitch attitude control as a primary element (straight and level flight, turns, climb and descent maneuvers, takeoff rotation and climb-out, landing approach, flare and touchdown) either as the actual means for performing the task or as an intermediate means for achieving the desired end result. Of the existing studies of pitch attitude control, Reference 5 provides an extensive review of previous investigations as well as a thorough analysis of pitch control of its own. Reference 6 also is an interesting analytical study of the problem and it provides some insights to the pilots' techniques in performing pitch attitude and altitude tracking tasks. Pitch attitude control with the elevator essentially reduces to direct control of the airplane's short period response. Although phugoid motion does appear in the open loop pitch response, the pilot has no difficulty in controlling pitch motions associated with this mode. Control of the short period pitch response may be characterized by the short period natural frequency, ω_{sp}, the short period damping ratio, ζ_{sp}, the numerator root of the pitch attitude to elevator transfer function, $1/T_{\theta_2}$, and the longitudinal control sensitivity, M_{δ_e} and F_s/g, or suitable combinations of any of the above. The short period frequency affects the quickness of the response of the airplane in pitch to elevator inputs. Furthermore, since it is so strongly related to the airplane's angle of attack stability, ($\omega_{sp}^2 \doteq M_\alpha - M_{\dot{\theta}} Z_\alpha / V_o$), the frequency is also associated with the airplane's static longitudinal stability and hence to the tendency of the airplane to hold a given trim airspeed. Short period damping ratio in general would be expected to influence the oscillatory character of the short period response. However, for the range of ζ_{sp} typically encountered for general aviation airplanes which is sufficient to prevent appreciable pitch oscillations, the damping ratio is more likely to manifest itself in terms of overshoots in pitch rate response. This is a characteristic which tends to be more important in maneuvering than steady level, climbing or descending flight. The pitch attitude numerator root affects the pilot's ability to achieve a tight control of pitch attitude over a wide band of frequencies.

Control of the airplane's flight path angle and altitude are also important. As Reference 6 points out, the pitch attitude numerator root, $1/T_{\theta_2}$, is predominantly determined by the lift curve slope ($1/T_{\theta_2} \doteq -Z_\alpha / V_o + Z_{\delta_e} M_\alpha / V_o M_{\delta_e}$). Because control of the airplane's flight path through changes in pitch attitude is strongly dependent on the magnitude of the lift curve slope, $1/T_{\theta_2}$ provides an indication of the pilot's ability to achieve precise flight path and altitude control with the elevator. The stability of closed loop control of flight path angle or altitude with the elevator is related to the parameter, $1/T_{h_1}$, which is the low frequency real root of the numerator of the altitude to elevator transfer function. Influences of this parameter are considered in detail in References 5, 6, and 7. It in turn is related to the operating point on the throttle required curve ($1/T_{h_1} \doteq -X_u + (X_\alpha - g) Z_u / Z_\alpha$) which defines flight path stability with speed.

Of these parameters, the short period frequency and damping (ω_{sp}, ζ_{sp}) and the pitch attitude numerator root ($1/T_{\theta_2}$) were chosen for the current test program. Phugoid dynamics were essentially constant ($\omega_{ph} \doteq .25$ rad/sec, $\zeta_{ph} \doteq .13$) with one exception where the phugoid decomposed into a pair of real roots, one of which represented a mildly unstable exponential divergence. Operation on the front side of the throttle required curve was achieved in every instance, thereby keeping $1/T_{h_1}$ in a satisfactory range ($1/T_{h_1} \doteq .04$ 1/sec). Longitudinal control sensitivity, M_{δ_e}, was set at the optimum value chosen for smooth air operation. These values corresponded to results reported in Reference 8 for optimum control sensitivity.

Test Matrix

Tables 2 and 3 list the turbulence configurations and open loop dynamic characteristics which were included in the test program. Specific combinations of turbulence and dynamics evaluated are given in Table 4. These particular combinations were chosen to

- permit an independent evaluation of the effects of turbulence on flying qualities for one particular set of good longitudinal dynamics - Configuration 1,

TABLE 2

TURBULENCE CONFIGURATION

Configuration	σ_Z	σ_M	ρ_{MZ}	ℓ_t / L	$M_{\alpha_w} / M_{\alpha_t}$	V_o / L	ω_{w_2}
1	.2	.12	+.39	.085	-1.08	1.0	18.5
2	.2	.14	-.62	.085	- .47	1.0	18.5
3	.2	.31	-.94	.085	.47	1.0	18.5
4	.2	.55	-.98	.085	1.72	1.0	18.5
5	.09	.14	-.62	.085	- .47	1.0	18.5
6	.09	.31	-.94	.085	.47	1.0	18.5
7	.09	.55	-.98	.085	1.72	1.0	18.5
8	.4	.14	-.62	.085	- .47	1.0	18.5
9	.4	.31	-.94	.085	.47	1.0	18.5
10	.4	.55	-.98	.085	1.72	1.0	18.5
11	.2	.14	-.62	.085	- .47	.314	18.5
12	.2	.31	-.94	.085	.47	.314	18.5
13	.2	.55	-.98	.085	1.72	.314	18.5
14	.09	.14	-.62	.085	- .47	.314	18.5
15	.09	.31	-.94	.085	.47	.314	18.5
16	.2	.14	-.62	.085	- .47	2.0	18.5
17	.2	.31	-.94	.085	.47	2.0	18.5

TABLE 2 (continued)

Configuration	σ_Z	σ_M	ρ_{MZ}	ℓ_t / L	$M_{\alpha_w} / M_{\alpha_t}$	V_o / L	ω_{wa}
18	.2	.55	-.98	.085	1.72	2.0	18.5
19	.09	.14	-.62	.085	- .47	2.0	18.5
20	.09	.31	-.94	.085	.47	2.0	18.5
21	.4	.14	-.62	.085	- .47	2.0	18.5
22	.11	.08	-.62	.085	- .47	.314	18.5
23	.36	.25	-.62	.085	- .47	1.0	18.5
24	.36	.25	-.62	.085	- .47	2.0	18.5
25	.2	.29	-.99	.03	.47	1.0	18.5
26	.2	.31	-.86	.2	.47	1.0	18.5
27	.2	.14	-.99	.085	6.6	1.0	18.5
28	.2	.55	-.98	.085	1.72	1.0	10.0

TABLE 3

DYNAMICS CONFIGURATION PARAMETERS AND DERIVATIVE VALUES

Configuration	ω_{sp} or $(-1/T_{sp_1})$	ζ_{sp} or $(-1/T_{sp_2})$	ω_{ph} or $(-1/T_{ph_1})$	ζ_{ph} or $(-1/T_{ph_2})$	$-1/T_{\theta_1}$	$-1/T_{\theta_2}$	$-1/T_{h_1}$	Z_α	M_α	$M_{\dot{\theta}}$	M_{δ_e}
1	3.0	.8	.19	.15	-.075	-2.0	-.043	-352.	- 5.22	-1.89	-.42
2	(-.57)	(-4.13)	(+.1)	(-.27)	-.075	-2.0	-.043	-352.	+ 1.0	-1.89	-.25
3	6.0	.4	.24	.13	-.075	-2.0	-.043	-352.	-20.6	-1.89	-.93
4	3.0	.8	.21	.13	-.084	- .89	-.011	-158.	- 6.31	-2.99	-.42
5	3.0	.5	.25	.11	-.075	-2.0	-.043	-352.	- 8.82	- .09	-.42
6	2.0	.75	.25	.08	-.075	-2.0	-.043	-352.	- 3.38	- .09	-.34

$X_u = -.069$ 1/sec

$X_\alpha = 6.0$ ft/sec^2 per rad

$X_{\delta_e} \doteq 0$

$Z_u = -.352$ 1/sec

$Z_{\delta_e} \doteq 0.$

$M_u \doteq 0.$

$M_{\dot{\alpha}} = -.9$ rad/sec^2 per rad/sec

$V_o = 176$ ft/sec

TABLE 4

COMBINATIONS OF TURBULENCE
AND DYNAMICS CONFIGURATIONS

Dynamics Configurations	Turbulence Configurations
1	All configurations 1-28
2	1, 2, 3, 4, 5, 8, 11, 16
3	2, 3, 4, 7, 10, 11, 13, 16, 18
4	2, 5, 6, 7, 11, 14, 16, 19
5	1, 2, 3, 4, 5, 8, 11, 12, 16, 17
6	2, 3, 8, 16

- determine the influence of short period frequency (angle of attack stability) for selective variations in rms pitch disturbance magnitude and bandwidth with lift curve slope and damping ratio constant,
- determine the influence of short period damping for selective variations in pitch disturbances and bandwidth with lift curve slope constant and for two values of short period frequency,
- determine the influence of lift curve slope emphasizing variations in pitch and heave disturbance magnitude and bandwidth with short period frequency and damping constant.

The variation in short period frequency simply reflects a variation in angle of attack stability and can as well be considered as a change in the airplane's static margin (c.g. position). Note that one case (Configuration 2) is actually composed of two real roots ($1/T_{sp_1} = .57$, $1/T_{sp_2} = 4.13$) instead of the typical complex pair, although the traditional short period notation is retained for sake of consistency with the other configurations. This particular configuration is statically unstable ($M_\alpha = +1.0$ rad/sec^2/rad, $M_u = 0$), which is reflected in a slightly positive real root comprising one of the so-called phugoid pair ($1/T_{ph_1} = -.1$, $1/T_{ph_2} = .27$).

Short period damping ($\zeta_{sp}\,\omega_{sp}$) is altered in this program entirely through the pitch damping derivative $M_{\dot{\theta}}$. This is an effect which can either be considered in terms of changes in aerodynamic pitch damping or as a contribution of an inertial pitch damper. The range of the derivative encompasses airplanes similar to the basic Navion at the high end to approximately zero pitch damping at the low end.

One lateral-directional dynamics configuration was used throughout the program. This configuration was consistent with good flying qualities as reported in References 1 and 9 ($T_R = .25$ sec, $\omega_d = 2.3$ rad/sec, $\zeta_d = .1$, $L_\beta = -16$ rad/sec^2/rad, L_{δ_a} and N_{δ_r} optimum). Light turbulence was simulated in roll and yaw.

Evaluation Task

Flight evaluations of the test configurations were obtained for an ILS approach task. A number of tasks were considered and some were test flown during preliminary evaluations in the process of selecting a practical and realistic method for studying longitudinal flying qualities in turbulence. Constant altitude tracking, steady climb and descent profiles, pitch attitude tracking, and the ILS approach were each studied before finally selecting the instrument approach as the most suitable for the flight program. Neither flying constant altitude nor maintaining steady rates of climb or descent (as monitored on an instantaneous vertical speed indicator) were found to be sufficiently demanding of the pilots to permit them to critically evaluate either the airplane's dynamics or turbulence response characteristics. Either of these tasks is more appropriate to the cruise segment of flight where precise flight control is generally unnecessary. Pitch attitude tracking, while being a primary task for many longitudinal control requirements of the pilot, is difficult to evaluate as a realistic task in and of itself. Of the tasks considered here, the ILS approach presents the most realistic and demanding requirements on longitudinal control of the airplane. While this task has the undesirable feature of the time varying sensitivity of the glide slope deviation indicator, it was still chosen as the best compromise of the available alternatives.

The entire flight test procedure is illustrated in Figure 7. Each test configuration was set up on the downwind leg of the approach whereupon the variable stability system was engaged and the evaluation pilot assumed control of the airplane. Approximately one minute was available to feel out the configuration before the pilot commenced a 135 degree turn to the left to intercept the localizer. After the localizer was acquired, the pilot had approximately one minute of level flight tracking prior to glide slope intercept. During this time the simulated turbulence was turned on. The ILS approach proceeded down to an altitude of 200 feet above the surface. At that point the evaluation pilot established visual contact with the ground and a VFR offset

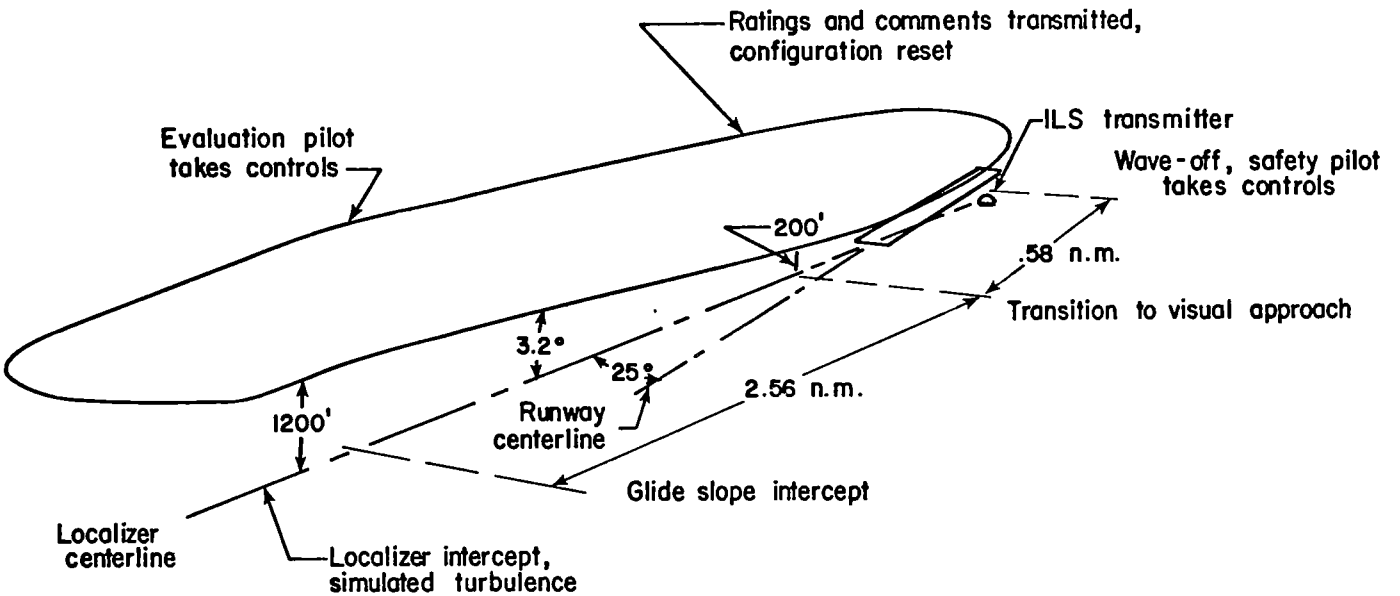

Figure 7. Diagram of Simulated Approach

maneuver, requiring a 25 degree heading change, was made to align with the runway. A waveoff was executed at 20 feet altitude and the safety pilot then assumed control of the airplane to permit the evaluation pilot to transmit his comments to the flight test monitor on the ground.

The ILS signals were provided by an ADCOLE microwave unit on loan from the Federal Aviation Administration's NAFEC facility. Standard cross-pointer cockpit instrumentation was used. Glide slope angle was set at 3.2 degrees as required for terrain avoidance. All approaches were flown at a trim speed of 105 knots (120 mph or 176 ft/ sec).

The pilot's evaluation of a configuration consisted of assigning an appropriate pilot opinion rating and providing detailed pilot commentary on several itemized factors for that configuration. Pilot ratings were based on the revised Cooper-Harper scale described in Reference 10 and reproduced in Table 5. Factors involved in the commentary were

- glide slope control - precision of performance and pilot workload, control technique;
- pitch attitude control - precision of control and pilot workload, effect of pitch excursions on glide slope tracking;
- airspeed control - ability to maintain the approach speed, effect of airspeed excursions on glide slope tracking;
- magnitude of turbulence - level of heave and pitch disturbances, effect on glide slope tracking;
- frequency content of turbulence - is frequency content apparent, effect on glide slope tracking.

If appropriate, the pilots distinguished in their comments between the IFR and VFR segments of the approach. Since the turbulence simulation was not considered to be representative of the characteristics of atmospheric turbulence below about 200 feet (Reference 1) any comments regarding maneuvers during the final stages of the approach immediately prior to what would be the initiation of flare (or in this case, the waveoff) were not given equal weight to

TABLE 5

PILOT OPINION RATING SCALE

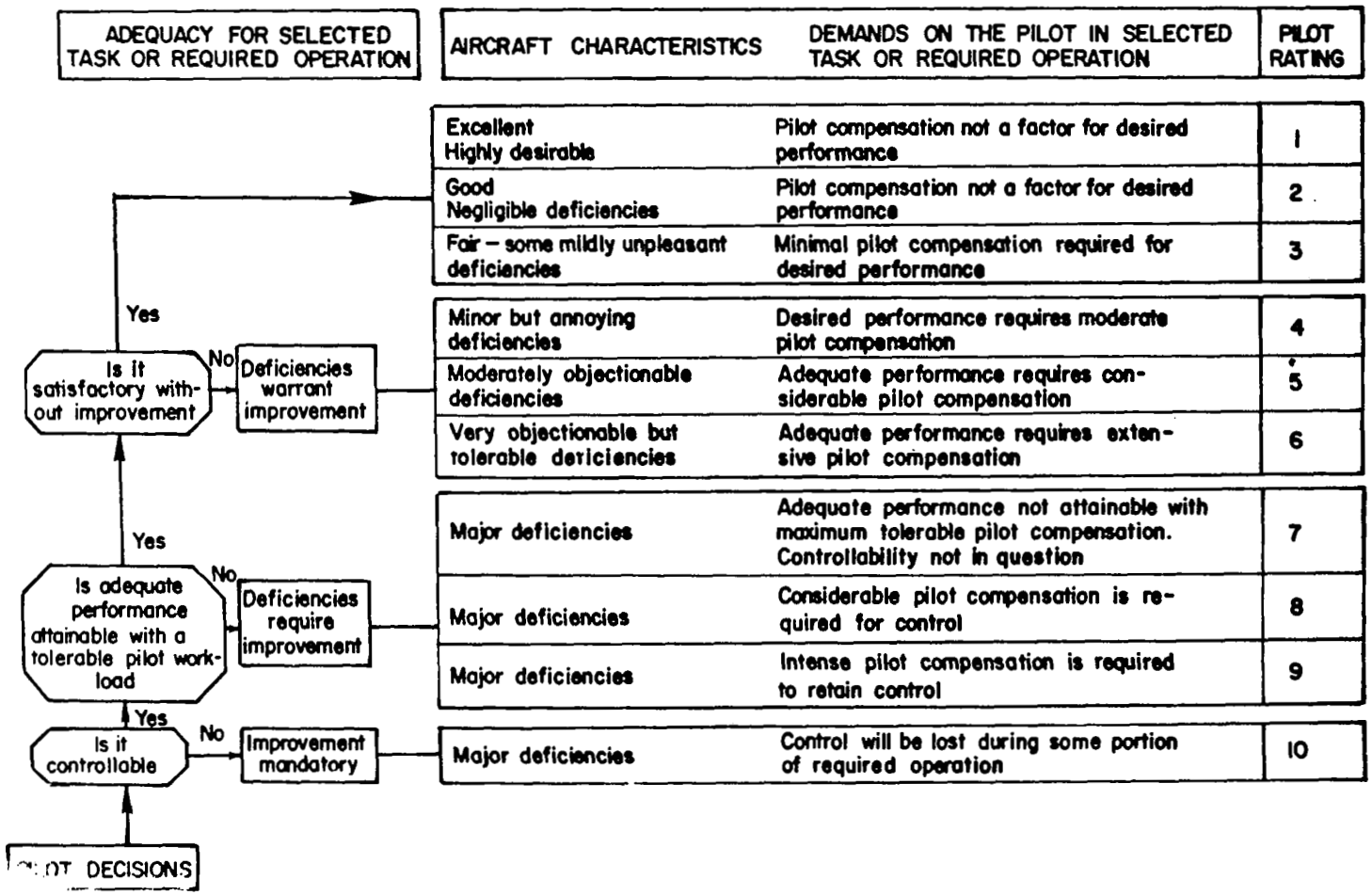

ratings and commentary related to the IFR segment of the approach. All evaluations were based on the duration of the approach. No attempt was made to factor fatigue or extended exposure time into the ratings.

The flight test program was carried out by four evaluation pilots. Three of the pilots had combined military and civil airplane backgrounds with current experience as flight test engineers and flying qualities evaluation pilots. The fourth pilot had an extensive background in civil aviation and had engineering experience in the areas of airplane stability and control and flying qualities. All were instrument rated.

Quantitative flight data was obtained in the form of on-line chart recorded time histories of telemetered signals for

longitudinal control motion
pitch attitude excursions
glide slope deviation
airspeed excursions
pitch turbulence

Tape recordings were made for the time histories of all the above variables and in addition for

pitch rate
normal acceleration
angle of attack
heave turbulence
flap motion

Test Facilities

Flight evaluations were made using an in-flight simulator, the Princeton Variable Stability Navion shown in Figure 8. This vehicle consists of a basic North American airframe modified to achieve a variable stability and control capability. The airplane and its systems are described in detail in Reference 1. To briefly summarize the longitudinal capabilities of the airplane, variable

Figure 8. Princeton Variable Stability Navion

stability is achieved through the response feedback technique illustrated in general in Figure 9. Angle of attack, pitch rate, and airspeed are fed back to the elevator and flap. In addition, airspeed and angle of attack may be fed to the throttle to achieve control of longitudinal force characteristics. Electric elevator and throttle controls are available to the pilot. The flaps may be used by the pilot in a direct lift control mode, although this control was not employed in the program. Hydraulic servo actuators provide control surface response which is flat on a frequency spectrum out to 10 cycles per second.

The cockpit environment of the Navion is shown in Figure 10. The evaluation pilot occupies the right seat and is provided with a standard instrument display (gyro horizon, directional gyro, ILS glide slope and localizer cross-pointer, airspeed indicator, altimeter, instantaneous vertical speed indicator, and turn and bank instrument). A center stick control using linear springs for control force gradient is provided. Stick geometry may be noted in Figure 10. The throttle control is at the pilot's left hand.

Analog matching was used to achieve proper correspondence between the airplane's response characteristics and the desired response produced by an analog computer simulation of the test configuration. The procedure and typical results are described in Reference 11.

The simulation of turbulence on board the airplane has been described fully in Reference 1. A block diagram of the system is reproduced from Reference 1 and shown in Figure 11. The vertical gust signal in the longitudinal channel consists of prefiltered Gaussian white noise, attenuated at 40 db/ decade below .05 cycles/ second by a high pass filter and attenuated at 20 db/ decade above 4 cycles/ second by a low pass filter. This signal is then introduced to the spectral shaping filters shown in Figure 12. Gain controls are adjusted to obtain amplitude characteristics of the pitch and heave disturbances appropriate to the rms vertical gust velocity and the aerodynamic stability derivatives, Z_{α}, M_{α_w}, and M_{α_t}. Filter corner frequencies are adjusted to match the corner frequencies of the turbulence models of Section 2.

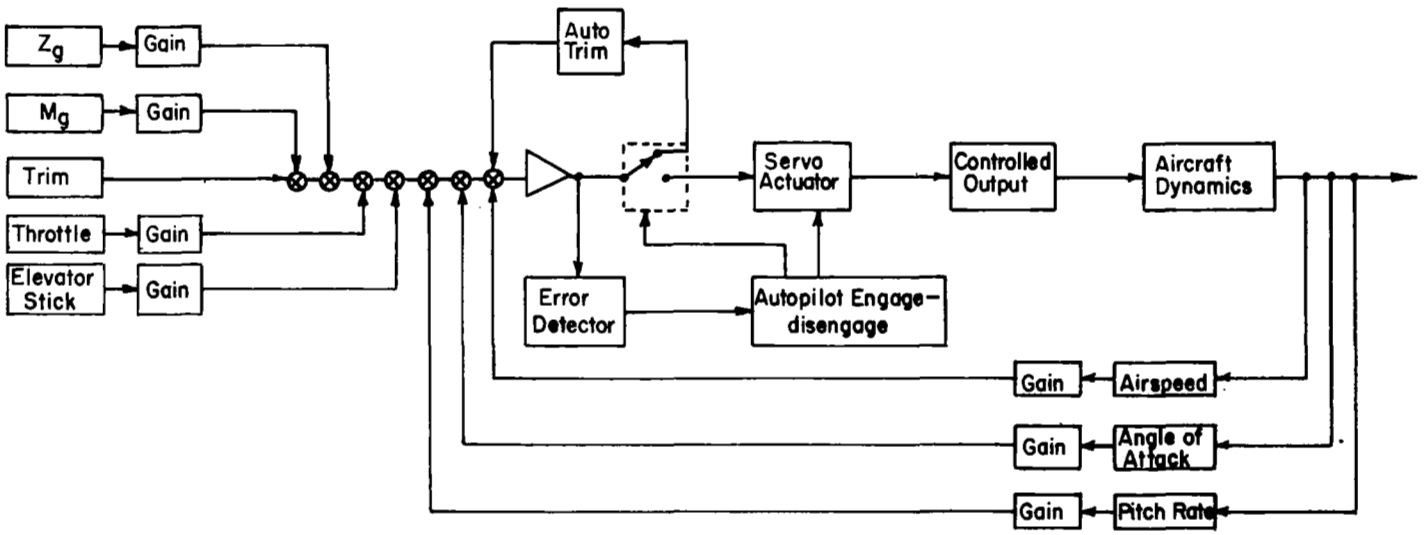

Figure 9. Typical Variable Stability Control System Channel - Longitudinal Mode

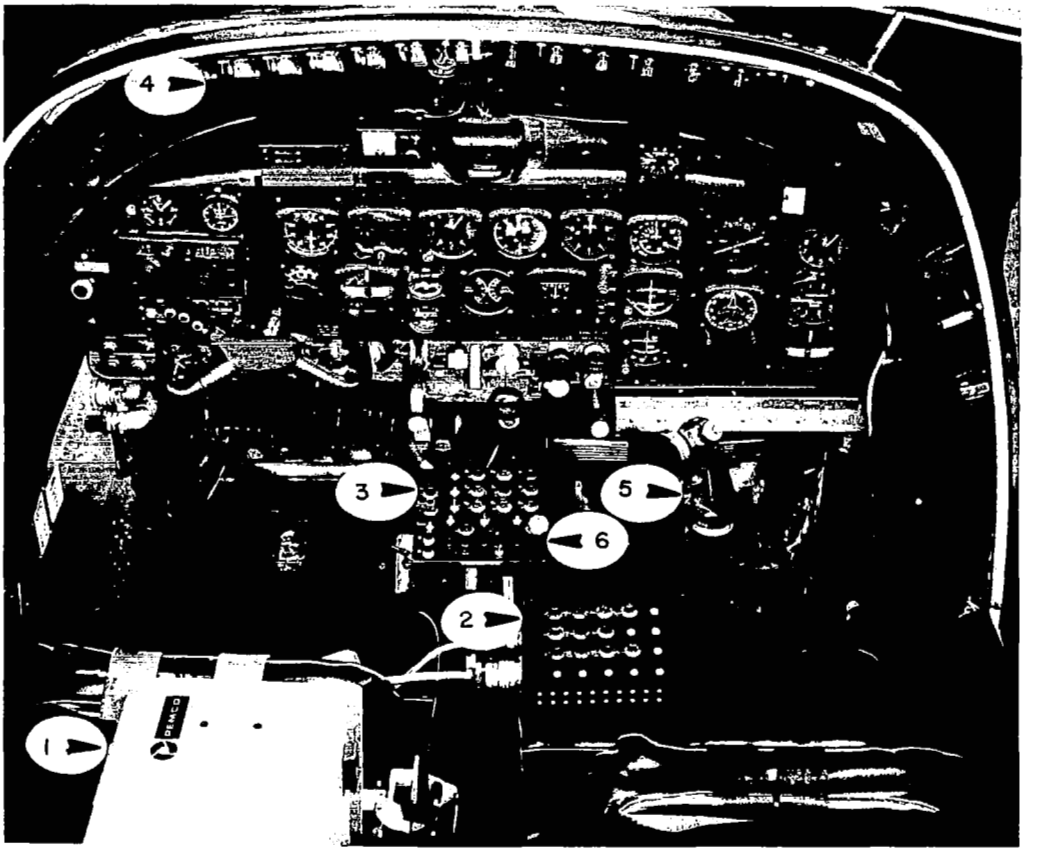

1. Tape Recorder
2. Turbulence Filter Circuitry
3. Individual Gain Controls
4. Variable Stability Feedback Gains
5. Control Stick (including DLC thumbwheel control)
6. Electric Throttle

CONTROL STICK GEOMETRY

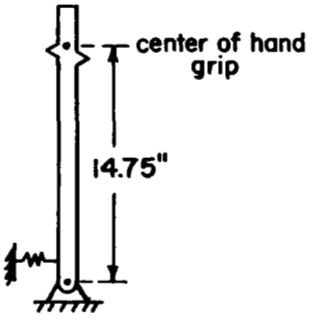

Longitudinal Force Gradient
5.2 lb/in at hand grip

Figure 10. Cockpit Environment and Control Stick Geometry

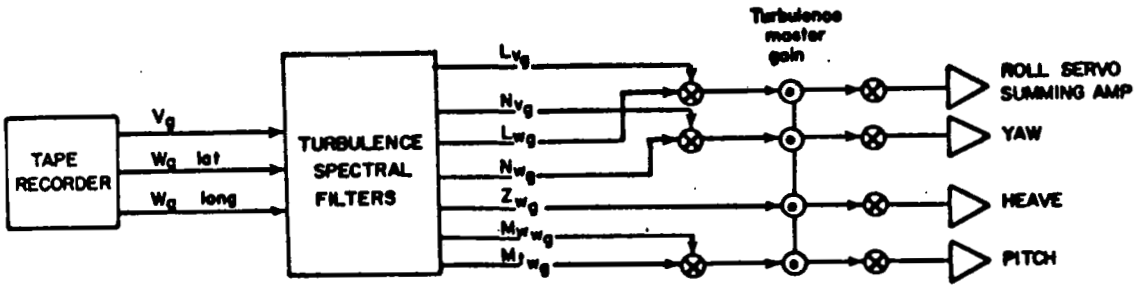

Figure 11. Turbulence Simulation System

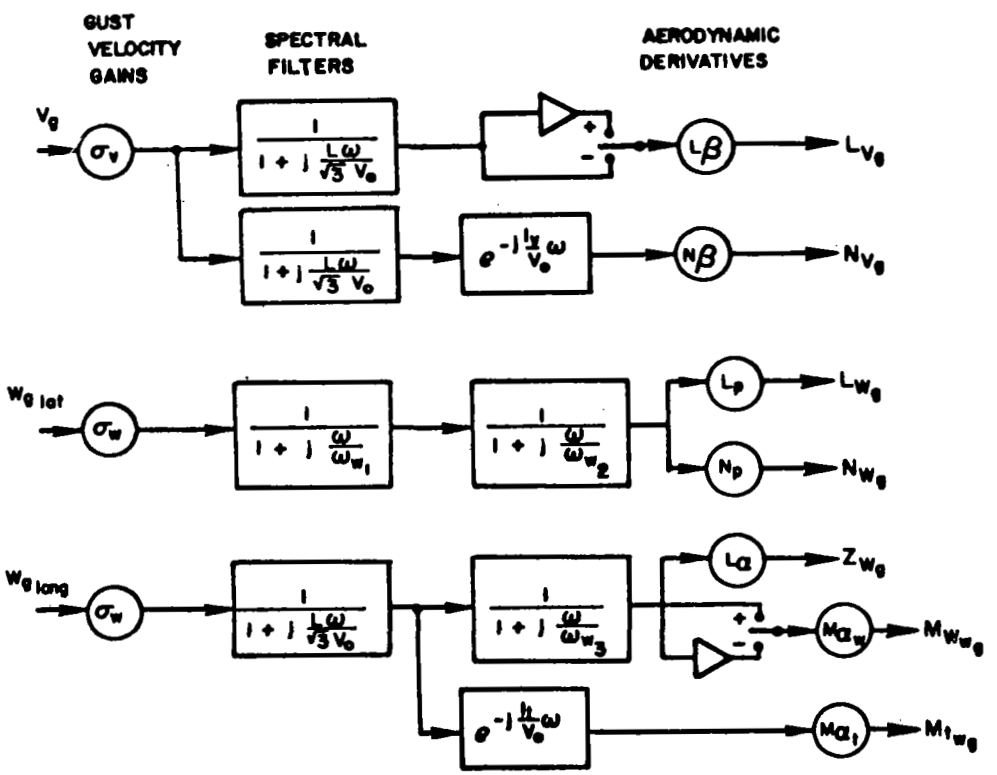

Figure 12. Turbulence Spectrum Filter System

A first order Pade transport lag representation is used to account for the separation of the wing and horizontal tail. A comparison of the simulated turbulence spectrum with the model of Section 2, which illustrates the low and high frequency pre-filtering in the simulation, is shown in Figure 13. A list of the functions of the longitudinal turbulence controls of Figures 11 and 12 is given in Table 6.

Following the scaling and filtering shown in Figure 12, the turbulence signal is fed to either the elevator or flap control servos. A comparison of the longitudinal force, vertical force, and pitching moment generated by the airplane's controls to the force and moment disturbances induced on an airplane in natural turbulence is shown below.

Natural Turbulence

$$\begin{bmatrix} X_{u_g} \\ Z_{u_g} \\ M_{u_g} \end{bmatrix} + \begin{bmatrix} X_{w_g} \\ Z_{w_g} \\ M_{w_g} \end{bmatrix}$$

Simulated Turbulence

$$\begin{bmatrix} X_{\delta_f} \\ Z_{\delta_f} \\ M_{\delta_f} \end{bmatrix} \left\{\frac{\delta_f}{w_g}\right\}_{w_g} + \begin{bmatrix} X_{\delta_e} \\ Z_{\delta_e} \\ M_{\delta_e} \end{bmatrix} \left\{\frac{\delta_e}{w_g}\right\}_{w_g}$$

where $\dfrac{\delta_f}{w_g} = \dfrac{Z_w}{Z_{\delta_f}}$; $\dfrac{\delta_e}{w_g} = \dfrac{(M_{w_w} + M_{w_t} e^{-\frac{\ell_t}{V_o} s})}{M_{\delta_e}}$

As was mentioned previously in this section, no attempt was made to simulate forces or moments due to longitudinal gusts. Longitudinal and vertical forces due to elevator deflection are negligible ($X_{\delta_e} \doteq 0$ and $Z_{\delta_e} \doteq 0$). Longitudinal forces produced by the flap in response to simulated vertical force signals, while small, are not negligible. However, these forces are in the proper direction to partially make up for the lack of X_{w_g} simulation. Pitching moments due to the flap are cancelled through an electric flap-elevator interconnect. Thus the final results of the simulation are pitching moment disturbances provided solely by the elevator and heave disturbances provided by the

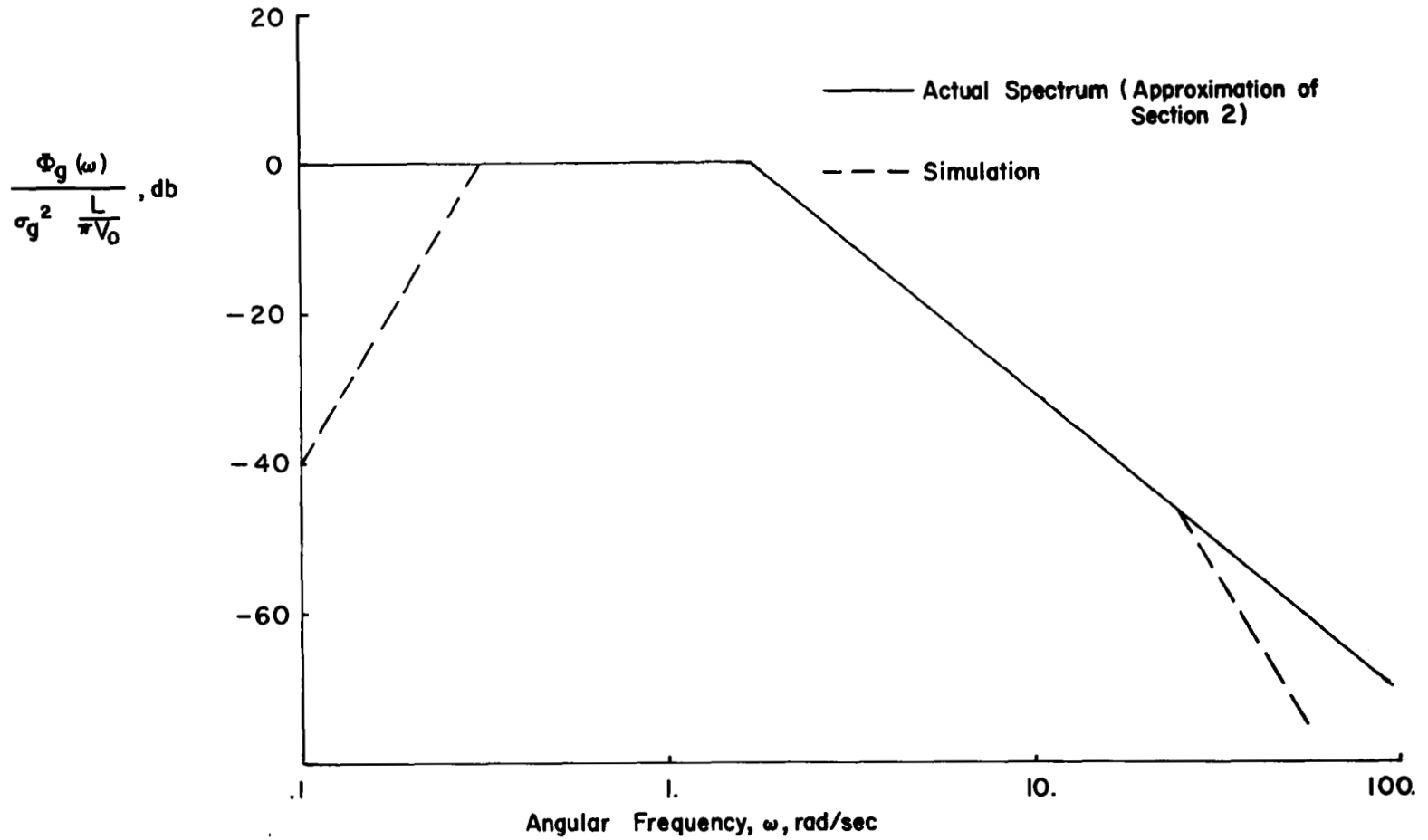

Figure 13. Asymptotes of Actual and Simulated Turbulence Spectra

TABLE 6

TURBULENCE SPECTRA CONTROLS

Pot	Parameter	Function	Spectra
σ_α	$\sqrt{\frac{L}{\pi V_o}}\left(\frac{\sigma_w}{V_o}\right)$	Vary σ_w to jointly control σ_M and σ_Z; Vary V_o/L to maintain constant σ with changes in ω_{w_1}	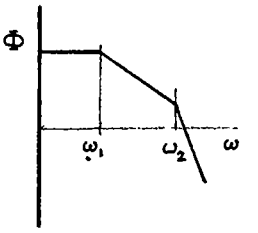
$\frac{V_o}{L}$	$\omega_{w_1} = \sqrt{3}\,\frac{V_o}{L}$	Vary low frequency break according to V_o/L	
ω_{w_3}	$\omega_{w_3} = \omega_{w_2} = \frac{V_o}{\sqrt{bc}}$	Vary high frequency break according to V_o/b and V_o/c	$\sigma_Z^2 = \frac{\sqrt{3}}{2}\left(\frac{\sigma_w}{V_o} Z_\alpha\right)^2$
$\ell_{t_{pot}}$	$e^{-\frac{\ell_t}{V_o}s} \doteq \frac{(1-\frac{\ell_t}{2V_o}s)}{(1+\frac{\ell_t}{2V_o}s)}$	Vary tail lag to change ρ_{MZ}	$\sigma_{M_w}^2 = \frac{\sqrt{3}}{2}\left(\frac{\sigma_w}{V_o} M_{\alpha_w}\right)^2$ For $L \gg \sqrt{3bc}$
	$\ell_{t_{pot}} = \frac{2V_o}{66.7}\left(\frac{\ell_t}{}\right)$		$\sigma_{M_t}^2 = \frac{\sqrt{3}}{2}\left(\frac{\sigma_w}{V_o} M_{\alpha_t}\right)^2$
L_α	L_α	Individual control over σ_Z	
M_{α_w}	M_{α_w}	Individual control over σ_M	
M_{α_t}	M_{α_t}	Control over σ_M and ρ_{MZ}	
M	Master gain	Control over σ_M, σ_Z, σ_L, σ_N	

flap (with small longitudinal forces as a by-product). Transient aerodynamic characteristics of the control surfaces were not accounted for in the simulation. Any attenuation of the aerodynamic disturbances produced by the controls due to transient lift development takes place at high frequency. The energy level of the disturbances at these frequencies is small and of no consequence to the simulation.

Of the four aerodynamic controls of the airplane, only the flap had restrictions on its authority which were reached or exceeded in the flight program. Flap travel on the Navion is limited to a range of 0 to 25 degrees, measured from the trail position to the down limit. Trim flap settings for the approach were in the mid-range of the full throw deflection. The incremental range of flap available imposed constraints on the magnitude of heave turbulence or the change in lift curve slope or a combination of both which could be simulated in flight. A full 25 degree flap deflection provides about one g incremental normal acceleration for the approach flight condition. This flap authority was adequate for simulation of an rms heave disturbance of .2 g's for either the low or high lift curve slope (Z_α / V_o = -.9 or -2.0 1/sec). However, the fidelity of the larger heave disturbance simulation (σ_Z = .4 g's) was compromised at the higher lift curve slope (which was the value of the basic Navion) and the simulation was not even attempted for the low lift curve configuration. Figure 14 illustrates the difficulty encountered. A plot of the probability density function for the simulated turbulence command to the flap and for the flap response is shown. The probability density corresponds to a Gaussian distribution. The flap deflection commanded by the simulated turbulence (Z_{w_g}) follows the Gaussian distribution without exception. Limitations on maximum attainable flap deflection produce a truncated Gaussian density function for flap response as indicated by the dashed lines. For the large heave disturbance simulation (σ_Z = .4 g's based on the Z_{w_g} signal) the flap deflection is truncated at about 40 percent (1.37 σ) above

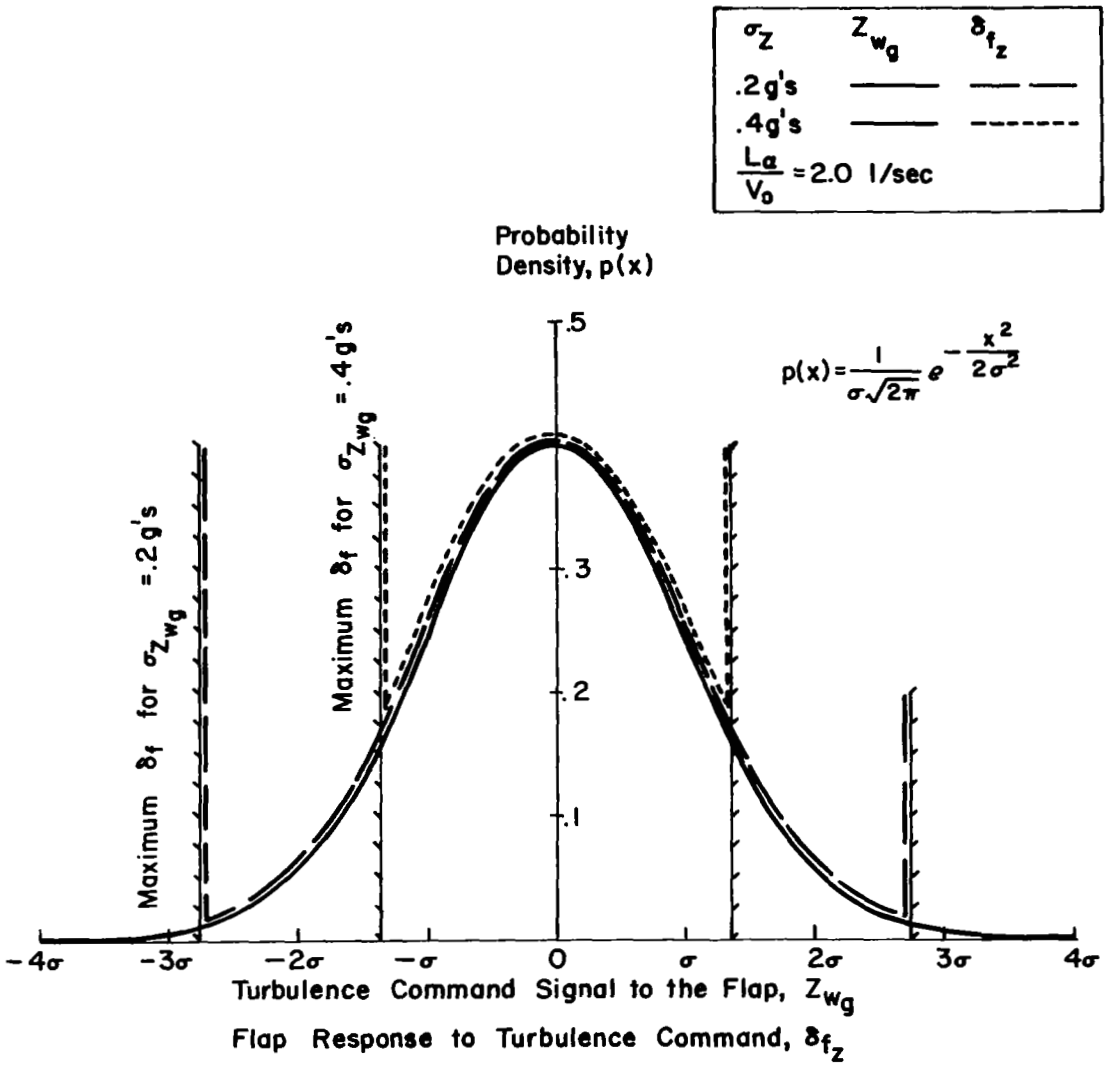

Figure 14. Comparison of the Probability Densities of the Turbulence Command to the Flap and the Flap Response

the rms level associated with the true Gaussian probability density. As a result, the rms values of the heave disturbances achieved in flight were lower than the rms magnitude of the heave disturbance commanded. Values of σ_Z determined from flap deflections measured in flight compared to the desired simulated values were

Desired of simulation	Achieved in flight
.09 g's	.09 g's
. 2 g's	.18 g's
. 4 g's	. 3 g's

This severe modification of the statistical properties for the large heave disturbance compromises that particular simulation since it significantly alters the maximum expected value of the disturbance (maximum Z_{w_g} encountered should be about 3 σ_Z for Gaussian distribution). However, the decision was made to retain the σ_Z = .4 g configuration in the test matrix for the sake of evaluating a condition with more frequent large heave disturbances than were encountered for the low disturbance cases where the Gaussian distribution was not violated. Therefore, when considering the flight data for large heave disturbances shown in the next section, the reader must recall that the maximum heave disturbance encountered did not exceed approximately .5 g's, instead of reaching approximately 1.2 g's as anticipated in the extreme for Gaussian turbulence.

Data Analysis

Flight test data in the form of continuous time histories of the airplane's motion, the pilot's control activity, and the simulated turbulence disturbances were converted to discrete time samples and analyzed for measures of precision of task performance and pilot control workload using the digital computer. The process of conversion of the data from analog to digital form is described in Reference 1. Rms values were computed for longitudinal control activity, pitch attitude excursions, incremental normal acceleration, glide slope deviation, airspeed excursions, magnitude of the heave and pitch disturbances, and flap deflection for heave turbulence simulation. Selective presentations of this data are made in the next section.

SECTION 4

ANALYSIS OF RESULTS

Synopsis of the Discussion

Data obtained during the flight test program consists to a considerable extent of pilot opinion ratings and commentary relating to the flying qualities of individual airplane configurations for various simulated turbulence environments. Supplementary data in the form of time history measurements of the airplane's motion, the pilot's control activity, and the simulated disturbance inputs were obtained for a selected number of configurations for one of the evaluation pilots. The first part of this section is concerned with the presentation and interpretation of the flight test data. As was noted in Reference 1, the limited number of pilots and the number of evaluations per pilot restrict the interpretation of this data to the identification of the significant influences of turbulence on longitudinal flying qualities. The objective of this analysis is to distinguish between important and unimportant effects rather than the determination of absolute levels of flying qualities as functions of dynamics and turbulence.

Measures of the precision of task performance and the pilot's control workload are compared with the pilot rating data and commentary to provide quantitative support for the pilot opinion trends. The primary measures of performance are rms pitch attitude excursions and deviation from the glide slope during the approach. Rms normal acceleration is also shown as an indication of the distraction and discomfort experienced by the pilot. Control workload is measured in terms of rms elevator stick force. Pilot opinion ratings and summaries of pilot commentary are included in Appendix C.

Following the presentation of the flight test results, a detailed closed loop pilot-airplane system analysis is undertaken. This study is useful in providing a more general understanding of the dynamics of the pilot-airplane

combination for various open loop airplane configurations. Based on this closed loop system theory closed loop performance and control workload are predicted and their trends as functions of longitudinal dynamics and turbulence characteristics are presented in this section.

Results of the Flight Test Program

Contribution of turbulence - Rms disturbance level

The effects of the rms magnitude of turbulence disturbances in heave and pitch on pilot opinion ratings are shown in Figure 15. Data for the primary evaluation pilot are shown in the upper diagram while data for the additional (secondary) evaluation pilots are presented in the lower diagram. It is the practice here and through the rest of the report as well to distinguish between the primary evaluation pilot, who flew every configuration in the test program at least twice, frequently three times, and occasionally more often, and the other (secondary) pilots, who flew only a portion of the configurations in the test matrix, generally with only one evaluation per configuration. Such a separation of the pilot rating data avoids obscuring the primary pilot's rating trends in the possible scatter of a number of singular ratings, while preserving these individual ratings and whatever message they may have in the way of each individual pilot's evaluations. The data are for a given set of longitudinal dynamics quite similar to those of the basic Navion (Configuration 1; $L_\alpha / V_o = 2.0$ 1/sec, $\omega_{sp} = 3.0$ rad/sec, $\zeta_{sp} = .8$) and for an intermediate spectral bandwidth corresponding to $V_o / L = 1.0$ radian/second. Average pilot ratings are noted adjacent to each test point and lines of constant pilot rating are faired to the primary pilot's data.

The degradation in pilot rating with increasing turbulence level is apparent. The gradient of pilot rating with turbulence level is not too severe and only for extreme pitch disturbances do the pilot ratings approach the unacceptable level for this case of good longitudinal dynamics. Combining and averaging the primary and secondary pilots' ratings does not alter these

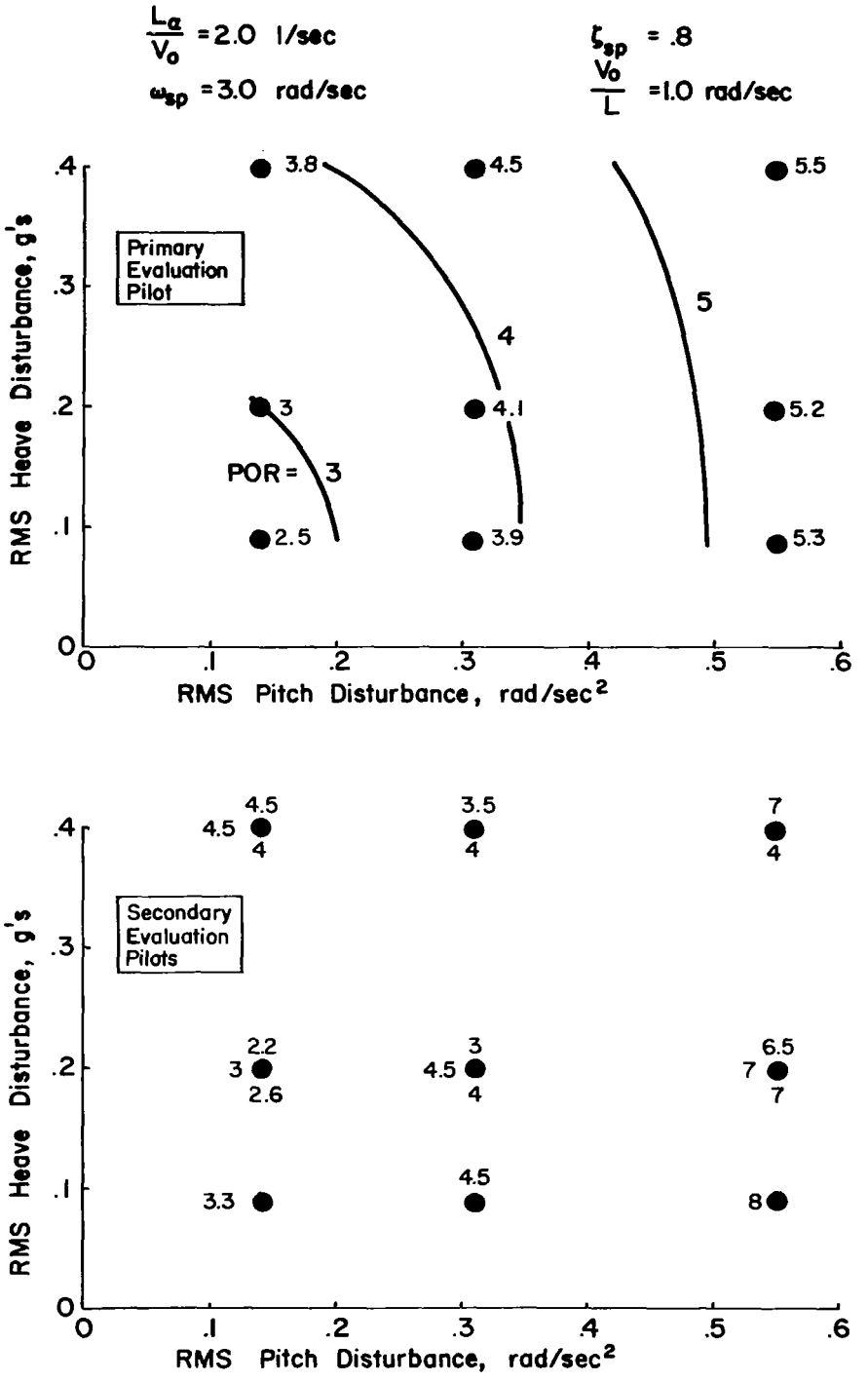

Figure 15. Effect of Rms Pitch and Heave Disturbances on Pilot Rating - Configuration 1

results to any significant extent. Composite ratings for all the pilots are shown in Figure 16. The rating trends with pitch and heave disturbances are in general agreement with Figure 15.

It should be recalled from Section 3 that the magnitude of simulated heave disturbances are limited by the restrictions on flap travel. The maximum incremental normal acceleration obtainable from the flap based on its trim setting for the approach condition is approximately one-half g. As was noted in Section 3, this restriction on the flap modifies the statistical properties of the heave disturbance from a true to a truncated Gaussian probability distribution. Furthermore the rms magnitude of the disturbance is reduced compared to the rms values corresponding to the true Gaussian probability distribution. Measured values of rms incremental normal acceleration due to the flap compared to the rms values expected for a Gaussian distribution were

True Gaussian	Truncated Gaussian
σ_Z - g's	σ_Z - g's
.09	.09
.2	.18
.4	.3

While the data is plotted for the rms heave magnitude corresponding to the true Gaussian distribution, the effect of the restricted flap deflection on the actual rms disturbance achieved in flight should be kept in mind.

Turning to the pilots' commentary and considering their remarks regarding the airplane's longitudinal dynamics for light turbulence (σ_M = .14 rad/sec^2, σ_Z = .09 or .2 g's), it is apparent that the airplane is quite easy to handle in the approach. Pitch attitude control is precise and pitch excursions and pilot workload (rms stick motion) are small. No problems were observed in flying the glide slope or in holding the trim airspeed for the approach (120 mph). The airplane is quite stable in pitch, has adequate normal acceleration response for altitude control and tracking the glide slope, and

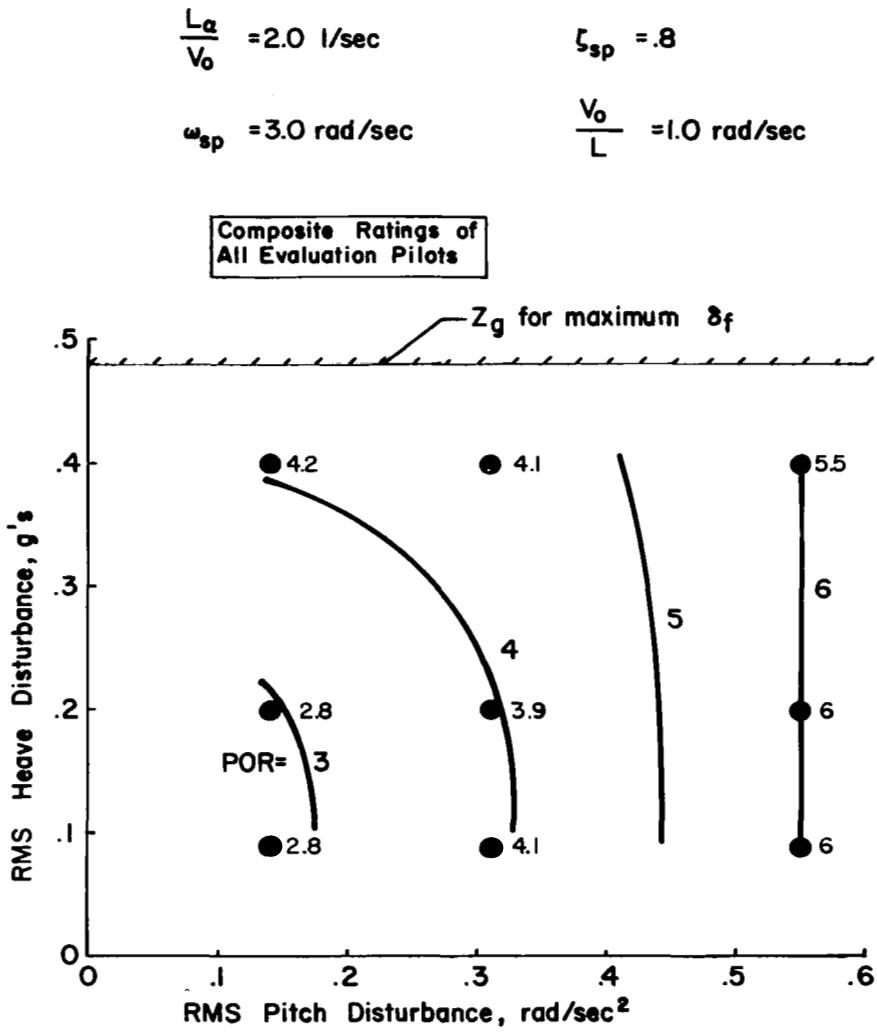

Figure 16. Composite Pilot Ratings for Variations in Pitch and Heave Disturbances - Configuration 1

has adequate speed stability associated with operation well on the front side of the throttle required curve ($1/T_{h_1} = .04$).

As pitch disturbances were increased the pilots began to complain of difficulty in achieving the precision of pitch attitude control desired for flying the glide slope. Increasing pitch excursions and control workload were the object of the pilots' complaints. In the extreme case ($\sigma_M = .55$ rad/ sec^2), large pitch excursions (on the order of ± 10 deg) detracted considerably from the pilots' ability to stay on the glide slope and to hold airspeed. Control workload in terms of rms stick force was noted to be considerable. One of the secondary pilots who gave the airplane an unacceptable rating (POR = 7) found glide slope control to be quite sensitive as he approached the 200 foot altitude for transition from IFR to VFR flight. Further out on the approach, in the vicinity of the outer marker, the glide slope sensitivity in presence of the large pitch excursions was less and his corresponding rating would have improved to a 5.5. The degradation in pitch attitude control and control workload is apparent in Figure 17. Rms values of pitch excursions, stick force, and normal acceleration are plotted in this figure for the lowest and highest levels of pitch disturbance ($\sigma_M = .14$ and $.55$ rad/ sec^2) and for two levels of heave disturbance ($\sigma_Z = .2$ and $.4$ g's). Not only do rms pitch attitude and stick force reflect the increase in pitch disturbances, but rms normal acceleration also increases due to the larger transient g loads associated with large pitching motion and a large lift curve slope configuration. A comparison of segments of the time histories of the ILS approach for the two levels of pitch disturbance are shown in Figures 18 and 19. The pilot's elevator control inputs, pitch attitude excursions, glide slope deviation, and indicated airspeed are shown for a one minute period extending to the end of the IFR segment. It is apparent that the pilot is having considerably more difficulty holding airspeed and a somewhat more difficult time staying on the glide slope for the approach of Figure 19 ($\sigma_M = .55$ rad/ sec^2) when compared to the approach of Figure 18 ($\sigma_M = .14$ rad/ sec^2).

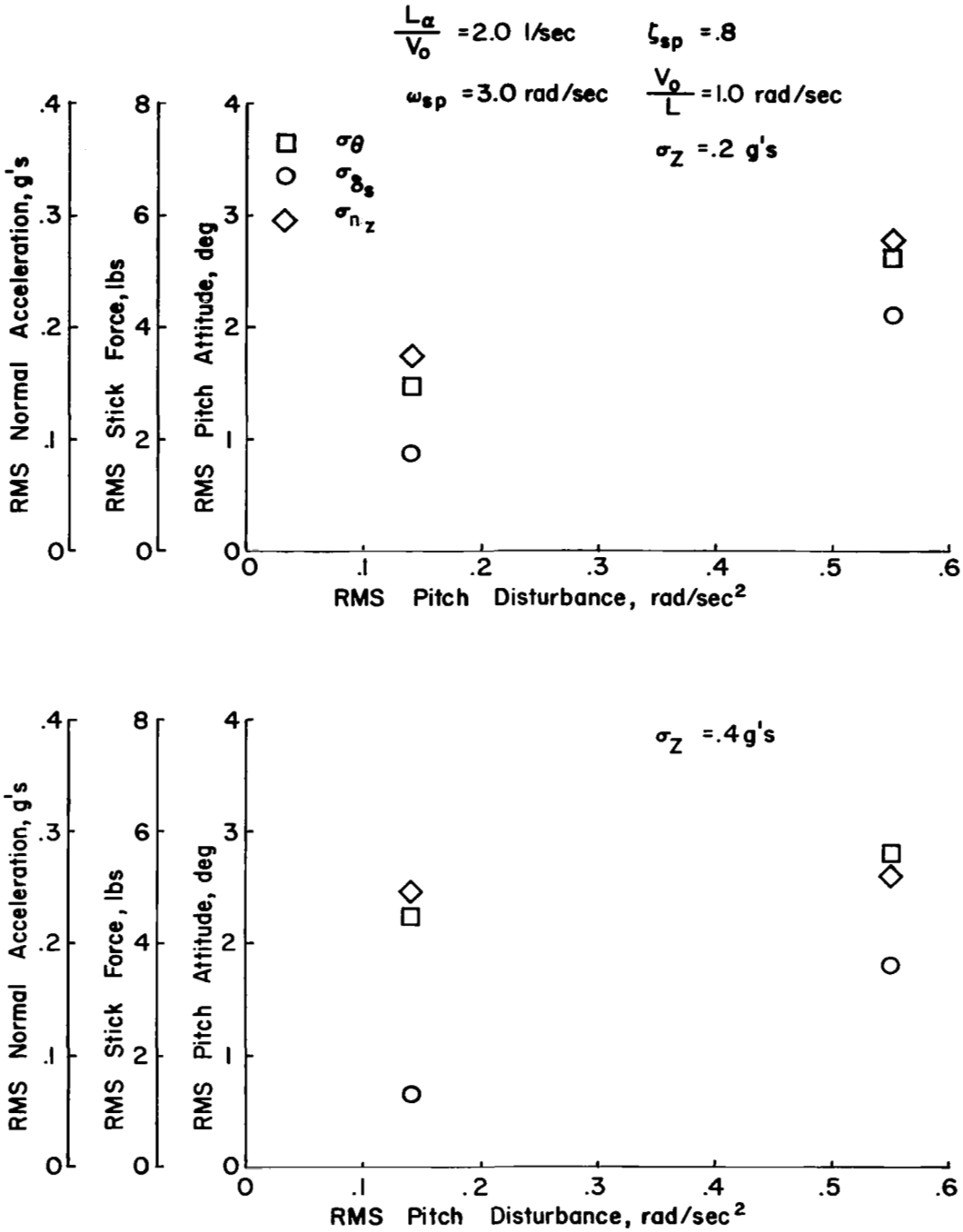

Figure 17. Trends of Task Performance and Control Workload with Pitch Disturbances - Configuration 1

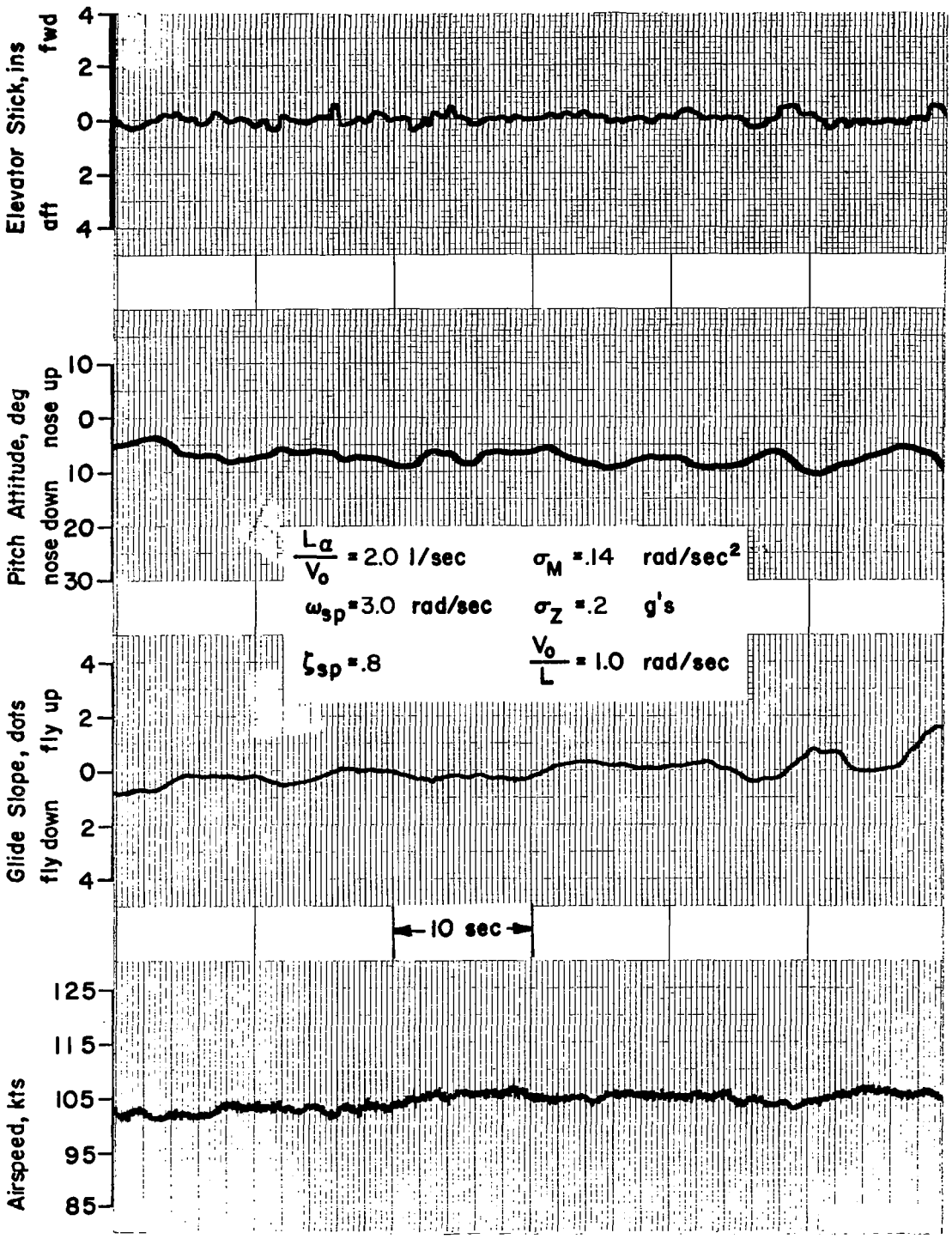

Figure 18. Time History of Longitudinal Control During the ILS Approach - Configuration 1/2

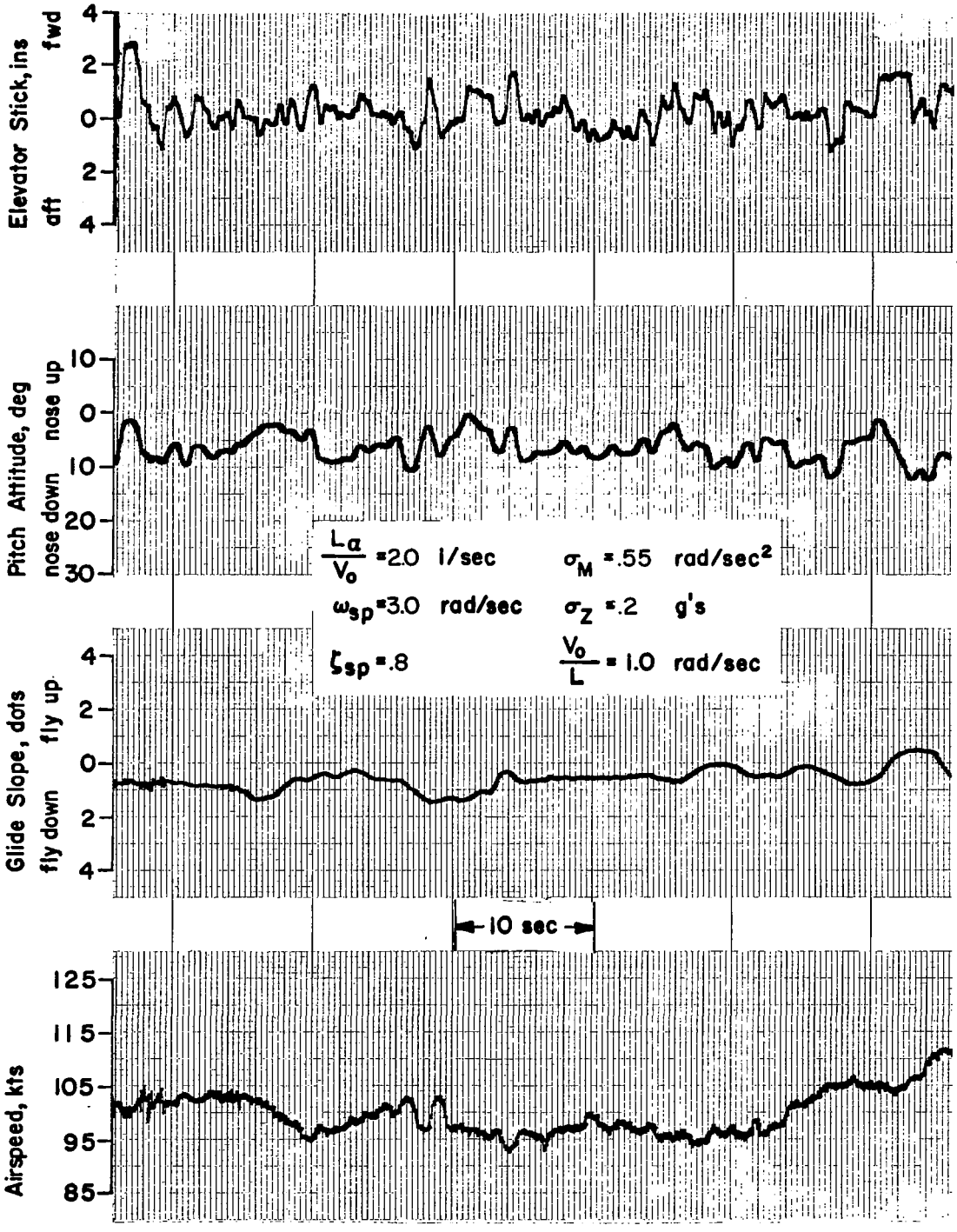

Figure 19. Time History of Longitudinal Control During the ILS Approach - Configuration 1/4

When heave disturbances were increased to the maximum value tested in the flight program (σ_Z = .4 g's for the Gaussian distribution, σ_Z = .3 g's measured in flight where $\Delta Z_{max} \doteq$ .5 g's), the pilots' objections related to the increase in discomfort and distraction associated with the increased level of normal acceleration. No appreciable degradation in pitch control precision, pilot workload, airspeed control, or glide slope tracking was noted for the highest level of heave disturbance. The performance-workload data of Figure 20, shown as a function of heave disturbance magnitude, support the pilots' commentary. Both the pilot ratings of Figure 15 and the performance-workload data of Figure 20 further indicate the dominant influence of pitch disturbances over heave when the pitch upsets are large. No degradation in pilot rating or in pitch attitude precision or control workload are observed when σ_Z is increased from .2 to .4 g's at σ_M = .55 rad/ sec^2. A segment of the time history of the approach for the largest heave disturbance is shown in Figure 21. Glide slope tracking and airspeed control are only slightly less precise than for the approach of Figure 18 for light pitch and heave disturbances.

Contributions of turbulence - Spectral bandwidth

The effects of bandwidth of the turbulence spectrum on pilot rating, in combination with variations in turbulence magnitude, may be noted in the data of Figure 22. The data are presented for the case of good longitudinal dynamics (Configuration 1) in terms of the rms vertical gust velocity (or the equivalent rms angle of attack for a trim speed, V_o = 176 ft/ sec) and the spectral corner frequency, V_o / L. The magnitude of rms pitch and heave disturbances are given in the upper right hand corner for the σ_{α_g} = 1.12 degree condition and corresponding to the aerodynamic stability derivatives associated with the dynamic configuration simulated. Variations in the rms gust velocity produce proportional variations in rms heave and pitch disturbances.

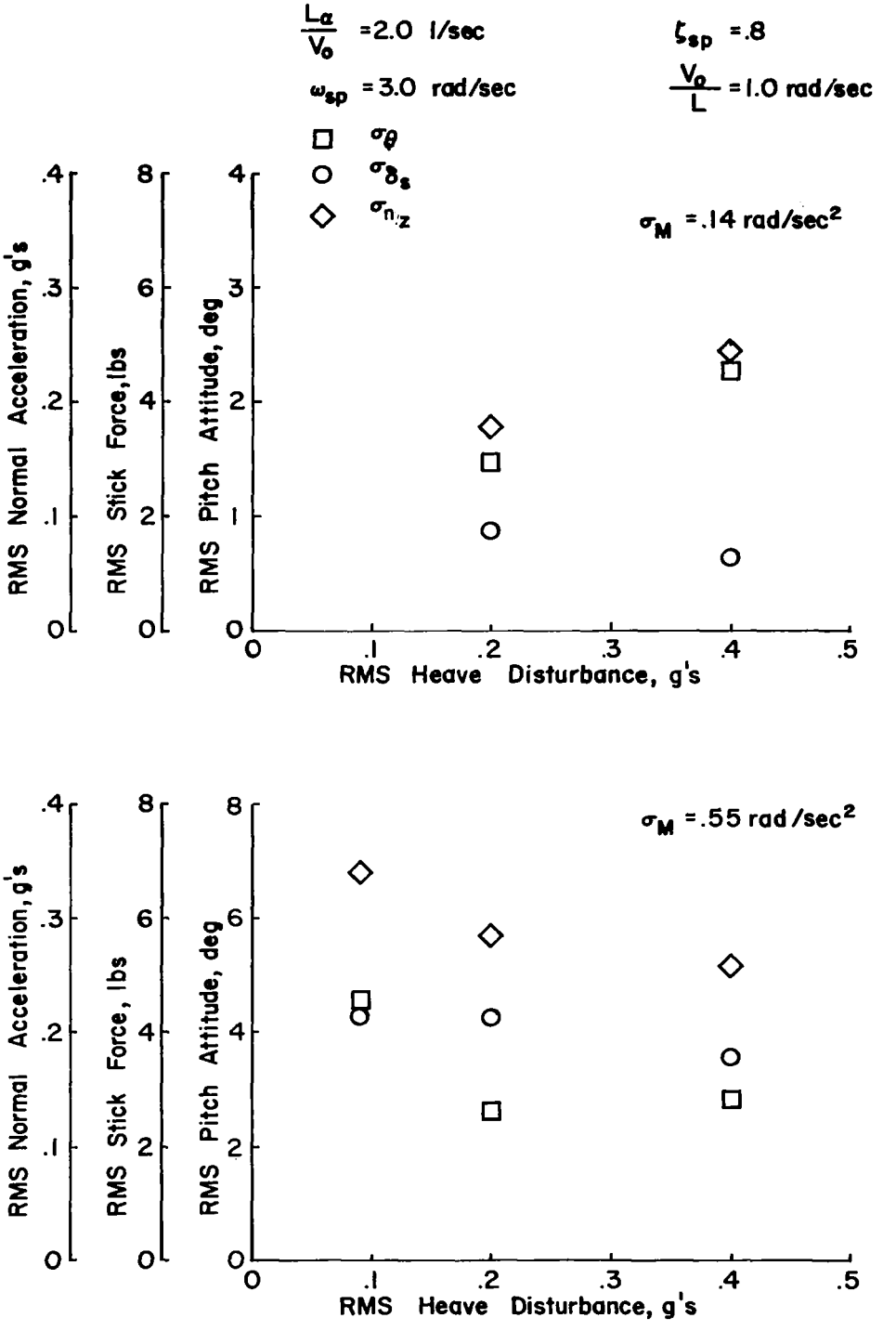

Figure 20. Trends of Task Performance and Control Workload with Heave Disturbances - Configuration 1

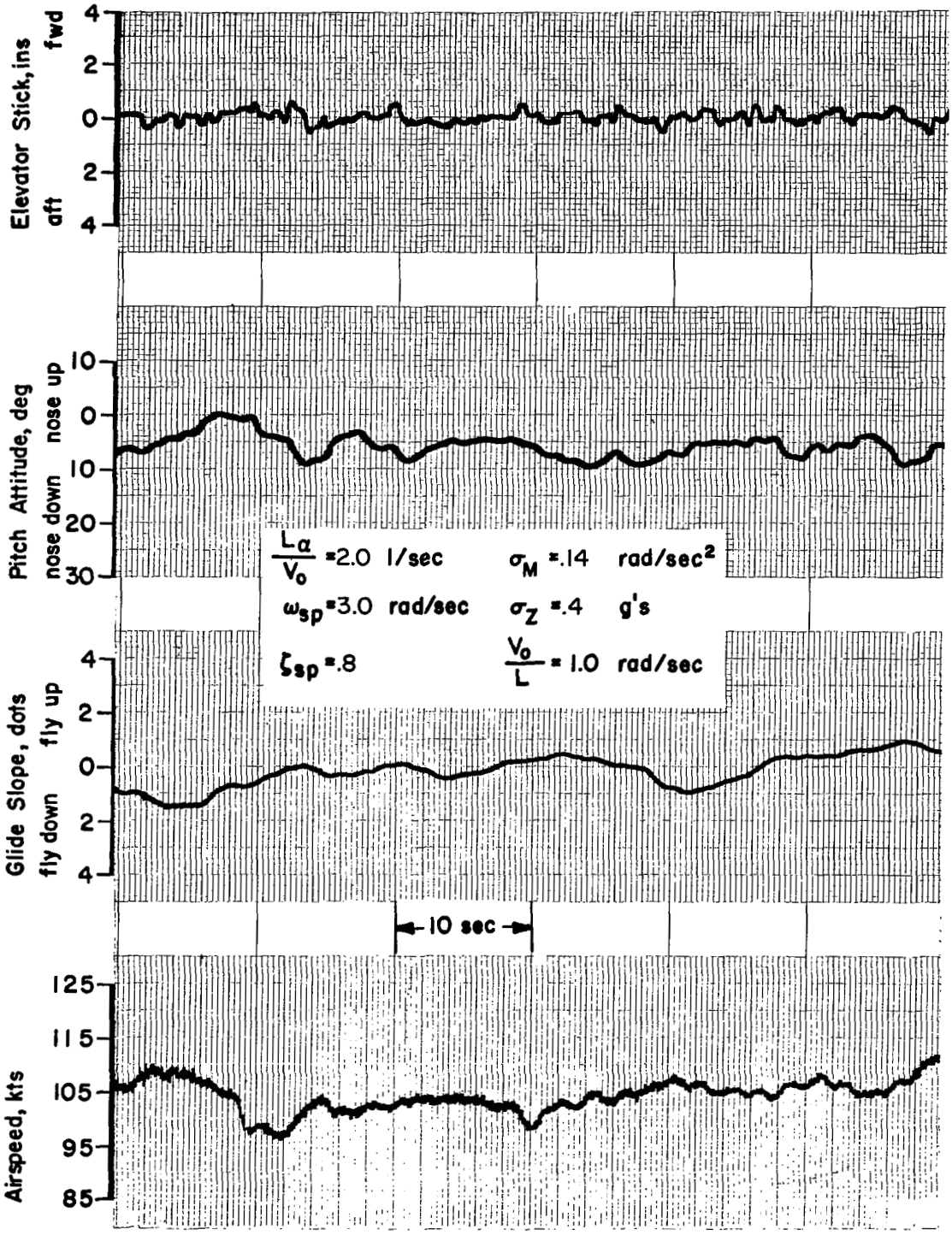

Figure 21. Time History of Longitudinal Control During the ILS Approach - Configuration 1/8

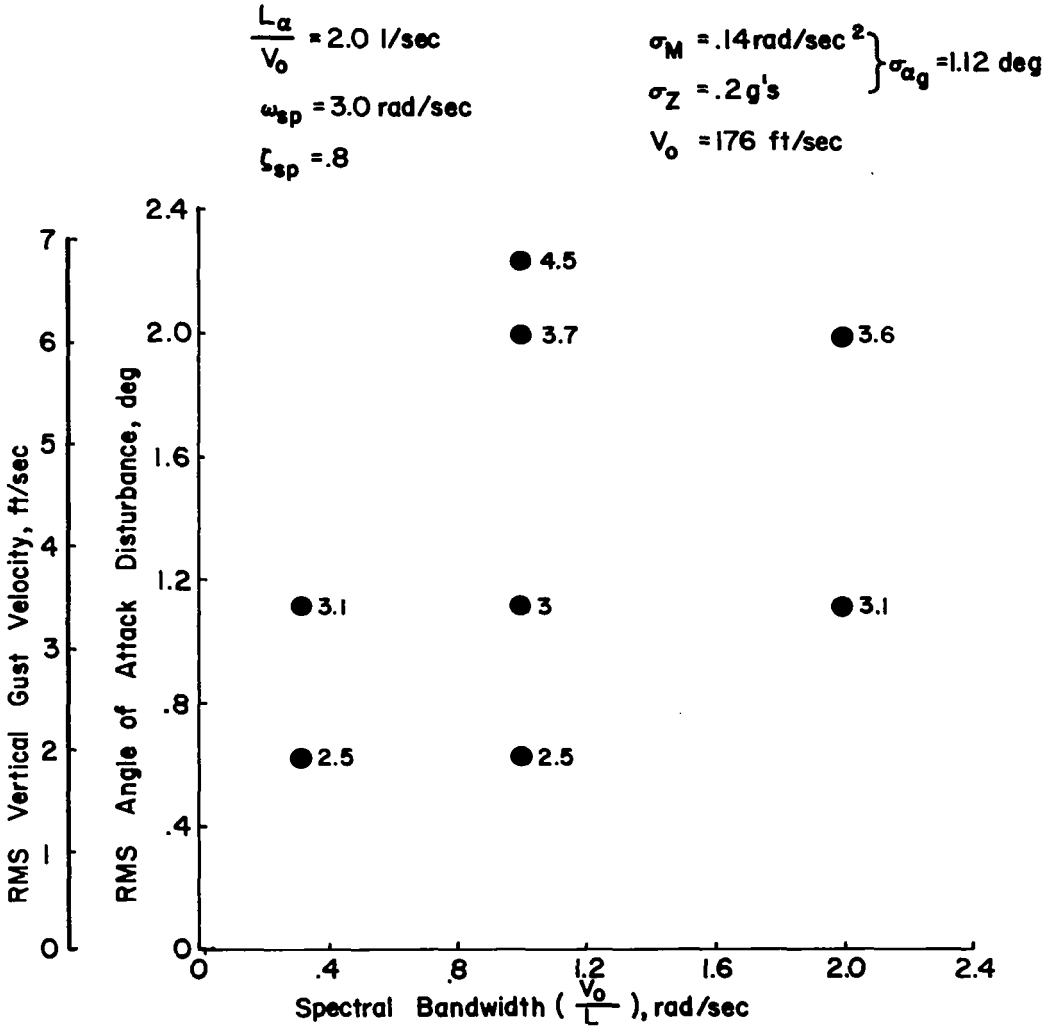

Figure 22. Influence of Spectral Bandwidth on Pilot Ratings - Configuration 1

Hardly any influence of turbulence bandwidth is apparent in the data of Figure 22. While a modest degradation in pilot rating occurs with the increase in magnitude of turbulence, there is essentially no change in rating for variations in bandwidth corresponding to $V_o / L = .314$ to 2.0 radians/second. If the combined effects of turbulence magnitude and bandwidth are considered for the heave and pitch axes separately, as shown in Figure 23, essentially the same results are noted. A slight degradation in pilot rating with increasing bandwidth seems to exist at the higher levels of pitch disturbance. However, the dominant influence of turbulence is still the disturbance mangitude. The pilots, according to their commentary, could discern changes in the frequency content of the turbulence. However, only for the turbulence with the highest bandwidth ($V_o / L = 2.0$ rad/sec) did the pilots indicate that frequency content of the disturbances had any direct influence on their evaluation. For $V_o / L = 2.0$ radians/second the pilots complained about high frequency pitch attitude excursions. When the pitch disturbance magnitude was sufficient to make these high frequency motions objectionable for glide slope tracking, the pilot ratings deteriorated somewhat. Typically, the pilots were unable to control the high frequency pitch excursions or did not choose to do so. They felt the effort required to track these motions would not yield a significant improvement in performance, and occasionally they remarked that the pitch control situation was aggravated if they attempted to attenuate the higher frequencies. Finally, it should be noted that high frequency attenuation of either the pitch or heave disturbances associated with the second corner frequency, ω_{w_2}, were only barely perceptible to the pilots due to the low energy level of the turbulence in this region of the spectrum. No change in pilot rating was noted for variations in ω_{w_2} from 10 to 18 radians/second.

Measures of precision of pitch attitude control and pilot workload for variations in spectral bandwidth confirm the pilot rating data just discussed. As may be noted in Figure 24, there are no significant variations in either rms pitch attitude, stick force, or normal acceleration over the range of bandwidths tested. The data are shown for a low and high level of pitch disturbance magnitude.

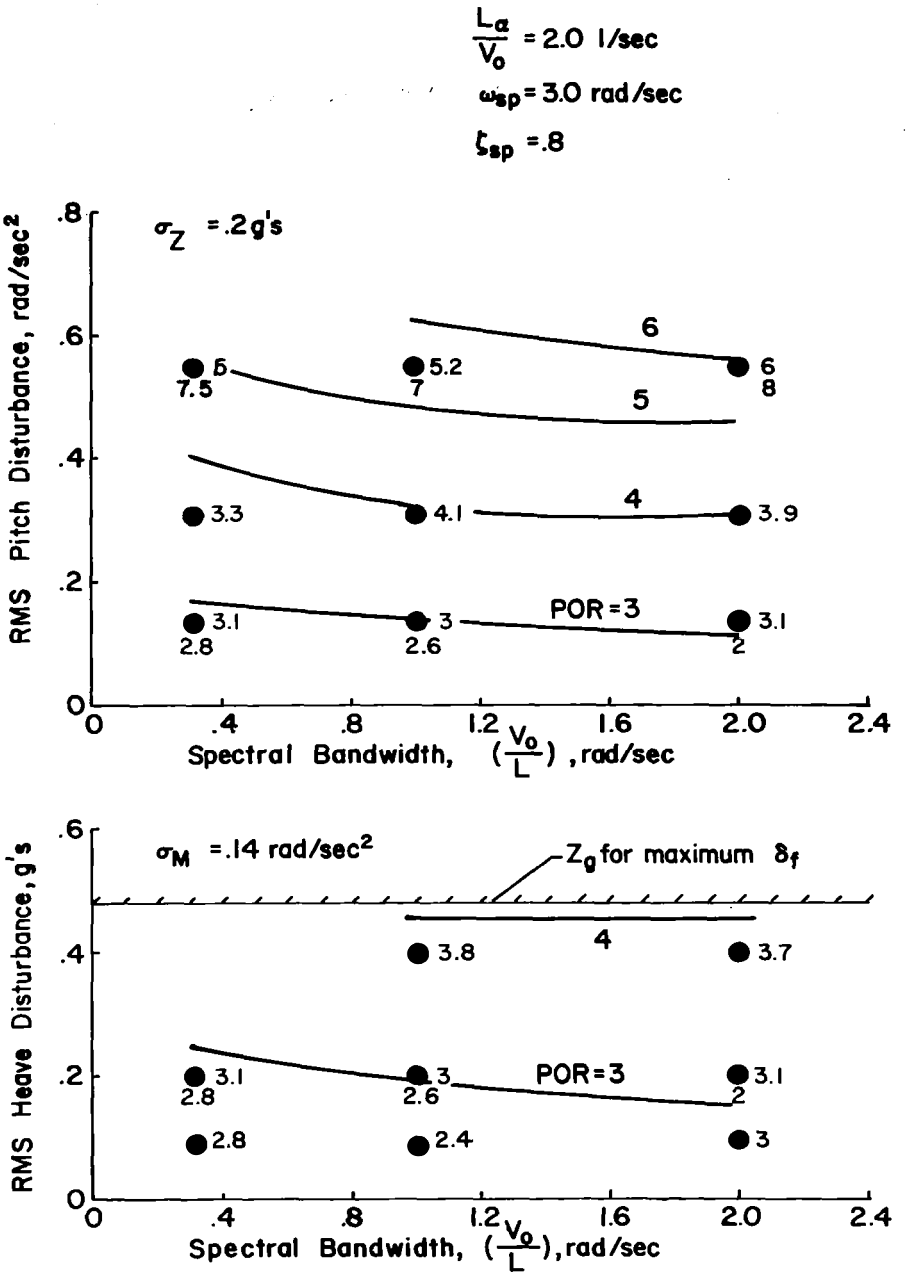

Figure 23. Combined Effects of Spectral Bandwidth, Pitch and Heave Disturbances on Pilot Rating - Configuration 1

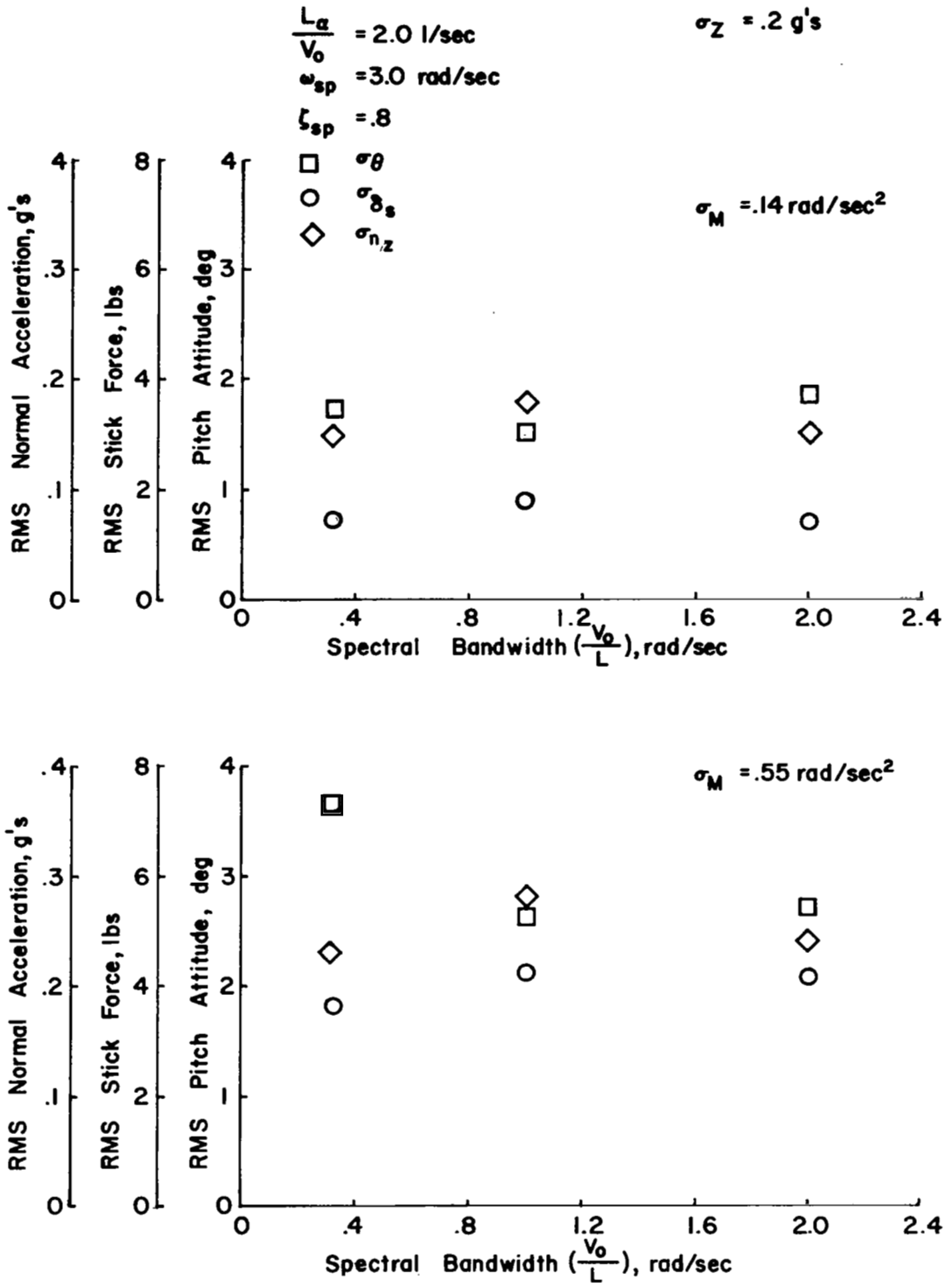

Figure 24. Trends of Task Performance and Control Workload with Spectral Bandwidth - Configuration 1

Contributions of turbulence - Pitch-heave correlation

The results of a limited evaluation of the effect of correlation between pitch and heave disturbances on pilot ratings are shown in Figure 25. Correlation between these disturbances was considered in this program because it can be shown theoretically to have some contribution to the magnitude of the airplane's response to turbulence, and because it was felt that the cues available to the pilot from his sensing of the disturbances might be favorably (or unfavorably) affected by this correlation. It appears from the data of Figure 25 that pitch-heave correlation is an innocuous influence so far as the pilot was concerned. Trends of pilot rating with the correlation coefficient are insignificant when compared to the variation in rating with pitch disturbance magnitude. Variations in the wing-tail separation for a range of the normalized tail length of $\ell_t / L = .03$ to $.2$ also had essentially no effect on pilot rating. Although the data are not included in Figure 25, the pilot rating over this range of tail lengths differed by less than one-half rating unit.

Contributions of short period frequency

To begin the consideration of the effects of longitudinal dynamics and turbulence on flying qualities, the combined effects of the longitudinal short period natural frequency with rms pitch disturbance and heave disturbance magnitudes are shown in Figure 26. These data are presented for constant values of slope of the lift curve, real damping of the short period mode, and spectral bandwidth ($L_\alpha / V_o = 2.0$ 1/ sec, $\zeta_{sp}\, \omega_{sp} = 2.4$ rad/ sec, $V_o / L =$ 1.0 rad/ sec). Average ratings from the primary evaluation pilot are shown to the right of each test point and contours of constant rating units are faired to these data. Ratings from one of the other pilots are also included.

Considering the trends of pilot rating in the upper diagram (for constant rms heave disturbances) it is apparent that independently increasing the level of pitch disturbances or reducing the short period frequency (angle of attack stability) is detrimental to the ILS task. The adverse influence of

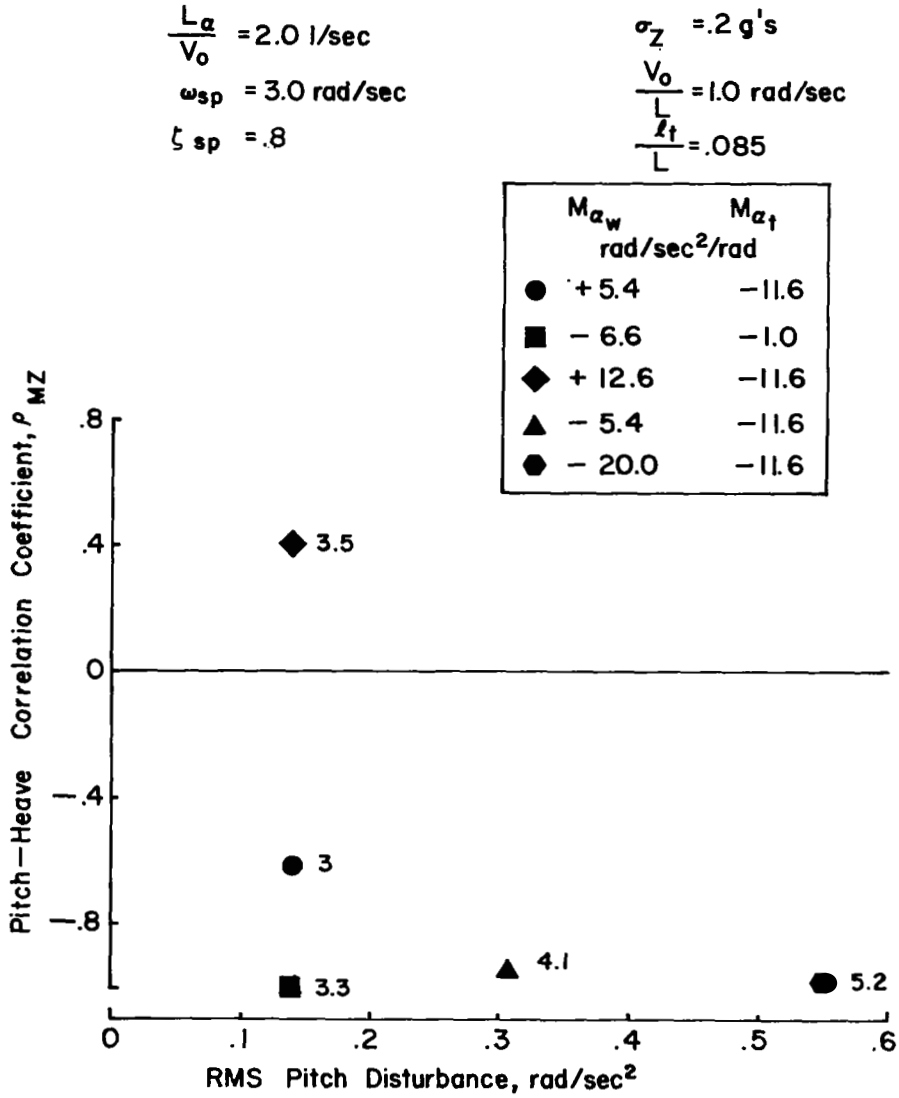

Figure 25. Effect of Pitch-Heave Correlation on Pilot Rating - Configuration 1

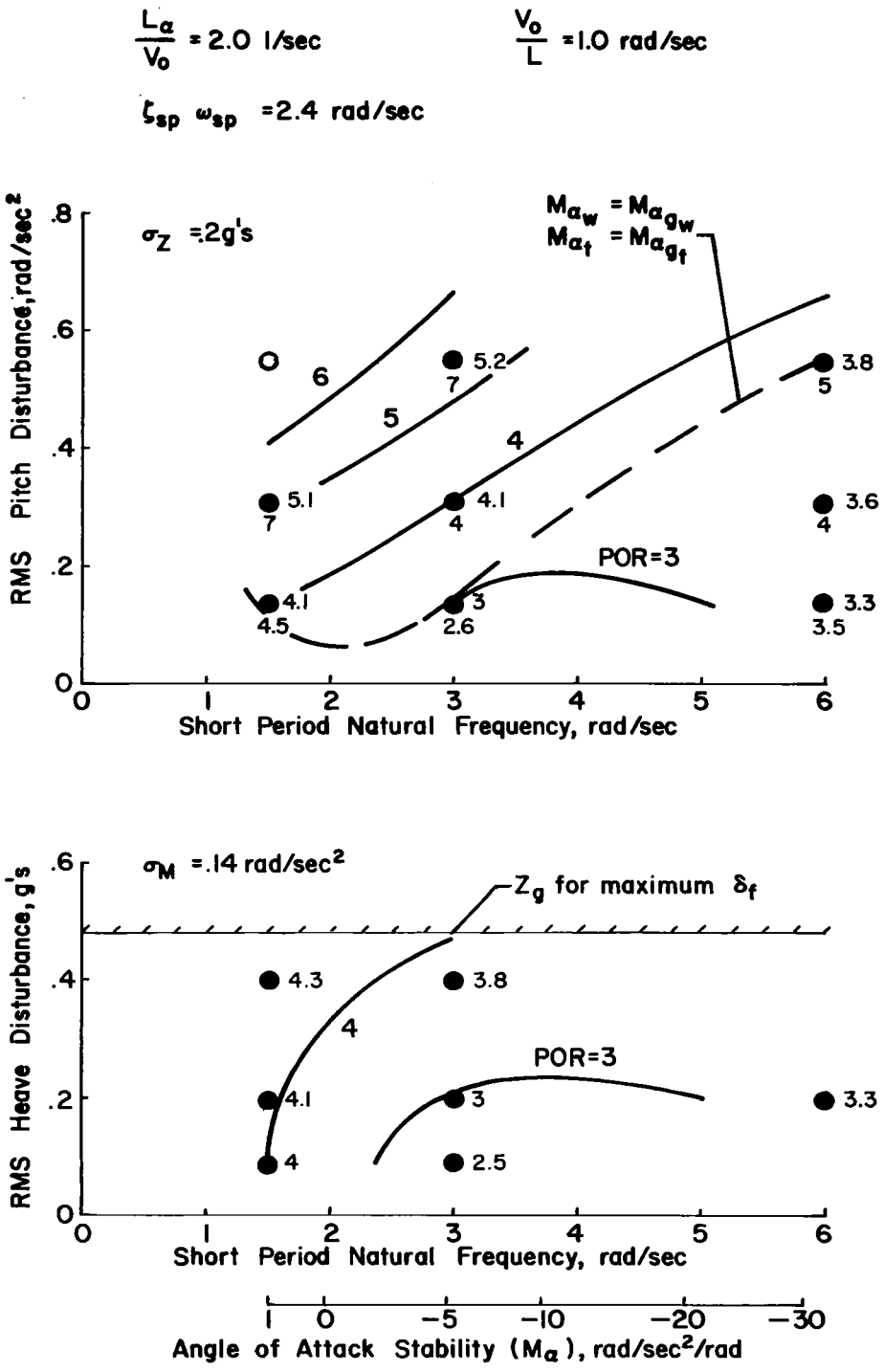

Figure 26. Effects of Short Period Frequency and Pitch and Heave Disturbances on Pilot Rating

independently increasing the pitch turbulence level had been demonstrated in Figure 15 for a satisfactory level of short period frequency. It is further apparent from Figure 26 that pilot rating becomes increasingly sensitive to pitch turbulence as the short period frequency is reduced. By the same token, changes in short period frequency have the greatest influence on pilot rating at the highest pitch disturbance level tested. In fact, when pitch disturbances are small, short period frequency has very little effect on pilot rating until the angle of attack stability boundary is approached. Perhaps the trends of this figure may best be summarized by saying that the pilot likes more static longitudinal stability when pitch disturbances are large.

It should be re-emphasized that the data points of the upper diagram of Figure 26 represent independent variations of short period frequency and pitch disturbance magnitude. While short period frequency and the magnitude of pitch disturbances can normally be interrelated through the aerodynamic pitching moment derivatives M_α and $M_{\dot\theta}$ (or M_{α_w} and M_{α_t}), i.e.

$$\omega_{sp}^2 \doteq -\left(M_\alpha + \frac{L_\alpha}{V_o} M_{\dot\theta}\right)$$

$$\sigma_M^2 = \left[M_{\alpha_{g_w}}^2 + M_{\alpha_{g_t}}^2 + 2\, M_{\alpha_{g_w}} M_{\alpha_{g_t}} e^{-\sqrt{3}\frac{\ell_t}{L}}\right] \frac{\sqrt{3}}{2} \left(\frac{\sigma_w}{V_o}\right)^2$$

$$M_\alpha,\ M_{\dot\theta} = f(M_{\alpha_w},\ M_{\alpha_t},\ \ell_t)$$

this interrelationship did not in general hold for the test configurations in Figure 26. To evaluate the combined effects of pitch dynamics and turbulence (ω_{sp} and σ_M in this case), configurations for which the interrelationship between ω_{sp} and σ_M hold are indicated by the dashed line. For the range of configurations shown, the dashed line shows a deterioration in pilot ratings for frequencies above or below $\omega_{sp} \doteq 2.0$ to 3.0 radians/second. At

the higher frequencies, increases in the level of pitch disturbances which accompany increases in static stability (or ω_{sp}) apparently override any improvement in pitch attitude control afforded by the greater stiffness in pitch. Pilot ratings degrade as a result. At the lower frequencies, approaching the case where $M_{\alpha} = 0$, pitch attitude, glide slope, and airspeed control problems begin to override any favorable influence of reducing pitch turbulence. Pilot ratings again degrade, but for reasons opposite to those which explained the poor ratings at high frequency.

Turning to the lower diagram, the modest influence of heave turbulence on pilot rating is again noted (for a low level of pitch disturbance). As the short period frequency is reduced and the airplane approaches neutral angle of attack stability, pitch attitude control characteristics associated with ω_{sp} begin to dominate the rating trends and heave turbulence accordingly has less influence.

Pilot commentary emphasizes difficulties in achieving precise pitch attitude control for the lowest short period frequency. It was necessary to pay close attention to pitch attitude and to airspeed in order to fly the glide slope acceptably. The pilots were aware of the slight static instability of the low frequency configuration and they complained of the tendency of pitch attitude and airspeed to get away from them if their attention was distracted to some other aspect of the task (such as lateral-directional control, power management, communications, etc.). Higher control workloads were apparent. Increases in pitch disturbances similar to those imposed on the higher frequency configurations brought more vociferous complaints about the size of pitch excursions and the effort required to control them. An inadvertent test run was made for the low frequency configuration with extremely large pitch disturbances ($\sigma_M = .55$ rad/sec^2, $\omega_{sp} = 1.5$ rad/sec). Although no numerical rating is shown for this configuration in Figure 26, the one unfortunate pilot who flew it rated it in the 9-10 category, emphasizing the likelihood that control could easily be lost since adequate pitch control power was not always available in the presence of such large disturbances. Turning to the highest frequency configuration, pilot commentary was

generally favorable with the exception of complaints about the high frequency pitch bobble excited by turbulence or by continuous control activity by the pilot. Sooner or later, the pilots would tire of tracking these high frequency motions, typically commenting that their effort was producing no commensuate improvement in pitch performance. In general, the bobble was considered an annoying and sometimes distracting characteristic of the configuration, but one which did not seriously affect the ILS task. Airspeed control and glide slope tracking were good. Increasing the level of pitch disturbances had much less influence than for the lower frequency configurations.

The combined influences of spectral bandwidth and short period frequency are shown in Figure 27 for constant lift curve slope, real damping, and heave turbulence (L_α / V_o = 2.0 1/ sec, $\zeta_{sp}\omega_{sp}$ = 2.4 rad/ sec, σ_Z = .2 g's), and for two levels of pitch turbulence. When pitch disturbances are low, as shown in the upper diagram, turbulence bandwidth has no apparent influence on pilot rating. At the higher pitch disturbance levels a slight degradation in rating with increasing bandwidth is noticeable for the lowest short period frequency shown (ω_{sp} = 3.0 rad/ sec). Pilot commentary reveals no direct influence of frequency content on pilot rating, with the exception that the high frequency disturbances were an annoyance which the pilots felt unable or unwilling to suppress.

Performance-workload measures for this series of configurations are presented in Figures 28 and 29. Rms pitch attitude excursions, stick force, and normal acceleration data in relation to short period frequency are shown in Figure 28 for otherwise constant longitudinal dynamics and turbulence characteristics. The apparent explanation of pilot rating degradation at the lowest frequency is the increase in control workload (rms stick force). Pitch attitude precision and incremental normal acceleration are essentially constant over the range of frequencies tested. It may well be that the rms stick force does not entirely reflect the pilots' workload for these low frequency configurations. The necessity to pay close attention to pitch attitude and airspeed control may represent an additional demand on the pilot which also

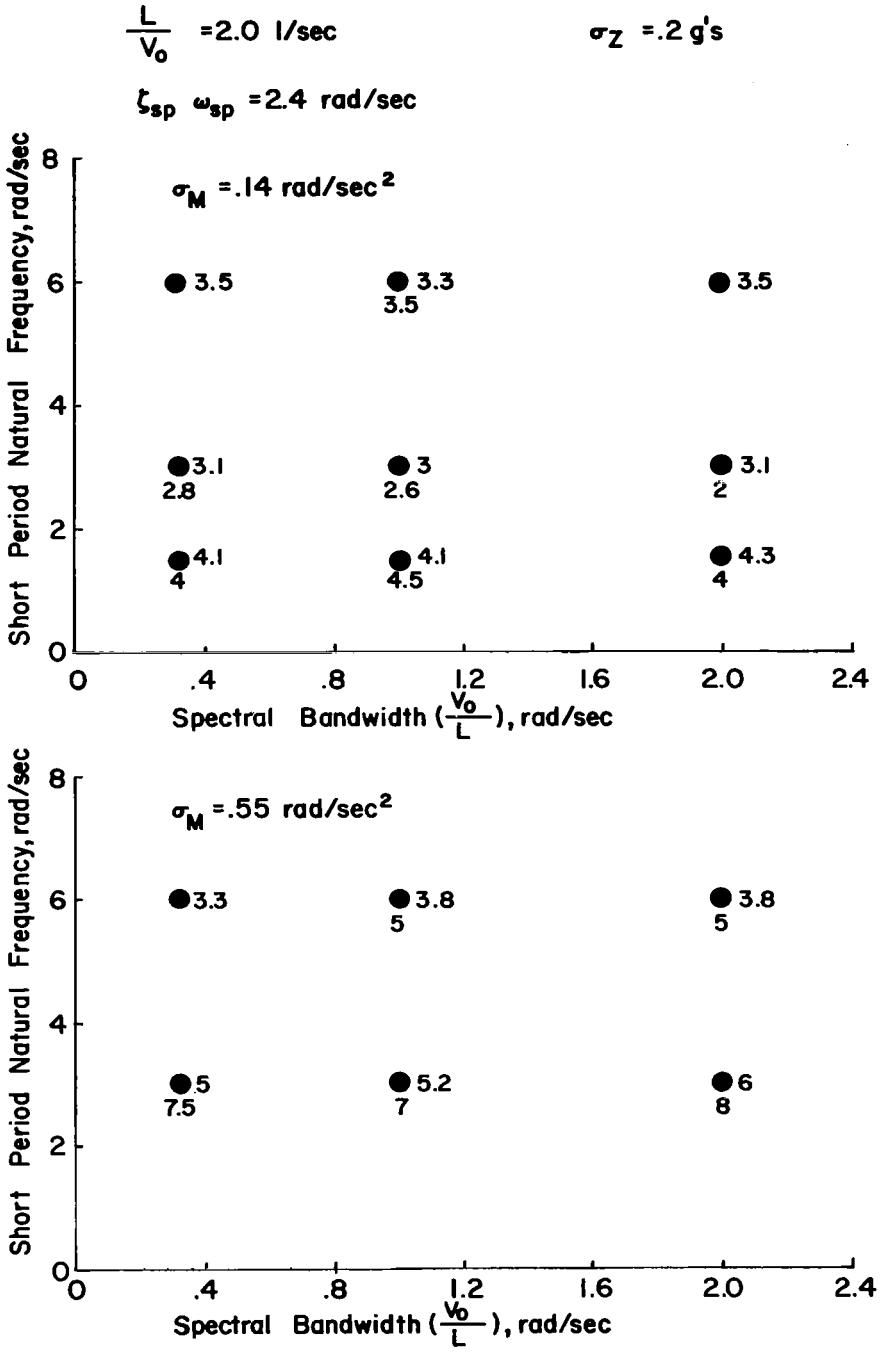

Figure 27. Combined Effects of Short Period Frequency and Spectral Bandwidth on Pilot Rating

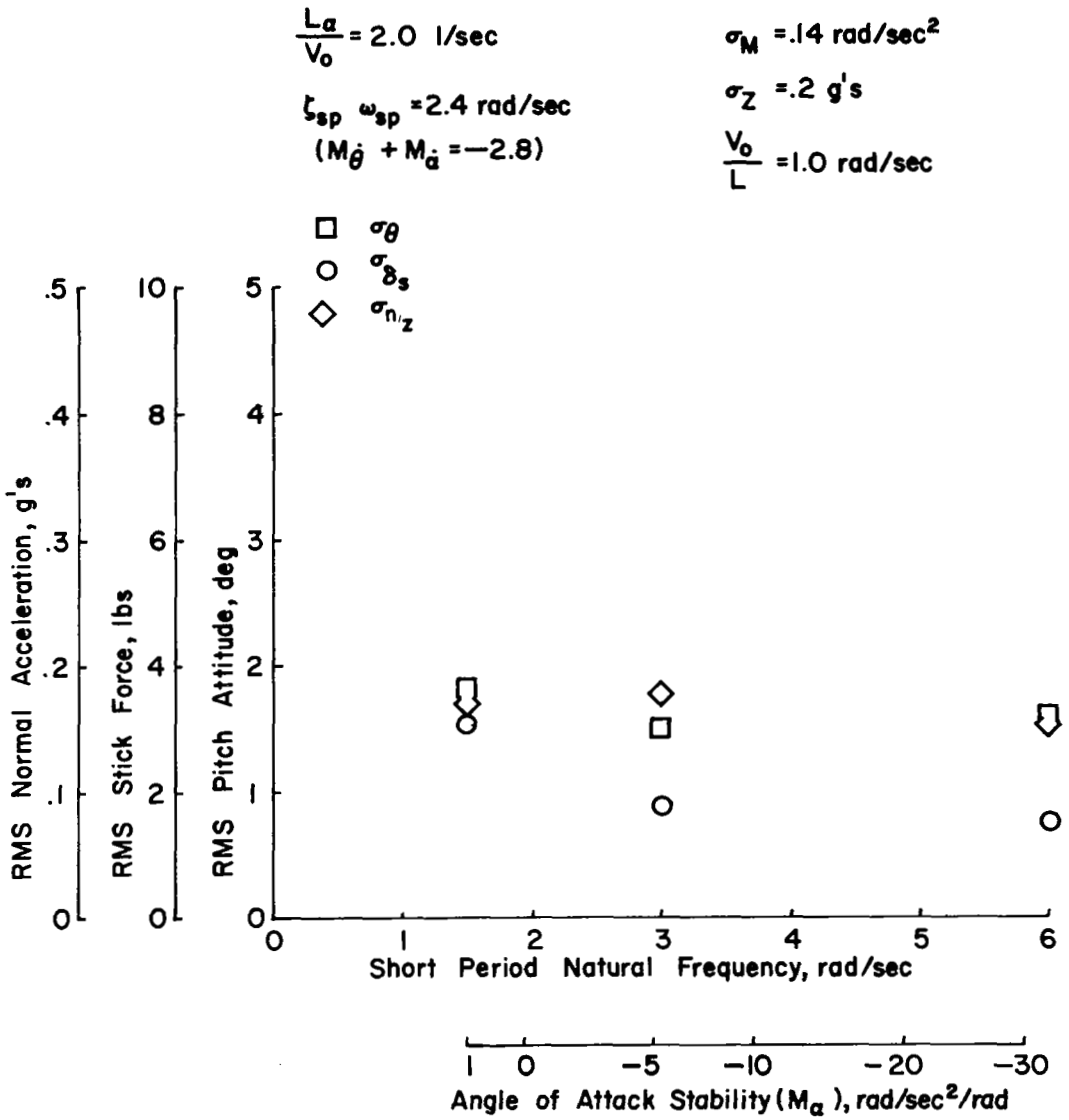

Figure 28. Trends of Task Performance and Control Workload with Short Period Frequency

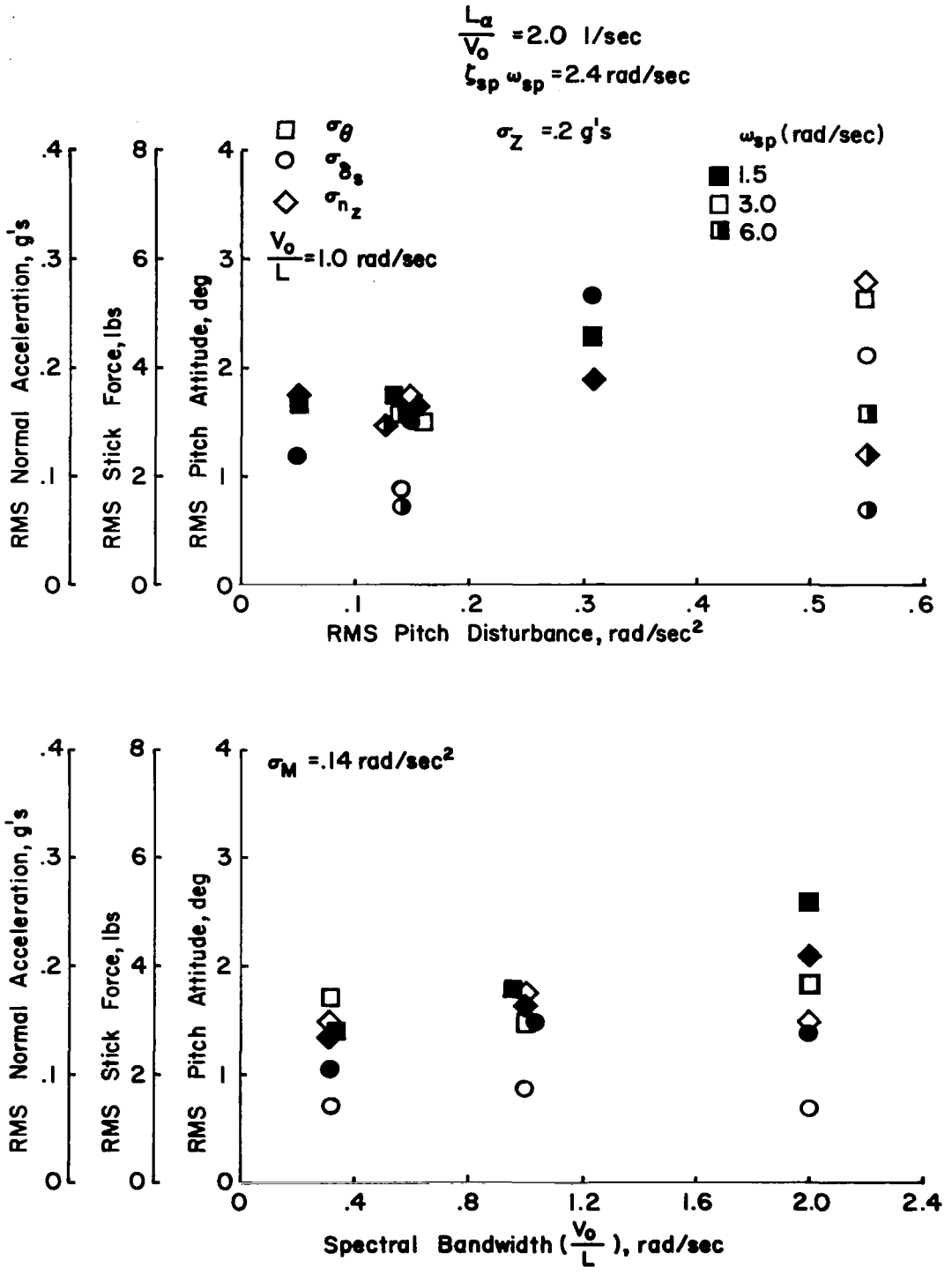

Figure 29. Combined Effects of Short Period Frequency, Pitch Disturbances and Spectral Bandwidth on Task Performance and Control Workload

accounts in part for the degraded ratings. The combined effects of short period frequency and pitch disturbance magnitude on performance-workload are indicated in the upper diagram of Figure 29 for constant heave disturbance and turbulence bandwidth. The variation of control workload with pitch disturbance magnitude increases to a considerable extent as short period frequency is reduced. Pitch attitude excursions and normal acceleration show trends similar to those of control activity. The control activity data in particular substantiate the pilot commentary and pilot rating trends of Figure 26. No significant trends in performance-workload data with spectral bandwidth are noted in the lower diagram of Figure 29. Although the pitch attitude excursions and to a lesser extent the normal acceleration excursions tend to increase with increasing bandwidth for the low short period frequency configuration, this behavior was not noted in pilot commentary and it apparently did not affect the ratings.

Finally, to complete the discussion of short period frequency, time histories of the ILS approach for the lowest and highest frequencies tested are shown in Figures 30 and 31. The turbulence disturbance magnitudes for these two configurations are defined by a constant rms gust field (σ_{α_g} = 1.12 degrees) and by the pitch and heave aerodynamic stability derivatives for the individual configurations. This means that the level of pitch disturbances for the high frequency configuration is larger than that for the low frequency case. The difficulty with pitch attitude, airspeed, and glide slope control previously mentioned for the low frequency configuration is apparent in Figure 30. Conversely, airspeed and glide slope are more precisely controlled for the high frequency configuration of Figure 31. The high frequency pitch response of this configuration which was annoying to the pilots is apparent. Note the relative absence of high frequency stick excursions in response to these pitch excursions.

Contributions of short period damping

The effect of variations in short period damping, either in terms of damping ratio, ζ_{sp}, or real damping, $\zeta_{sp}\omega_{sp}$, are presented in Figure 32. Lift curve slope, heave disturbance magnitude, and spectral bandwidth are

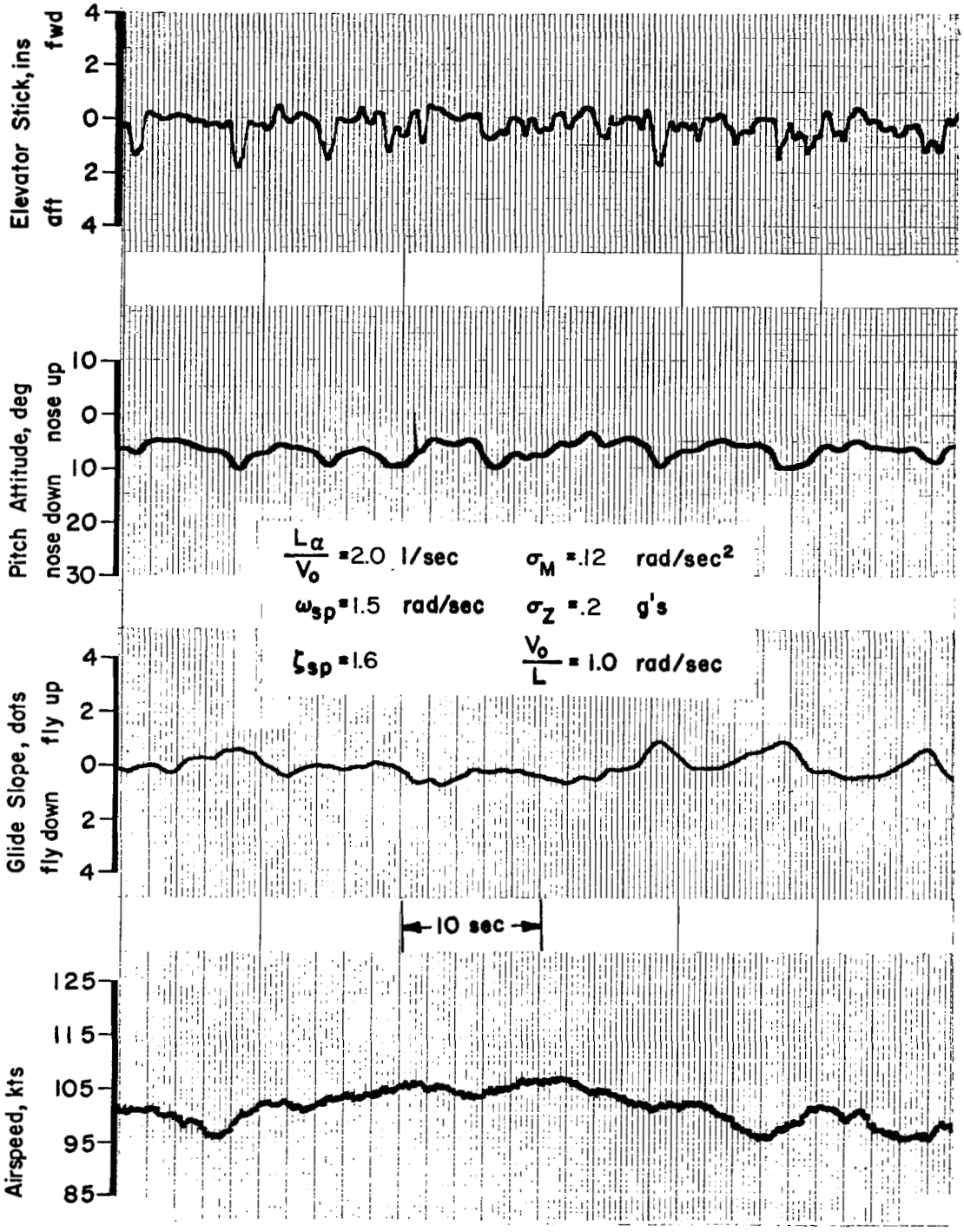

Figure 30. Time History of Longitudinal Control During the ILS Approach - Configuration 2/1

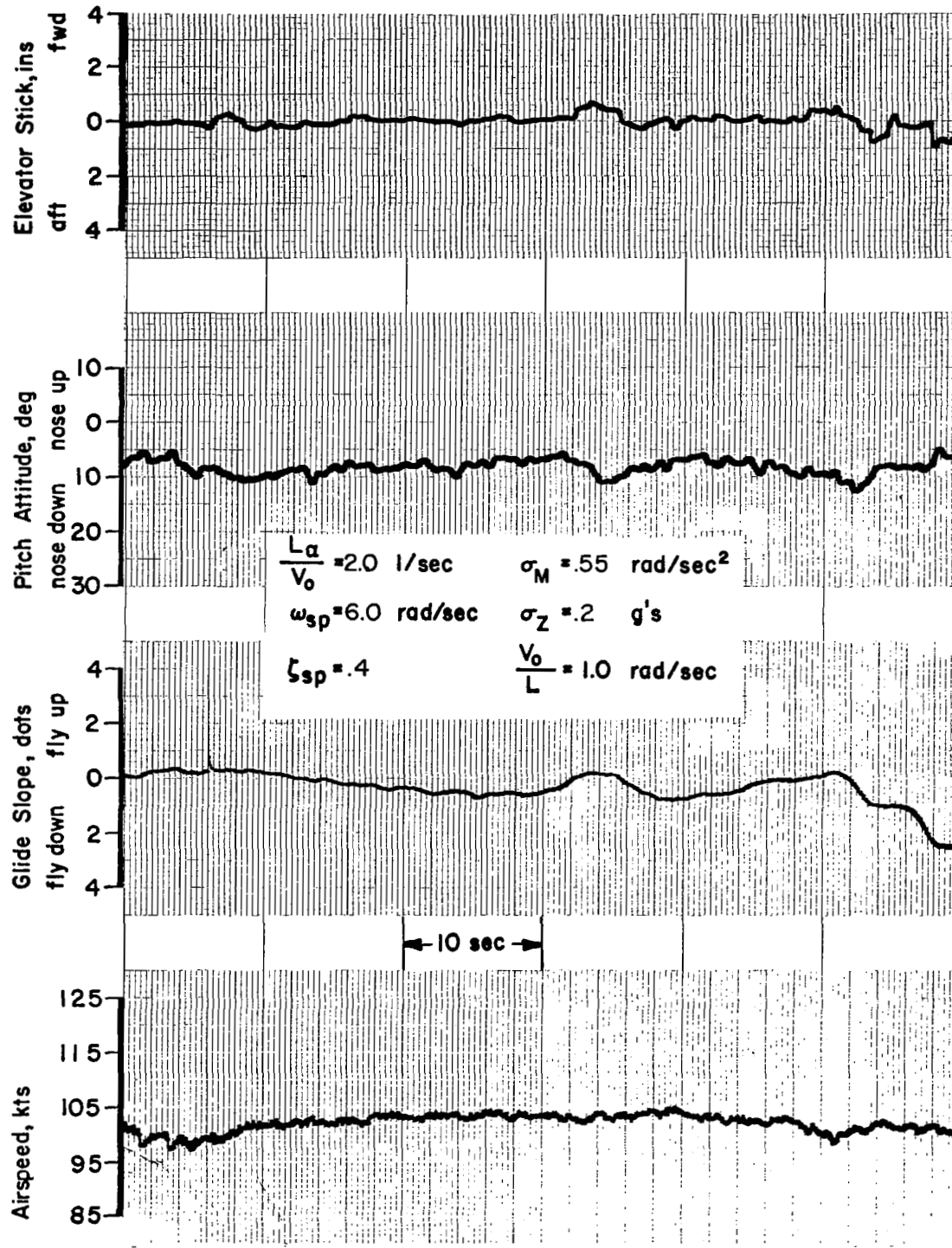

Figure 31. Time History of Longitudinal Control During the ILS Approach - Configuration 3/4

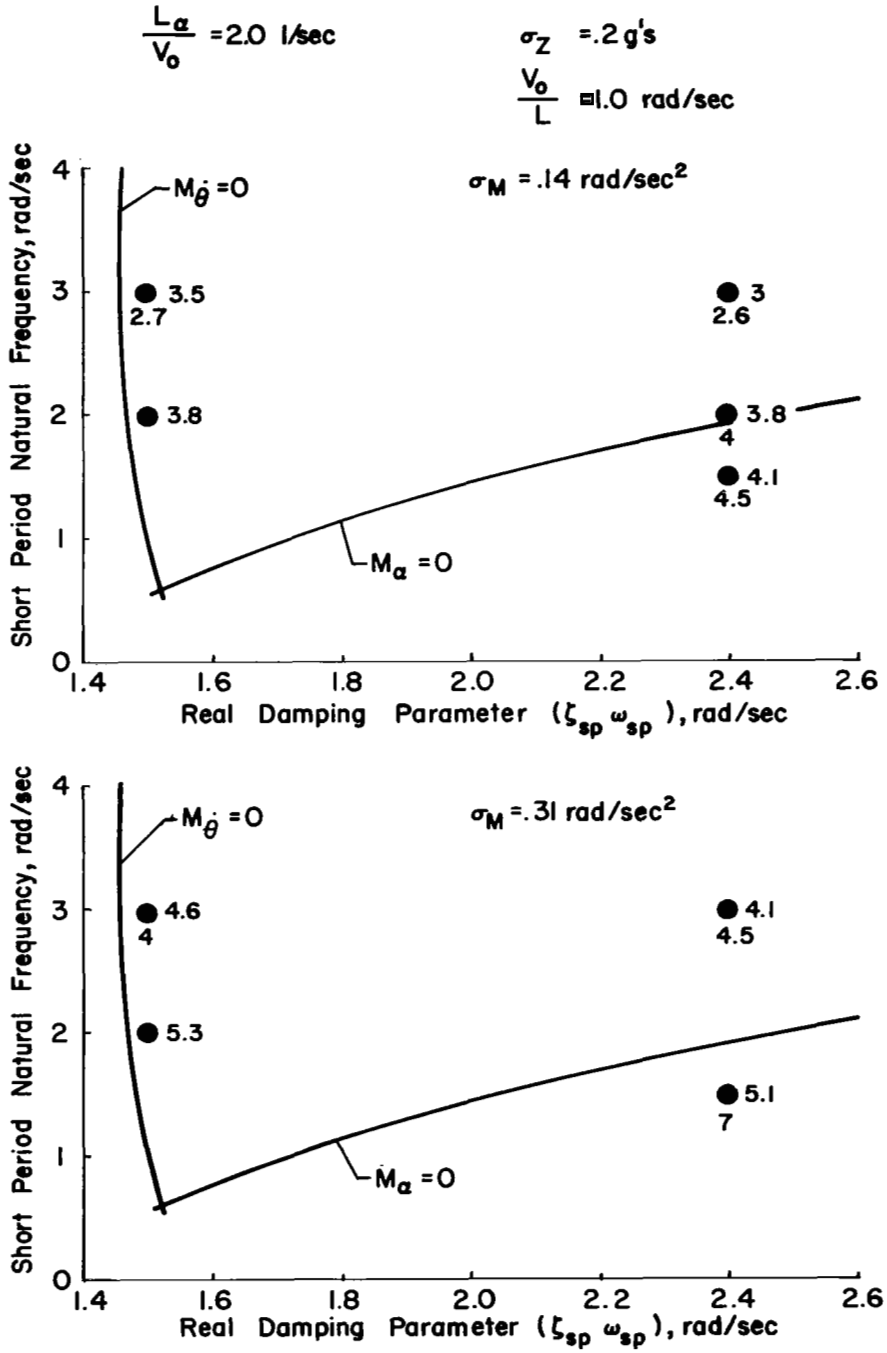

Figure 32. Effects of Short Period Frequency and Damping on Pilot Rating

constant (L_α / V_o = 2.0 1/sec, σ_Z = .2 g's, V_o / L = 1.0 rad/sec). Two levels of real damping are shown, ranging from a value comparable to the basic Navion at the given flight condition down to a value corresponding closely to neutral pitch damping. Damping ratios range from .5 to 1.6.

Short period damping has only a modest influence on pilot rating up to the point of neutral pitch damping. This conclusion applies for either of the values of short period frequency shown and for the two levels of pitch disturbance. According to their commentary, the pilots were aware of reduced pitch damping of the $\zeta_{sp}\omega_{sp}$ = 1.5 radian/second configurations primarily through increased pitch rate overshoots associated with the lower damping ratio. However, the pilots remarked that the pitch overshoot tendency did not have any significant effect on their ability to fly the approach. At the higher short period frequency (ω_{sp} = 3.0 rad/sec), control workload was considered light to moderate, and airspeed control and glide slope tracking were satisfactory. The same remarks would apply as well to the case of larger pitch disturbances shown in the lower diagram, except that the level of difficulty of the task in terms of pitch attitude precision and control workload increased with the turbulence magnitude.

Reducing the short period damping does not alter the influence of turbulence bandwidth on pilot rating. The combined effect of real damping and bandwidth are shown in Figure 33 for two values of short period frequency. In no case do pilot ratings vary with frequency any more than the trends noted previously in Figure 23.

Performance-workload data of Figures 34 and 35 confirm the insensitivity of pilot ratings over the range of short period damping tested. For constant turbulence characteristics, it may be noted in Figure 34 that only a slight increase in control workload accompanies the reduction in pitch damping from ζ_{sp} = .8 to .5. Pitch attitude excursions do increase with the reduction in damping; however, by the pilot's own account, the increased pitch response did not degrade the glide slope tracking performance significantly. Moving on to Figure 35, the trends of rms pitch attitude, stick force,

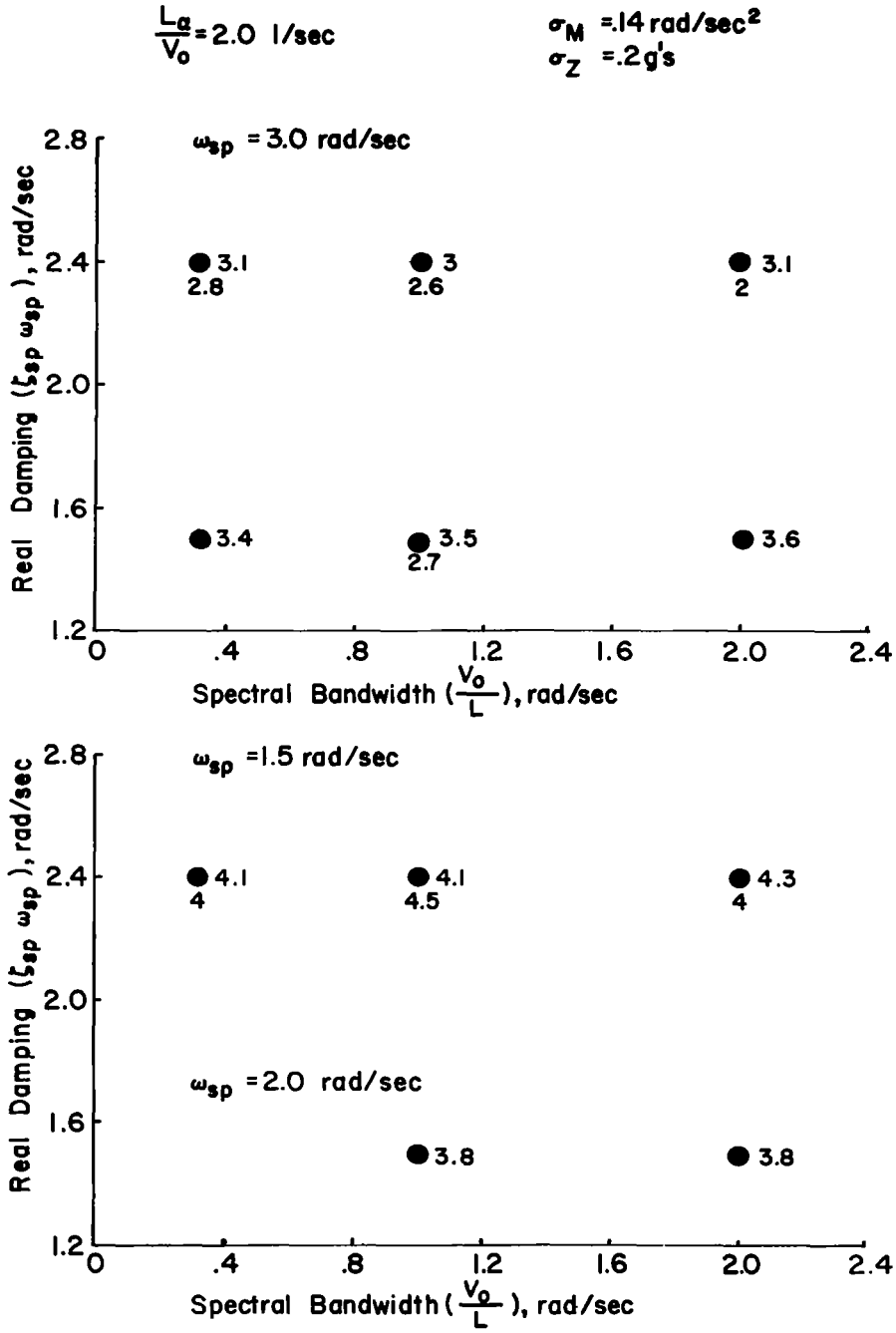

Figure 33. Combined Effects of Short Period Damping and Spectral Bandwidth on Pilot Ratings

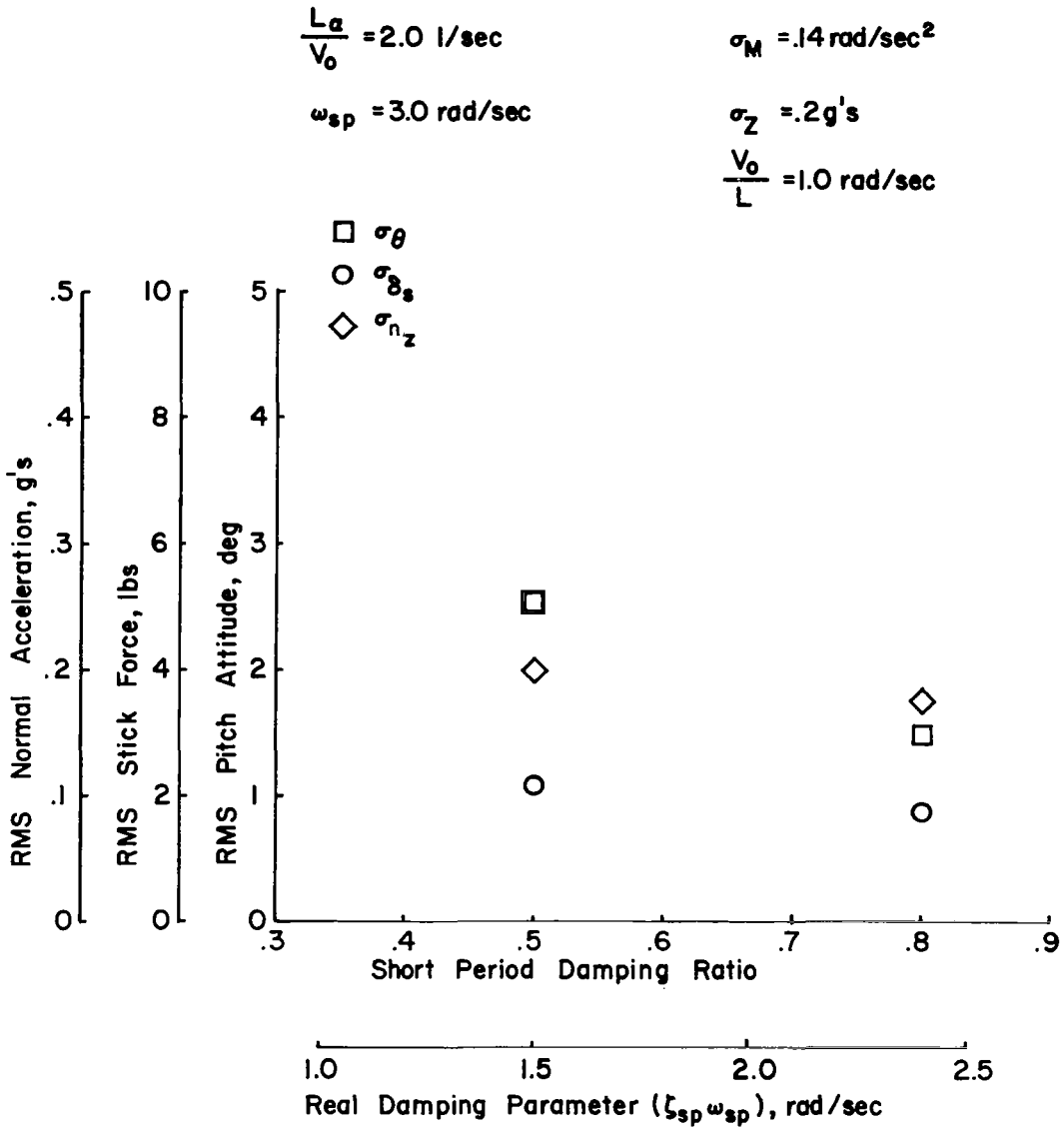

Figure 34. Effect of Short Period Damping on Task Performance and Control Workload

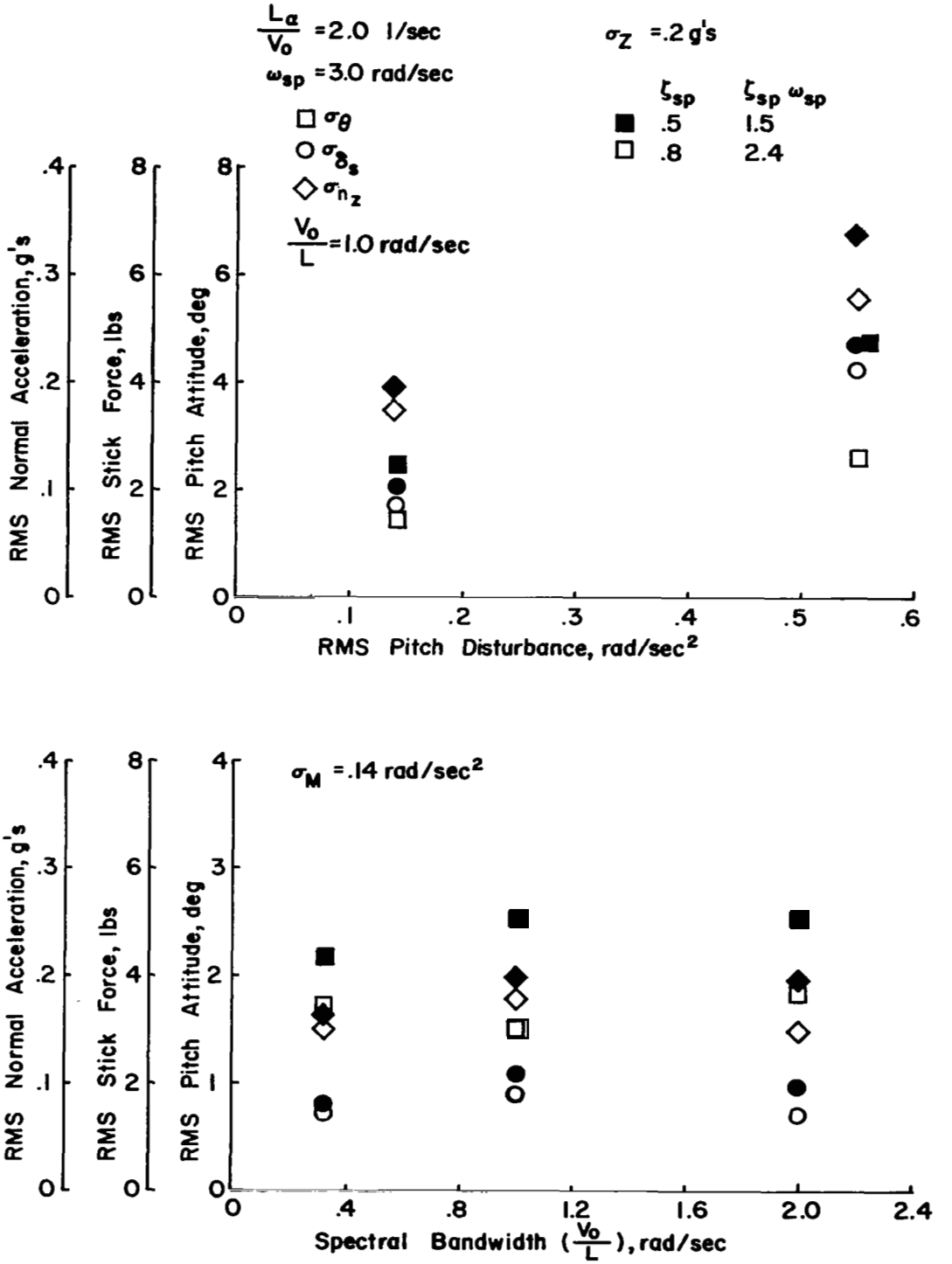

Figure 35. Combined Effects of Short Period Damping, Pitch Disturbances, and Spectral Bandwidth on Task Performance and Control Workload

and normal acceleration with pitch disturbance magnitude and spectral bandwidth are essentially the same for either value of pitch damping. This observation is particularly true of control workload. While the trend of pitch excursions with pitch disturbances does increase as pitch damping is reduced, this behavior is apparently not a serious factor in the pilot's ratings.

The time history of a segment of the ILS approach for one of the low damping configurations shown in Figure 36 substantiates the previous comments. Compared to the approach shown in Figure 18, which only differs from the conditions of this figure in short period damping, the more lightly damped airplane of Figure 36 does exhibit a somewhat larger and more oscillatory pitch response. However, neither airspeed control or glide slope deviations are appreciably different for the two approaches. The pilot is working somewhat harder for the more lightly damped airplane, and it is this factor which appears in his commentary and apparently accounts for what little influence pitch damping has on his ratings.

Contributions of lift curve slope

The final aspect of longitudinal dynamics to be considered is the influence of the slope of the lift curve on the ILS approach. Pilot rating data for combined variations in the parameter L_α / V_o, and pitch and heave disturbance magnitude are shown in Figure 37. Short period dynamics and the turbulence bandwidth are constant ($\omega_{sp} = 3.0$ rad/sec, $\zeta_{sp} = .8$, $V_o / L = 1.0$ rad/sec). Similar to the previous plots of pilot ratings, the primary evaluation pilot's average ratings are shown to the right of each test configuration. One of the secondary pilots also flew some of the same configurations and his data are included in the figure as well.

Reducing the lift curve slope to a little less than half that of the basic Navion (reducing L_α / V_o from 2.0 to .9 1/sec) has only a modest influence on the ILS approach, so long as pitch upsets are light ($\sigma_M \doteq .14$ rad/sec^2). The primary pilot's ratings degrade less than one-half unit for this reduction in L_α / V_o, while the secondary pilot's rating degrades by about a full rating unit. Pilot commentary indicates an awareness of the reduced lift curve

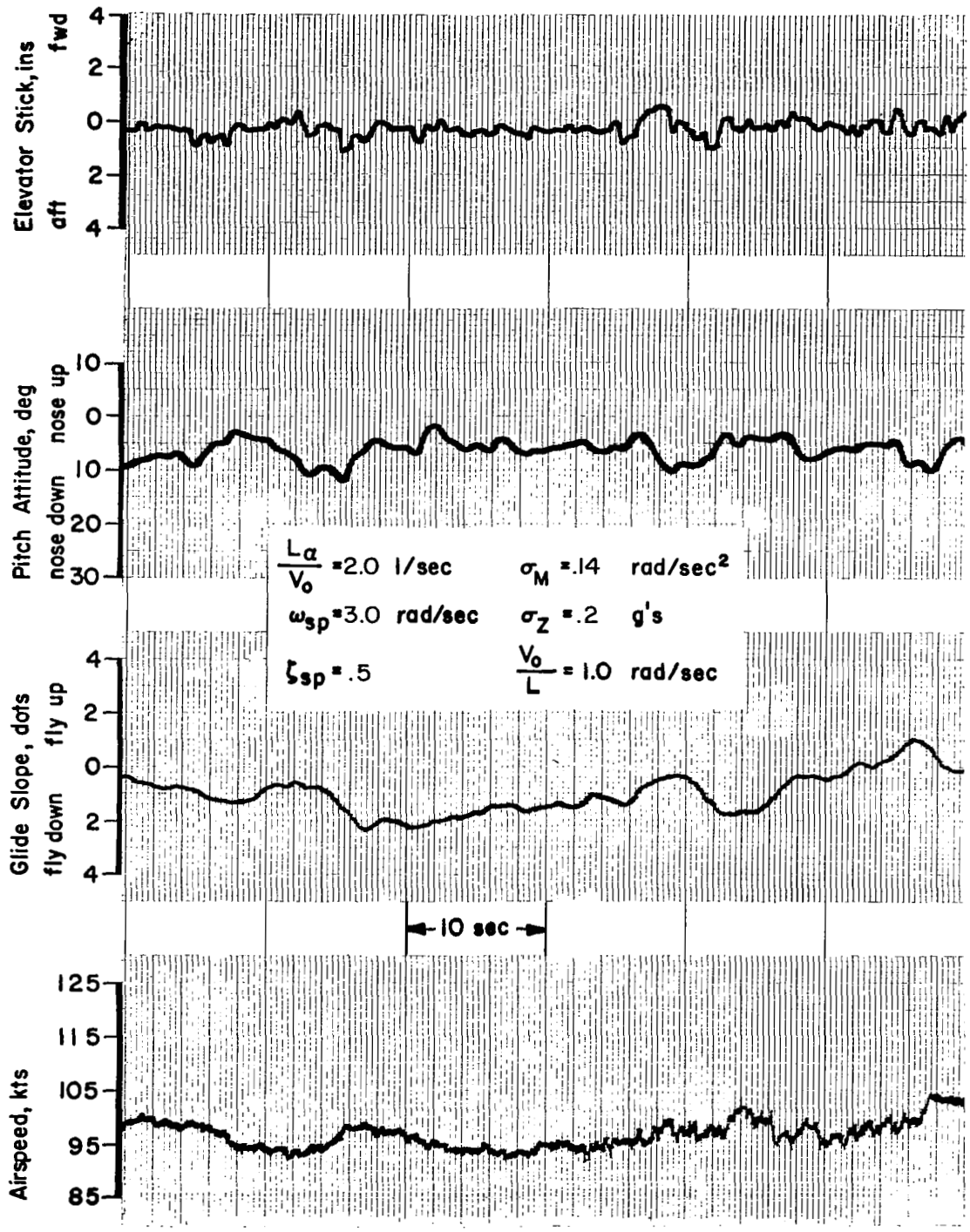

Figure 36. Time History of Longitudinal Control During the ILS Approach - Configuration 5/2

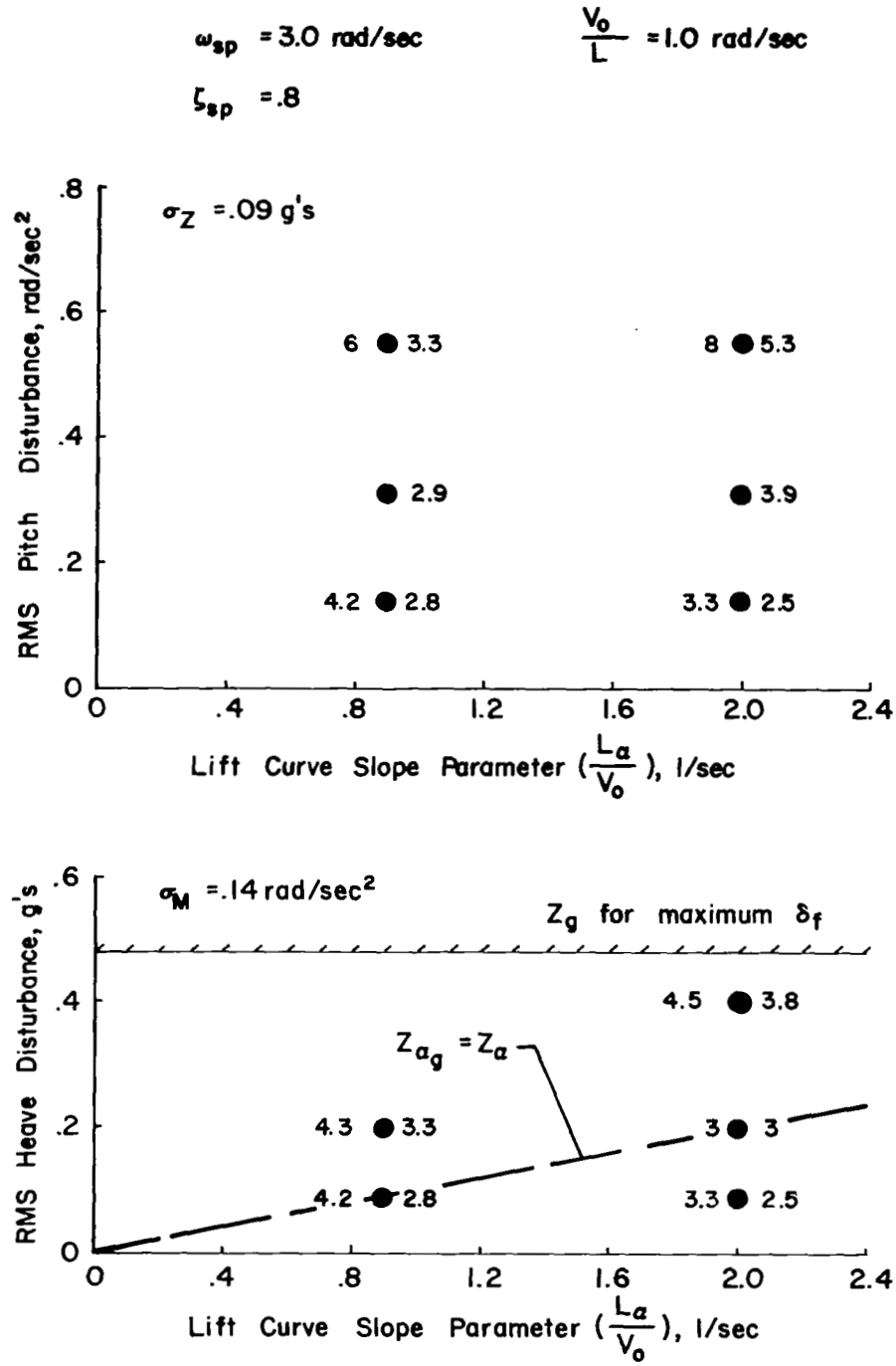

Figure 37. Combined Effects of Lift Curve Slope with Pitch and Heave Disturbances on Pilot Rating

slope and the degraded ratings, when they are observed, relate to the slower flight path response to pitch attitude commands. Longer time was required to make glide slope corrections and as a result glide slope control demanded more attention by the pilot during the approach. Airspeed control was good for the lower L_α / V_o configuration.

All of what has just been said applies when pitch disturbances are light, as is the case for the lower diagram of Figure 37 and for a portion of the upper diagram. Regarding the upper diagram, which shows the influences of lift curve slope and pitch disturbance magnitude (σ_Z = .09 g's), it is apparent that a reduction in lift curve slope improves the pilot's rating of the ILS approach when pitch disturbances are large. For the extreme pitch disturbances shown (σ_M = .55 rad/sec^2), an improvement in pilot rating of two units accompanies the reduction in L_α / V_o from 2.0 to .9 1/seconds. Depending on which pilot's ratings are considered, the approach is improved from one which is moderately objectionable to one which is generally satisfactory (primary pilot), or it is improved from an inadequate to an adequate, though very objectionable approach due to a high workload (secondary pilot). The reason for this improvement in rating for the lower L_α / V_o configuration is its reduced heave response to pitch excursions. Glide slope excursions are smaller when L_α / V_o is low and the ride itself is not as uncomfortable or distracting as when L_α / V_o is on the order of the basic Navion. While the pilots still object to the large pitch excursions associated with large pitch disturbances and will work to reduce their magnitude, the pilot difficulty in flying the ILS is distinctly reduced for the lower L_α / V_o airplane.

The data presented in Figure 37 serve to define the independent influences of lift curve slope and turbulence disturbances on pilot evaluations of the ILS approach. While the lift curve slope and the magnitude of heave disturbances are normally related to each other, i.e.,

$$\sigma_Z^2 = \frac{\sqrt{3}}{2} \left(\frac{\sigma_w}{V_o} Z_{\alpha_g}\right)^2$$

$$Z_{\alpha_g} = Z_\alpha = -L_\alpha$$

this relationship was not in general enforced for the test configurations of Figure 37. An evaluation of the combined effects of lift curve slope related to pitch attitude and glide slope control ($1/T_{\theta_2}$ influences discussed later in this section) and to the heave disturbance magnitude (σ_Z) may be made by considering the configurations of the lower diagram where $Z_{\alpha_g} = Z_\alpha$ as indicated by the dashed line. The trend in pilot ratings along this line for the range in L_α / V_o and σ_Z shown is either insignificant (for the primary pilot) or moderately degrading as the lift curve slope is reduced (secondary pilot). The influences of lift curve slope on pitch attitude and glide slope control and on heave disturbance magnitude tend to counteract each other and the consequent effect on pilot rating of these combined contributions of L_α / V_o are apparently only modest if, indeed, there is any trend at all.

Performance-workload data are shown in Figure 38 as a function of lift curve slope alone. Short period dynamics and turbulence magnitude and bandwidth are constant. Certainly no trends of any consequence in rms pitch attitude, control activity, or normal acceleration can be observed in this figure. Even the slight decrease in rms normal acceleration as L_α / V_o is reduced is unlikely to be significant to the pilot. A time history of the ILS approach is shown in Figure 39 for the low L_α / V_o configuration. Comparing this approach to that of Configuration 1 (Figure 18) reveals no appreciable differences in their overall performance. Glide slope error for the low L_α / V_o airplane is somewhat larger toward the end of the approach and seems to be corrected more slowly than are the errors which developed for Configuration 1. Airspeed control is also less precise for low L_α / V_o, although there is no indication that these errors are a consequence of exaggerated pitch attitude control used to make glide slope corrections.

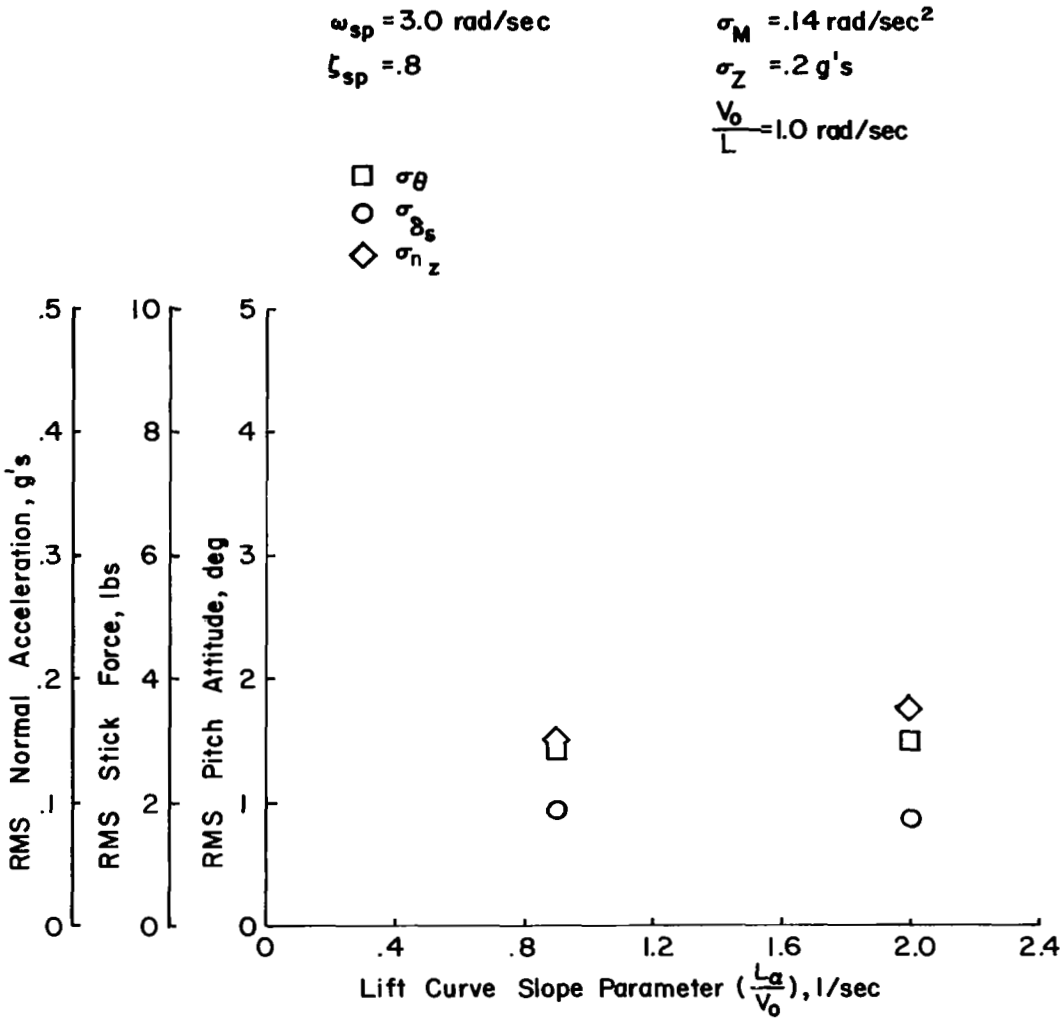

Figure 38. Trends of Task Performance and Control Workload with Lift Curve Slope

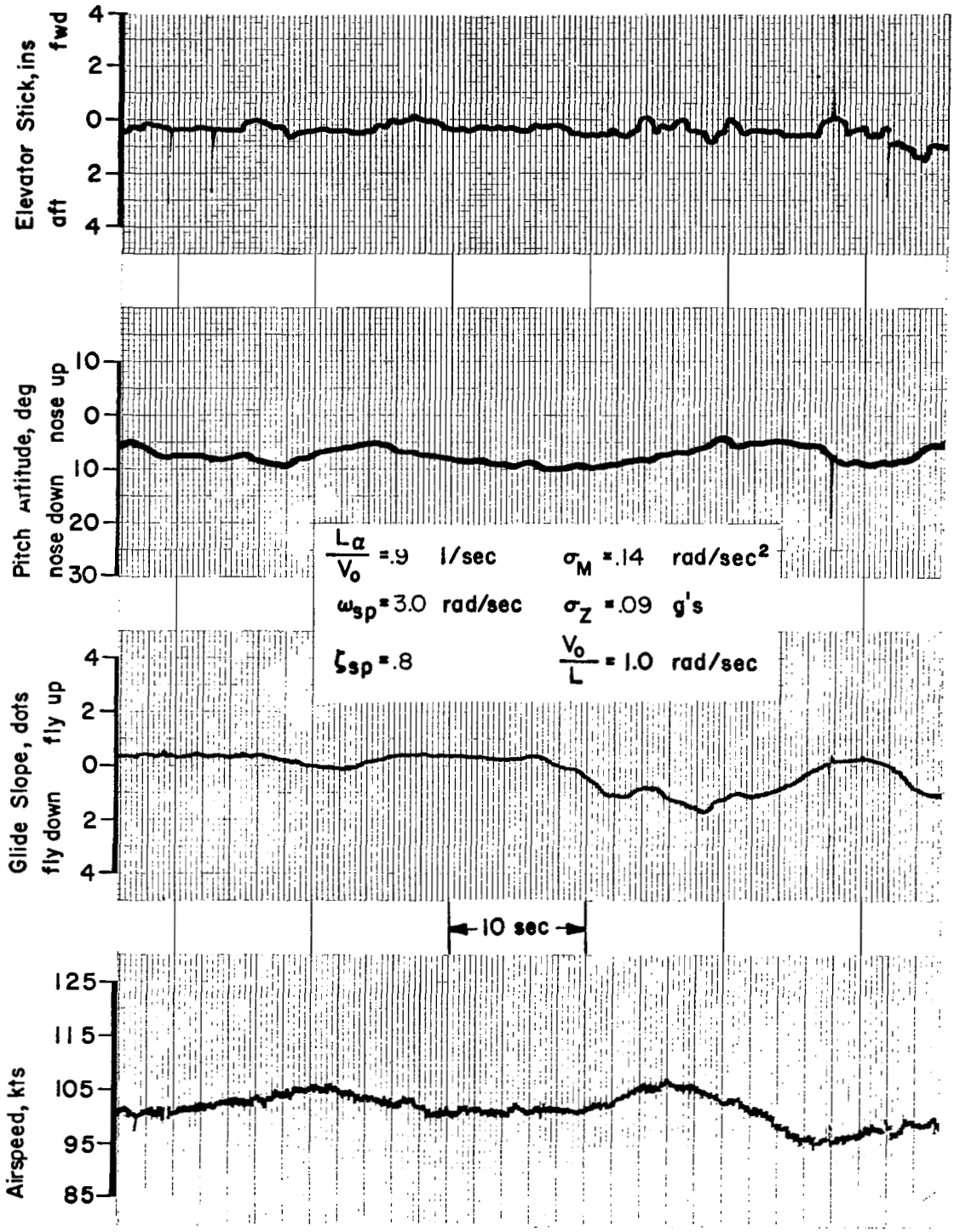

Figure 39. Time History of Longitudinal Control During the ILS Approach - Configuration 4/5

Turning to Figure 40 and considering the upper diagram first, heave disturbance magnitude has no significant influence on pitch attitude or control activity. The increase in normal acceleration is in accord with pilot commentary and apparently is the basis for the slight trend in rating with σ_Z which is observed in Figure 37. Data of the lower diagram of Figure 40 make it apparent why lowering L_α / V_o improves pilot rating in the presence of large pitch disturbances. These data show the effect of pitch disturbance magnitude on the usual performance-workload measures for the two levels of L_α / V_o tested. The significant improvement in rms pitch attitude, stick force and normal acceleration at the extreme pitch disturbance level (σ_M = .55 rad/ sec^2) as L_α / V_o is reduced concurs with the pilots' commentary and, along with a similar improvement in glide slope performance, offers the basis for their ratings.

To conclude the data related to lift curve slope, Figure 41 includes pilot rating data showing the effect of turbulence bandwidth for two levels of L_α / V_o. Short period dynamics and pitch and heave disturbance magnitude are constant (ω_{sp} = 3.0 rad/ sec, ζ_{sp} = .8, σ_M = .14 rad/ sec^2, σ_Z = .2 g's). No trend in pilot rating is apparent for either the high or low levels of lift curve slope. Performance-workload data shown in Figure 42 for the same conditions also have no significant variation over the range of bandwidths tested.

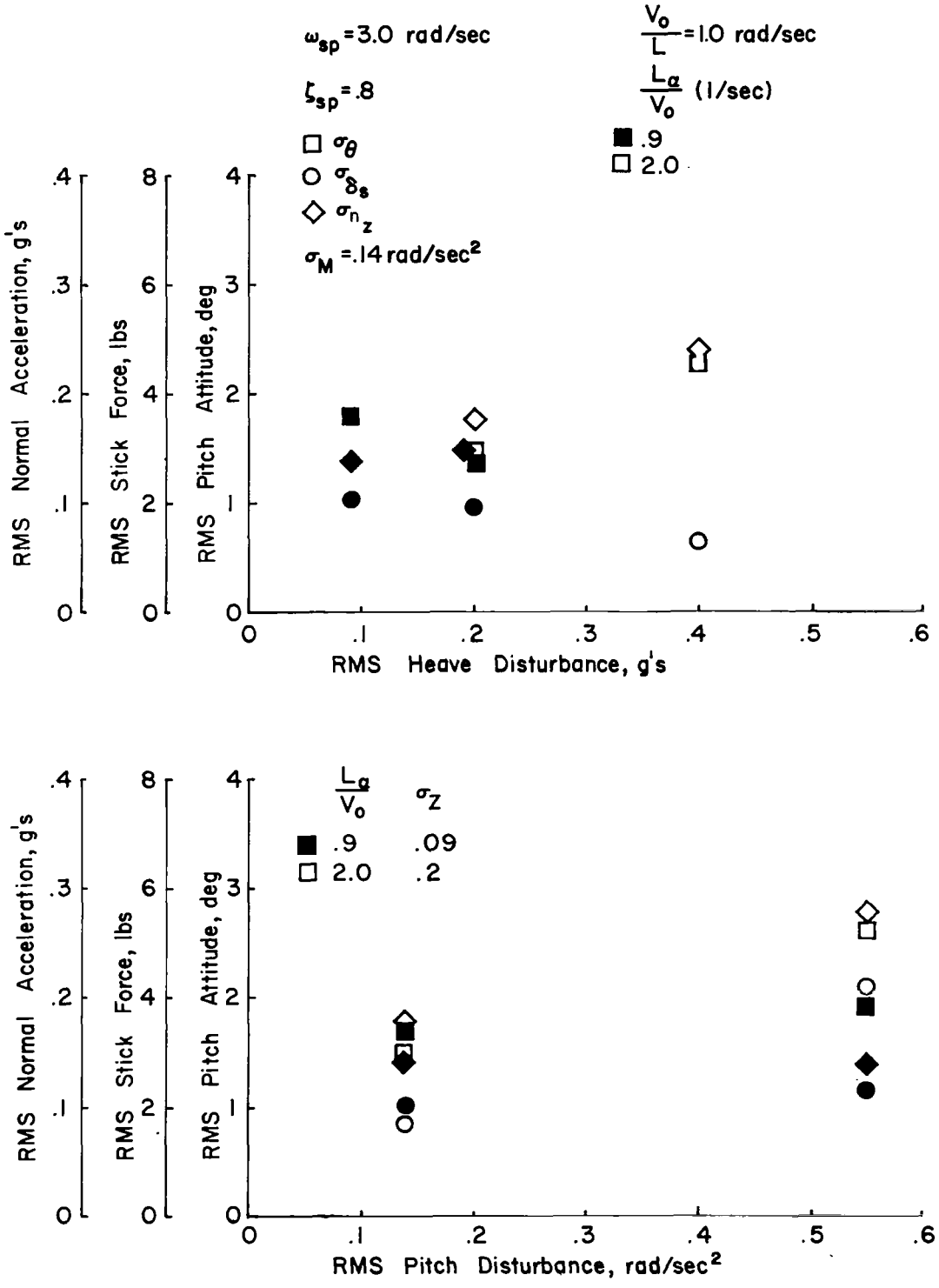

Figure 40. Combined Effects of Lift Curve Slope, Pitch and Heave Disturbances on Task Performance and Control Workload

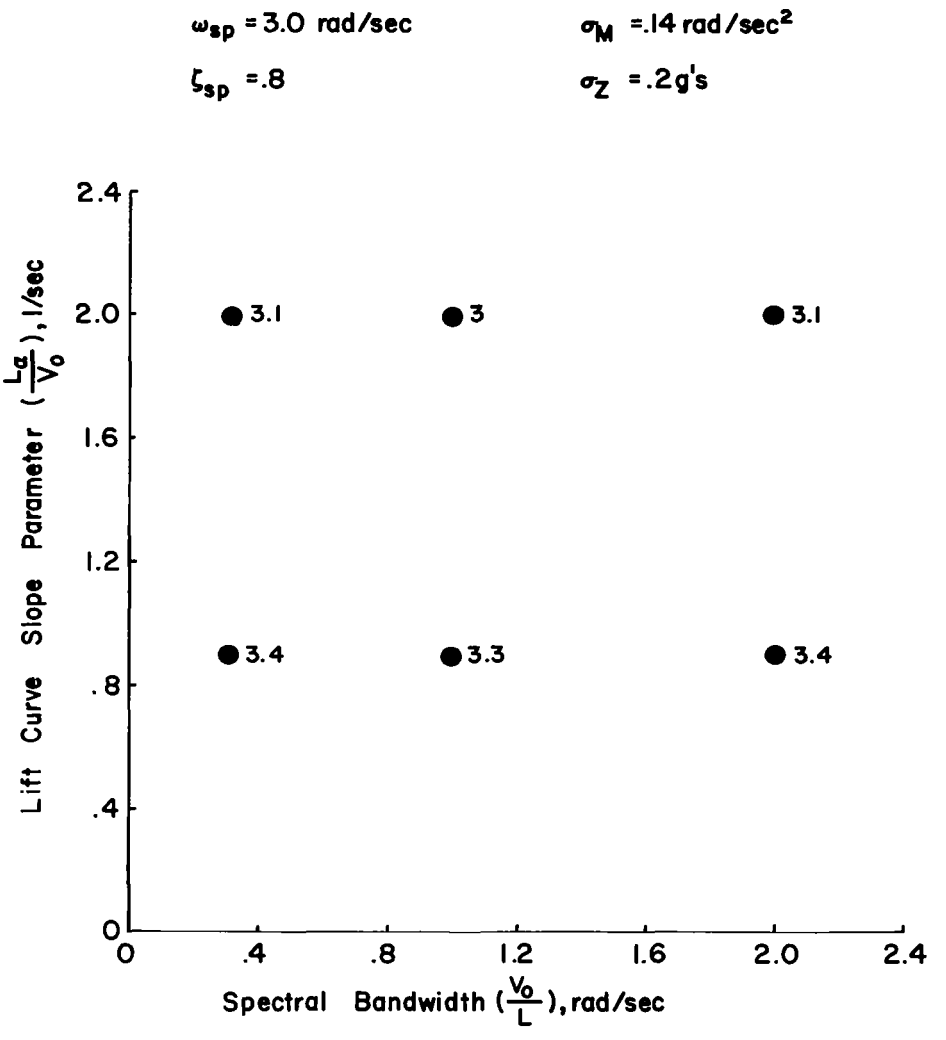

Figure 41. Combined Effects of Lift Curve Slope and Spectral Bandwidth on Pilot Rating

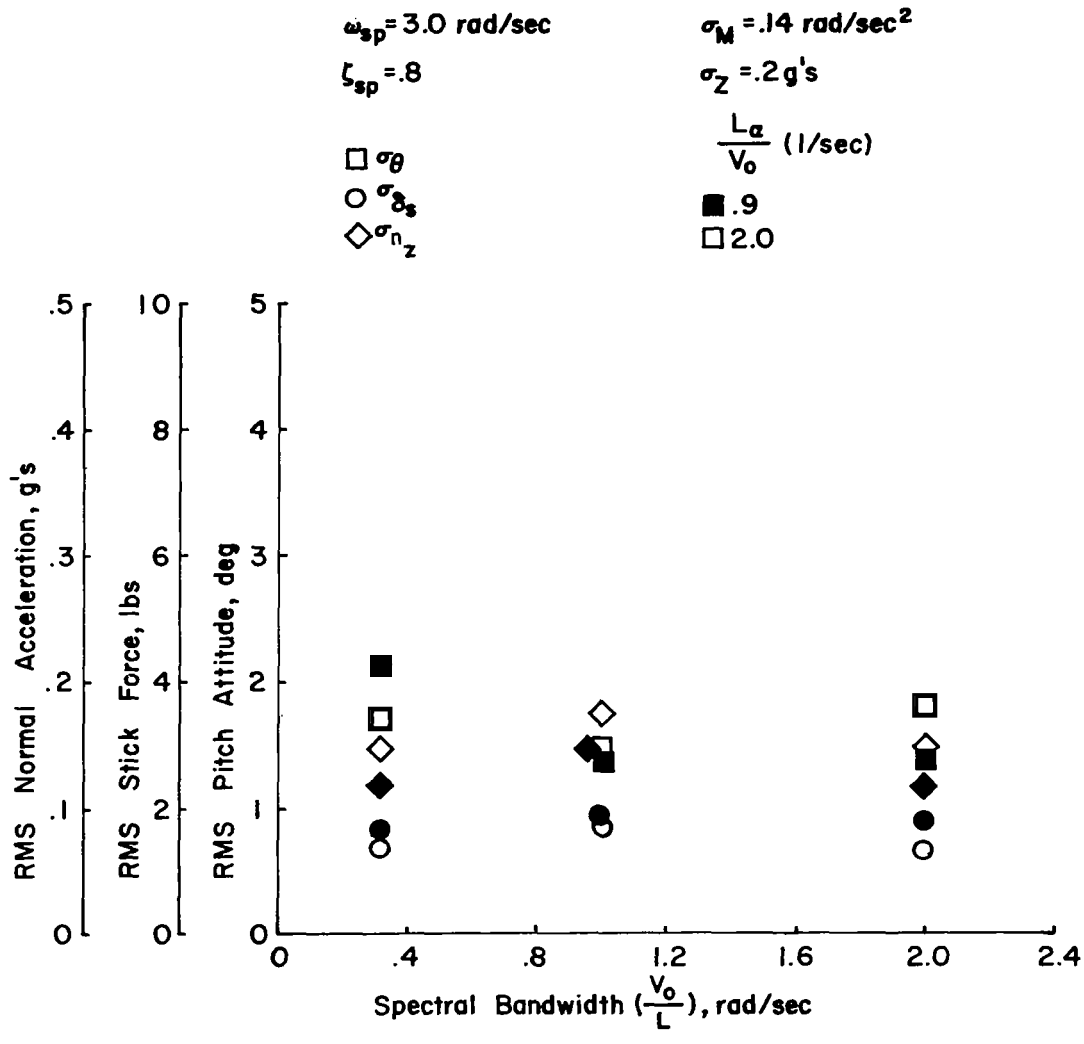

Figure 42. Trends of Task Performance and Control Workload with Lift Curve Slope and Spectral Bandwidth

Pilot-Airplane System Analysis

Background

The discussion of results up to this point has attempted to define the influences of turbulence and airplane dynamics in terms of pilot ratings and quantitative measures of the precision of task performance and the pilot's control workload. It is now of interest to consider the problem of longitudinal control of the airplane in turbulence through an analysis of the closed loop pilot-airplane system. The objective of this analytical study is to identify problems relating to closed loop longitudinal control and to predict the effects of turbulence and airplane dynamics on precision of performance and control workload for comparison with similar data obtained in flight.

The response of the piloted airplane to turbulence disturbances was expressed in general by equation (1), in terms of the power spectral density of the response

$$\Phi_{rr} = \left|\frac{Y_G}{1 + Y_p Y_A}\right|^2 \Phi_{ff}$$

assuming command inputs to the airplane are neglected. Longitudinal control of the airplane in the landing approach in the presence of turbulence may be simplified to the elements contained in Figure 43. Glide slope tracking is reduced to a basic requirement for control of the airplane's attitude, altitude, and speed at any point along the approach. Pitch attitude is controlled with the elevator for the purpose of compensating for deficiencies in longitudinal dynamics, either associated with the long period, poorly damped phugoid mode, or with the short period response, and to suppress pitch excursions caused by turbulence. In addition, pitch attitude control is used as a means of making changes in altitude, that is to say altitude is controlled in series with pitch attitude using the elevator. Airspeed control is not represented in the block diagram, nor will it be considered in the analysis to follow. It is assumed that the airplane is operated well on the front side of the throttle

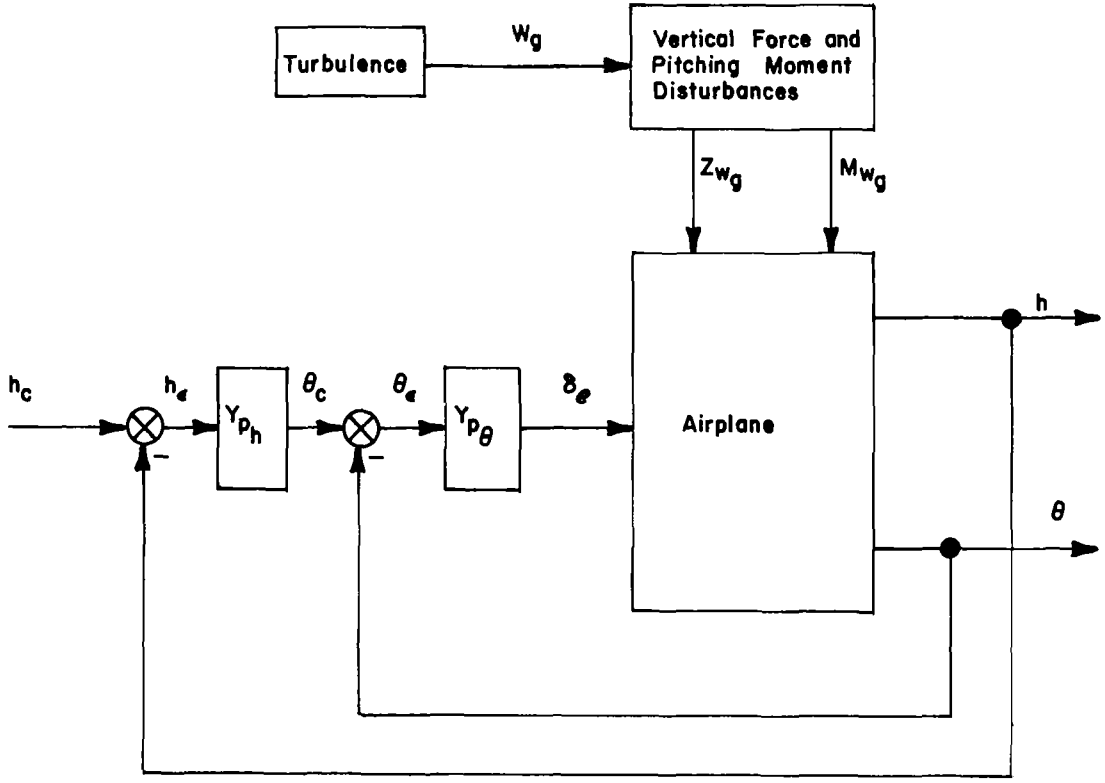

Figure 43. Block Diagram of Pitch Attitude and Altitude Control in Turbulence

required curve and hence that it has adequate flight path stability. Under these circumstances, corrections in pitch attitude and altitude may be made with the elevator about a trimmed descent condition without having to make corresponding corrections to airspeed or altitude with the throttle.

In the analysis to follow, pitch attitude control in the presence of vertical gusts (perhaps pitch attitude regulation is a more proper description) will be discussed first, then the problem of altitude control with the pitch attitude inner loop closed will be considered. In general, it will be assumed that the pilot is attempting to fly constant attitude or altitude (hence the reference to regulation of θ or h) and that the command inputs are constant or zero.

Pitch Attitude Control - Applying equation (1) to pitch attitude control gives

$$\Phi_{\theta_\epsilon} = \left| \frac{\frac{N_{w_g}^{\theta}}{\Delta}}{1 + Y_{p_\theta} \frac{N_{\delta e}^{\theta}}{\Delta}} \right|^2 \Phi_{w_g} \tag{38}$$

for the power spectrum of pitch attitude excursions due to vertical gusts. This expression for the closed loop pitch attitude spectrum may also be written

$$\Phi_{\theta_\epsilon} = \frac{\Phi_{\theta_{O.L.}}}{\left| 1 + Y_{p_\theta} \frac{N_{\delta e}^{\theta}}{\Delta} \right|^2} \tag{39}$$

where the numerator is the spectrum for open loop pitch response to vertical gusts

$$\Phi_{\theta_{O.L.}} = \left| \frac{N_{w_g}^{\theta}}{\Delta} \right|^2 \Phi_{w_g} \tag{40}$$

To gain further insight into the nature of closed loop pitch attitude response it is necessary to understand the nature of the pilot's contribution in

the pitch attitude to elevator loop. Some general criteria for the pilot's contribution to control of the airplane in turbulence were noted in Reference 1, based on the studies of the human controller in Reference 11. To reiterate these criteria, the pilot will try to achieve the following results

- $Y_p Y_A >> 1$ for $\omega << \omega_c$ in order to suppress the effects of turbulence disturbances and to follow command inputs over a sufficient bandwidth, where ω_c, the crossover frequency, is defined by $|Y_p Y_A|_{\omega=\omega_c} = 1.0$,
- $Y_p Y_A << 1$ for $\omega >> \omega_c$ for adequate closed loop stability,
- $Y_p Y_A$ in the crossover region of the form $\omega_c e^{-j\omega\tau_e}/j\omega$, with bandwidth to exceed the disturbance bandwidth, $\omega_c > \omega_f$, and with sufficient stability margin to avoid a poorly damped dominant mode.

To accomplish these objectives, the pilot may increase his own gain, observing the constraints imposed by excessive workload and stability considerations. He may also provide compensation to improve system stability, to achieve the K/s character in the region of crossover, and to increase the system gain at low frequency. As indicated in Reference 11, this compensation may take the form of a first order lead (where the pilot makes use of angular and linear rate cues), a reduction in the effective time delay of the pilot's response, or a first order lag (where the pilot uses the control to smooth the airplane's response, ignoring high frequency inputs).

Pitch attitude control with the elevator is defined by the transfer function

$$\frac{N^{\theta}_{\delta e}}{\Delta} = \frac{A_\theta (s + \frac{1}{T_{\theta_1}})(s + \frac{1}{T_{\theta_2}})}{(s^2 + 2\zeta_{ph}\omega_{ph}s + \omega^2_{ph})(s^2 + 2\zeta_{sp}\omega_{sp}s + \omega^2_{sp})} \tag{41}$$

where according to Reference 12

$$A_\theta = M_{\delta e}$$

$$\frac{1}{T_{\theta_1}} \doteq - X_u + \frac{X_\alpha}{Z_\alpha} Z_u \left(\frac{1 - \frac{Z_{\delta e} M_u}{M_{\delta e} Z_u}}{1 - \frac{Z_{\delta e} M_\alpha}{M_{\delta e} Z_\alpha}} \right)$$

$$\frac{1}{T_{\theta_2}} \doteq \frac{1}{V_o} \left(- Z_\alpha + \frac{M_\alpha}{M_{\delta e}} Z_{\delta e} \right)$$

The numerator root, $1/T_{\theta_1}$, is typically located in the vicinity of the origin, while $1/T_{\theta_2}$, as previously noted, is approximately the value of L_α / V_o. The pilot's contribution to the control loop is assumed to be of the form

$$Y_{p_\theta} = K_\theta T_{L_\theta} \left(s + \frac{1}{T_{L_\theta}} \right) e^{-\tau_e s} \tag{42}$$

which incorporates lead compensation and an effective time delay to account for the pilot's transport delay and neuromuscular dynamics. The effective time delay is in turn represented by a first order Pade approximation

$$e^{-\tau_e s} = - \frac{\left(s - \frac{2}{\tau_e} \right)}{\left(s + \frac{2}{\tau_e} \right)} \tag{43}$$

The complete pilot-airplane transfer function becomes

$$\frac{\theta}{\theta_e} = - \frac{K_\theta T_{L_\theta} M_{\delta e} \left(s + \frac{1}{T_{L_\theta}} \right)\left(s - \frac{2}{\tau_e} \right)\left(s + \frac{1}{T_{\theta_1}} \right)\left(s + \frac{1}{T_{\theta_2}} \right)}{\left(s^2 + 2\zeta_{ph}\omega_{ph} s + \omega_{ph}^2 \right)\left(s^2 + 2\zeta_{sp}\omega_{sp} s + 1 \right)\left(s + \frac{2}{\tau_e} \right)} \tag{44}$$

A root locus and Bode diagram of this transfer function is shown in Figure 44 for characteristics typical of the basic Navion.

It is apparent from the Bode diagram of Figure 44 that adequate gain exists at low frequency, i.e., $|\theta/\theta_\varepsilon| \gg 1$ for low frequencies in the region of the phugoid mode. Thus, as is well recognized, the pitch attitude to elevator loop is very effective in suppressing phugoid mode response and it becomes reasonable to represent the $\theta/\theta_\varepsilon$ transfer function by the short period approximation of Reference 12

$$\frac{\theta}{\theta_\varepsilon} \doteq \frac{-K_\theta T_{L_\theta} M_{\delta e} (s + \frac{1}{T_{L_\theta}})(s - \frac{2}{\tau_e})(s + \frac{1}{T_{\theta_2}})}{s(s^2 + 2\zeta_{sp}\omega_{sp}s + \omega_{sp}^2)(s + \frac{2}{\tau_e})} \tag{45}$$

It has been pointed out in Reference 6 that the bandwidth of this loop closure is strongly influenced by short period frequency. Asymptotes of the closed loop pitch attitude response (heavy solid line) indicate a closed loop bandwidth on the order of the short period frequency, with the exception of the droop in the asymptote associated with the pole-zero combination near $1/T_{\theta_2}$. This droop, which compromises the precision of pitch attitude control in this frequency region, is reduced by increasing $1/T_{\theta_2}$. Short period damping affects stability or phase margin in the crossover region and hence it indirectly influences the crossover frequency.

The pilot's contribution should include sufficient lead compensation to achieve the K/s behavior in the crossover region and to provide adequate stability at crossover. Typical values of the pilot's effective time delay are on the order of .2 to .4 seconds according to Reference 11. The magnitude of this time delay will affect phase margin at crossover.

For pitch attitude control, Reference 11 suggests that crossover frequencies of approximately 4.5 radians/second are appropriate and that the pilot's effective time delay should be on the order of .25 seconds. The

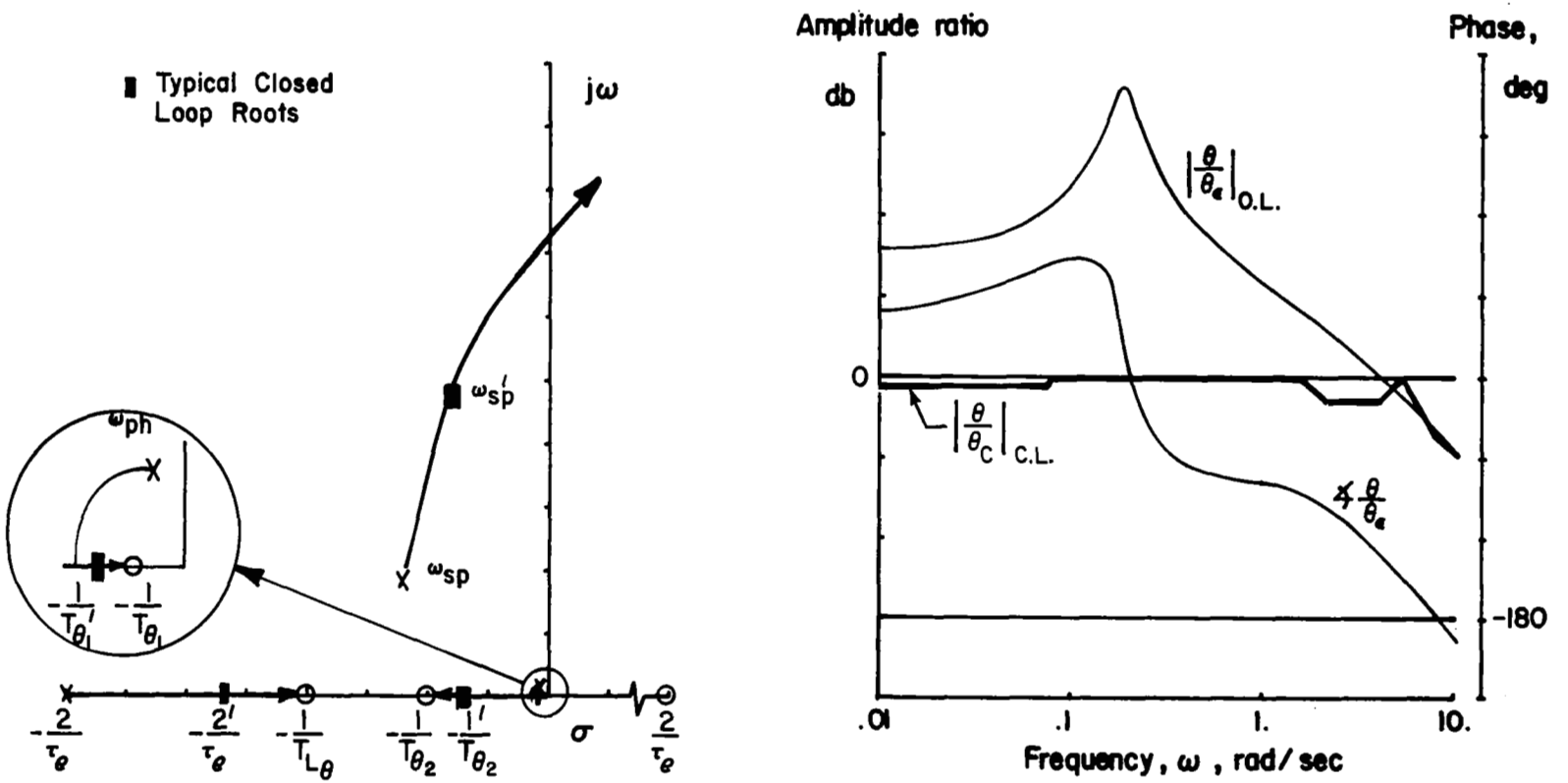

Figure 44. Characteristics of Pitch Attitude Control with Elevator

acceptability of flying qualities associated with pitch control would be expected to depend on the effort required of the pilot to achieve the desired bandwidth and the amount of compensation required to maintain adequate closed loop stability.

Open loop pitch attitude response to vertical gusts is defined by

$$\Phi_{\theta_{O.L.}} = \left|\frac{N_w^\theta}{\frac{g}{\Delta}}\right|^2 \Phi_{w_g} = \left|\frac{s(A_w^\theta s^2 + B_w^\theta s + C_w^\theta)}{V_o(s^2 + 2\zeta_{ph}\omega_{ph}s + \omega_{ph}^2)(s^2 + 2\zeta_{sp}\omega_{sp}s + \omega_{sp}^2)}\right|^2 \frac{\sigma_w^2 \frac{L}{\pi V_o}}{(\frac{\omega L}{V_o})^2 + 1} \quad (46)$$

where

$$A_w^\theta = M_{\dot\theta} - M_{\dot\alpha}$$

$$B_w^\theta = -M_\alpha - \frac{Z_\alpha}{V_o} M_{\dot\theta} - X_u(M_{\dot\theta} - M_{\dot\alpha})$$

$$C_w^\theta = X_u\left(M_\alpha + \frac{Z_\alpha}{V_o} M_{\dot\theta}\right) - \frac{X_\alpha}{V_o}(V_o M_u + Z_u M_{\dot\theta})$$

The open loop power spectrum, $\Phi_{\theta_{O.L.}}$ is shown in Figure 45. It is characterized by the dominant response associated with the phugoid mode, and otherwise by a fairly broad spectrum extending to the frequency of the short period mode.

The attenuation of the open loop turbulence response through the pitch attitude loop closure as represented by equation (39) is graphically shown in Figure 45. Turbulence response is reduced for frequencies less than the crossover frequency of the open loop pitch attitude spectrum. Phugoid response in particular is completely suppressed. More effective attenuation of pitch response in the frequency range defined by the corners of the asymptotes of $|1/(1 + Y_p Y_A)|^2$ at $1/T'_{\theta_2}$ and ω_{sp} is possible if $1/T_{\theta_2}$ is increased. The reduced effectiveness of pitch attitude suppression in this frequency region corresponds to the droop in the closed loop asymptotes of Figure 44.

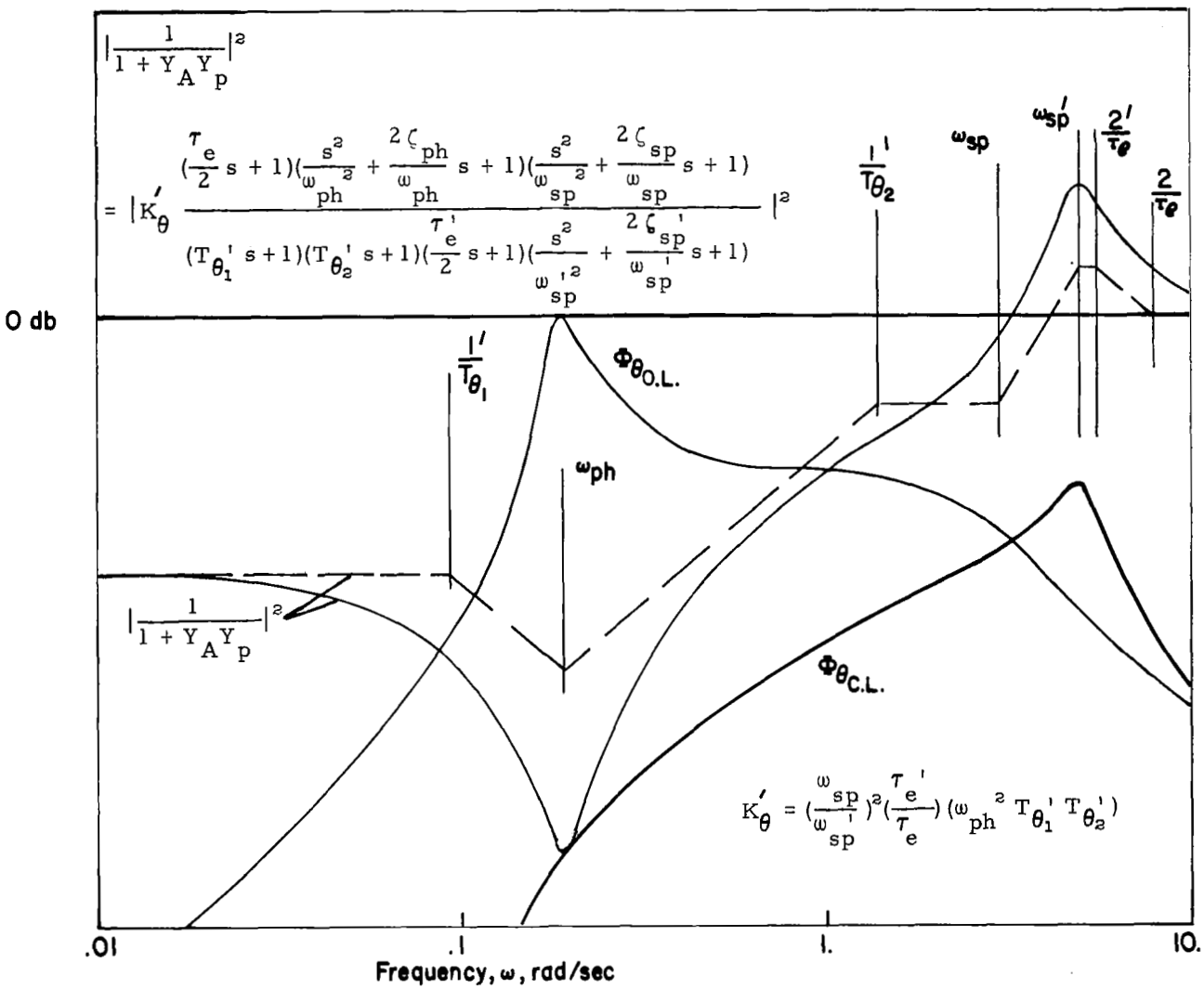

Figure 45. Closed Loop Pitch Attitude Response to Vertical Gusts

Depending on how tightly the pilot closes the pitch attitude loop, pitch response may or may not be accentuated at high frequencies, above the airplane's short period frequency. Because of the peak in the spectrum around ω'_{sp}, increasing the turbulence bandwidth will increase pitch attitude response, assuming the pilot maintains the same loop closure. It is more likely that the pilot would relax somewhat in the control of pitch so as to reduce the high frequency peak. In fact, this is exactly what the pilots appear to do, according to their comments.

Altitude Control - If equation (1) is applied to altitude control with the elevator, assuming a pitch attitude to elevator inner loop, the result is

$$\Phi_{h_\epsilon} = \frac{\left| \frac{N^h_{w_g} + Y_{p_\theta} N^h_{w_g} N^\theta_{\delta e}}{\Delta + Y_{p_\theta} N^\theta_{\delta e}} \right|^2 \Phi_{w_g}}{\left| 1 + Y_{p_h} Y_{p_\theta} \frac{N^h_{\delta e}}{\Delta'} \right|^2} \tag{47}$$

where the numerator is equivalent to the spectrum of altitude response to vertical gusts with pitch attitude controlled by the elevator. Equation (47) may be rewritten

$$\Phi_{h_\epsilon} = \frac{\Phi_{h_{\theta \to \delta e}}}{\left| 1 + Y_{p_h} Y_{p_\theta} \frac{N^h_{\delta e}}{\Delta'} \right|^2} \tag{48}$$

where

$$\Phi_{h_{\theta \to \delta e}} = \left| \frac{N^h_{w_g} + Y_{p_\theta} N^h_{w_g} N^\theta_{\delta e}}{\Delta'} \right|^2 \Phi_{w_g} \tag{49}$$

and

$$\Delta' = \Delta + Y_{p_\theta} N^\theta_{\delta e} \tag{50}$$

The outer loop closure of altitude to elevator in Figure 43 is defined by the transfer function

$$\frac{h}{h_c}_{\theta \rightarrow \delta e} = Y_{p_h} Y_{p_\theta} \frac{N^h_{\delta e}}{\Delta'} \tag{51}$$

where

$$\frac{N^h_{\delta e}}{\Delta'} = \frac{A_h (s + \frac{1}{T_{h_1}})(s + \frac{1}{T_{h_2}})(s + \frac{1}{T_{h_3}})(s + \frac{2}{\tau_e})}{s(s + \frac{1}{T_{\theta_1}'})(s + \frac{1}{T_{\theta_2}'})(s + \frac{2}{\tau_e'})(s^2 + 2\zeta_{sp}' \omega_{sp}' s + \omega_{sp}'^2)} \tag{52}$$

and the numerator factors according to Reference 12 are

$$A_h = - Z_{\delta e}$$

$$\frac{1}{T_{h_1}} \doteq - X_u + (X_\alpha - g) \frac{Z_u}{Z_\alpha}$$

$$\frac{1}{T_{h_2}} \doteq (M_\alpha - \frac{M_{\delta e}}{Z_{\delta e}})^{\frac{1}{2}}$$

$$\frac{1}{T_{h_3}} \doteq - \frac{1}{T_{h_2}}$$

Y_{p_θ} was defined in equation (42) and

$$Y_{p_h} = K_h$$

which neglects higher frequency contributions of the pilot in the altitude control loop. For this analysis, elevator lift is neglected ($Z_{\delta e} \doteq 0$). The numerator thus reduces to first order with a root at $1/T_{h_1}$, typically located at low frequency, and the root locus gain, A_h, is equal to $(-M_{\delta e} Z_\alpha)$. The characteristic roots (Δ') resulting from the pitch attitude loop closure are

- $1/T'_{\theta_1}$ - a low frequency root associated with the respective numerator term of the $\theta \rightarrow \delta e$ transfer function,
- $1/T'_{\theta_2}$ - a root related to the $1/T_{\theta_2}$ numerator term and largely determined by L_α / V_o,
- $2/\tau'_e$ - a root related to the pilot's time delay, and
- ζ'_{sp}, ω'_{sp} - the short period root as modified by the $\theta \rightarrow \delta e$ loop.

A root locus and Bode diagram of the altitude control transfer function is shown in Figure 46. As was noted in Reference 6, the crossover frequency of this transfer function is strongly related to $1/T_{\theta_2}$, inasmuch as the closed loop roots designated by ω''_h are determined to a large extent by the pole at $1/T_{\theta_2}'$. The closed loop asymptotes of altitude response (heavy solid line) show a flat response out to a frequency on the order of the open loop crossover frequency, and it is reasonable to expect good altitude tracking capability out to this frequency.

An example of altitude response to vertical gusts is demonstrated by the spectrum, $\Phi_{h_{\theta \rightarrow \delta e}}$, in Figure 47. Assuming tight control of pitch attitude, this spectrum may be approximated according to Reference 6

$$\Phi_{h_{\theta \rightarrow \delta e}} = \left| \frac{N^h_{w_g} + Y_{p_\theta} N^{h\ \theta}_{w_g\ \delta e}}{\Delta + Y_{p_\theta} N^{\theta}_{\delta e}} \right|^2 \Phi_{w_g}$$

$$\doteq \left| \frac{N^{h\ \theta}_{w_g\ \delta e}}{N^{\theta}_{\delta e}} \right|^2 \Phi_{w_g}$$

$$\doteq \left| \frac{1}{s(T_{\theta_2} s + 1)} \right|^2 \Phi_{w_g} \qquad (53)$$

Thus, the energy content in the altitude response at higher frequencies is related to $1/T_{\theta_2}$ as well as to the bandwidth of the vertical gust spectrum, Φ_{w_g}.

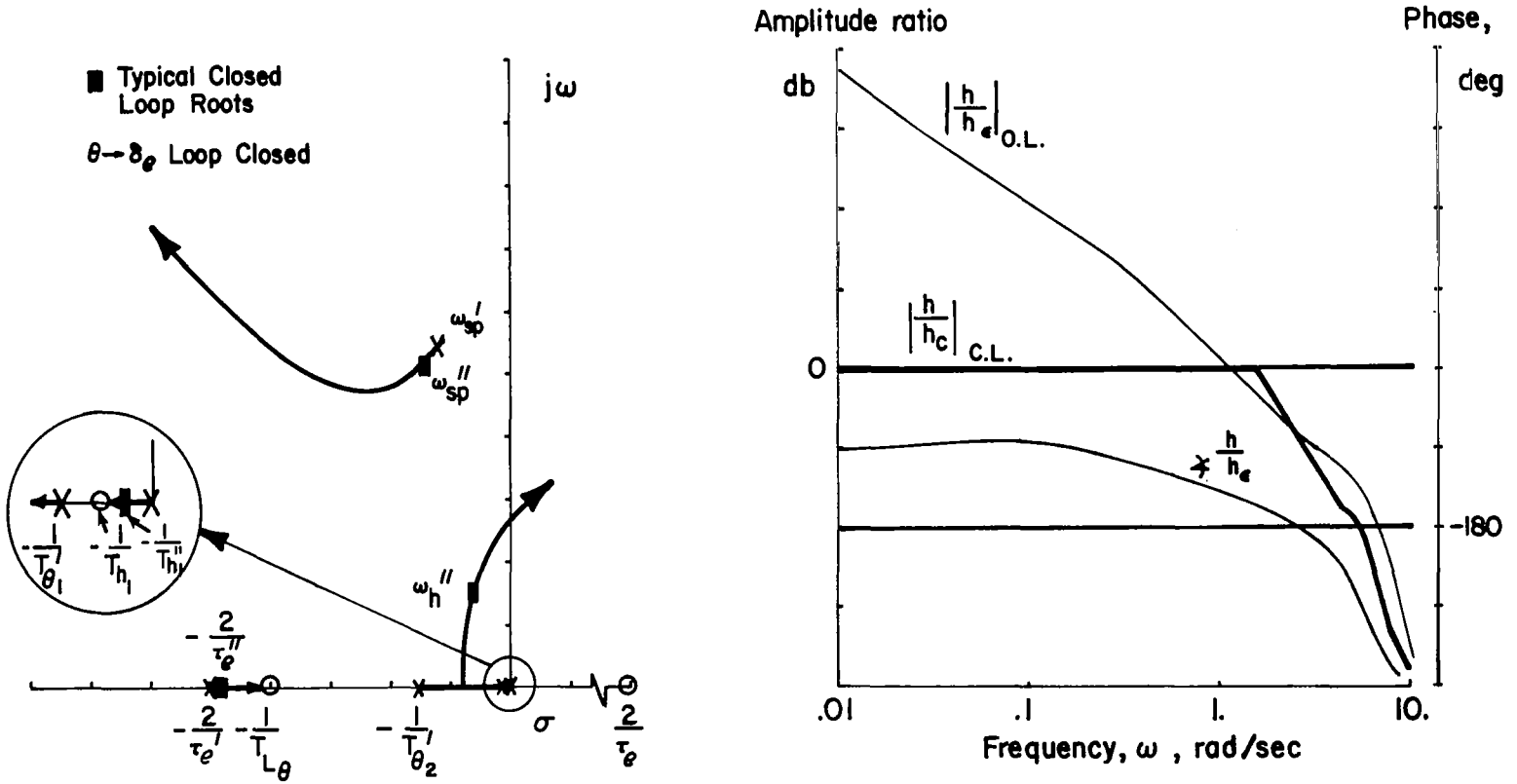

Figure 46. Characteristics of Altitude Control with Elevator - $\theta \rightarrow \delta e$ Loop Closed

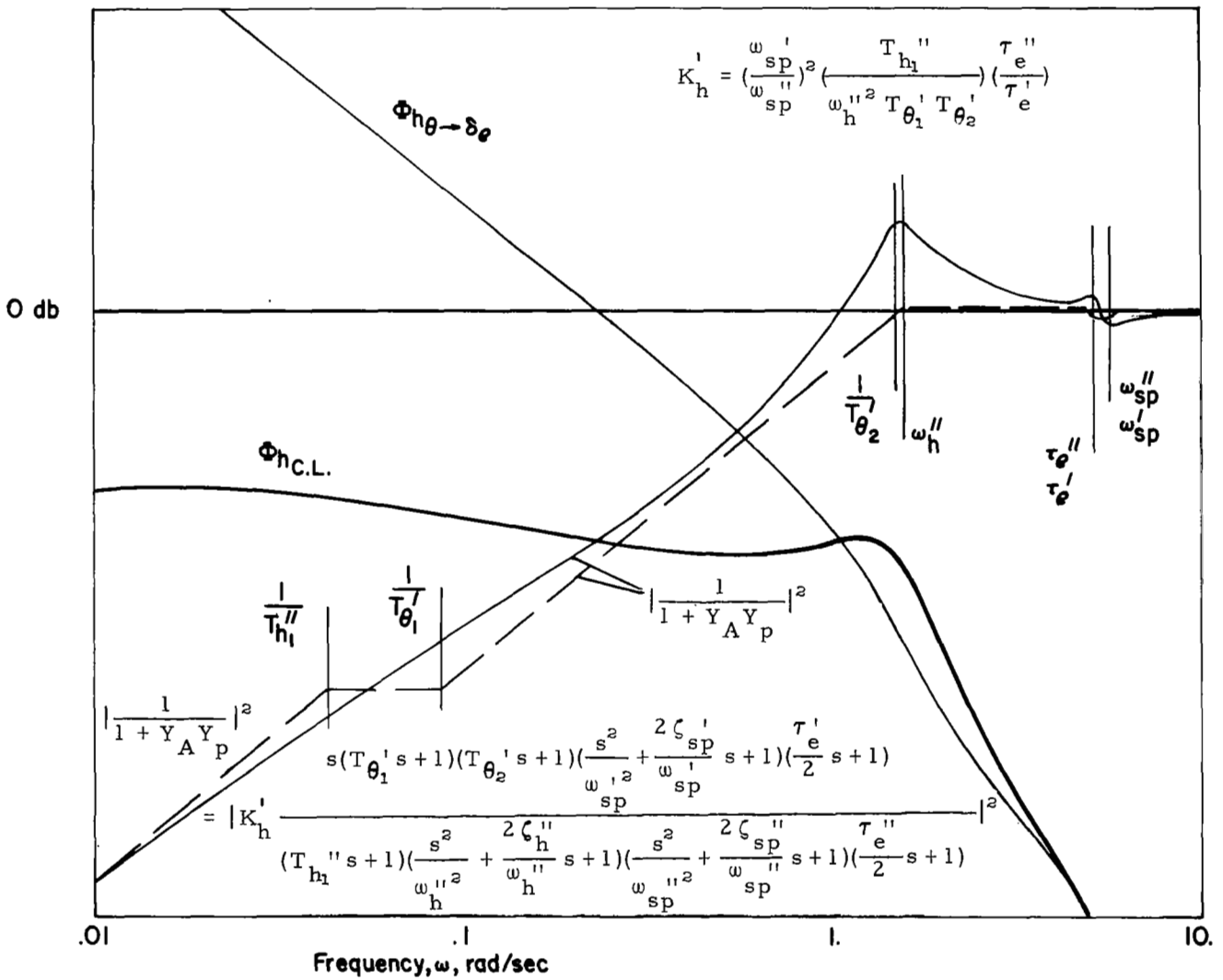

Figure 47. Closed Loop Altitude Response to Vertical Gusts

Attenuation of altitude response is quite effective for frequencies below the crossover frequency of the altitude control loop. The closed loop altitude spectrum is shown in Figure 47 along with $\Phi_{h_\theta \rightarrow \delta e}$ and $|1/(1 + Y_p Y_A)|^2$, and its bandwidth is on the order of the corner frequency ω_h'' of $|1/(1+Y_p Y_A)|^2$. Since the spectrum is essentially flat out to ω_h'', changes in turbulence bandwidth are unlikely to substantially affect the rms magnitude of altitude response.

Task Performance and Control Workload - Considerable evidence exists in pilot commentary and in the measures of the precision of task performance and the pilot's control workload to indicate a dominant relationship between performance-workload and pilot rating. This relationship is particularly strong between control workload and pilot rating. Similar behavior was also noted in Reference 1 for bank angle and heading control in turbulence. Pilot rating data for configurations in the current program are plotted against the available data for rms elevator stick activity and rms pitch attitude in Figure 48. These data reflect a range in pilot rating from 2.8 to 6.0, that is from a satisfactory airplane to an unsatisfactory and very objectionable vehicle. Corresponding variations in elevator workload and precision of pitch control are

$$\left.\begin{matrix} .26 \text{ in} \\ \\ 1.3 \text{ lbs} \end{matrix}\right\} \leq \sigma_{\delta_s} \leq \left\{\begin{matrix} 1.04 \text{ in} \\ \\ 5.3 \text{ lbs} \end{matrix}\right. \qquad 1.4 \leq \sigma_\theta \leq 4.75 \text{ deg}$$

Correlation between pilot rating and elevator workload show a scatter of ±.8 rating units in the extreme or, if the two lowest points are neglected, ±.6 units. Rms pitch excursions correlate with pilot ratings to within ±1.0 unit. The POR - σ_{δ_s} correlation is reasonably good and, interestingly enough, it closely resembles the pilot rating correlation with aileron workload shown in Reference 1 in that the POR - σ_δ gradient and rating scatter are similar.

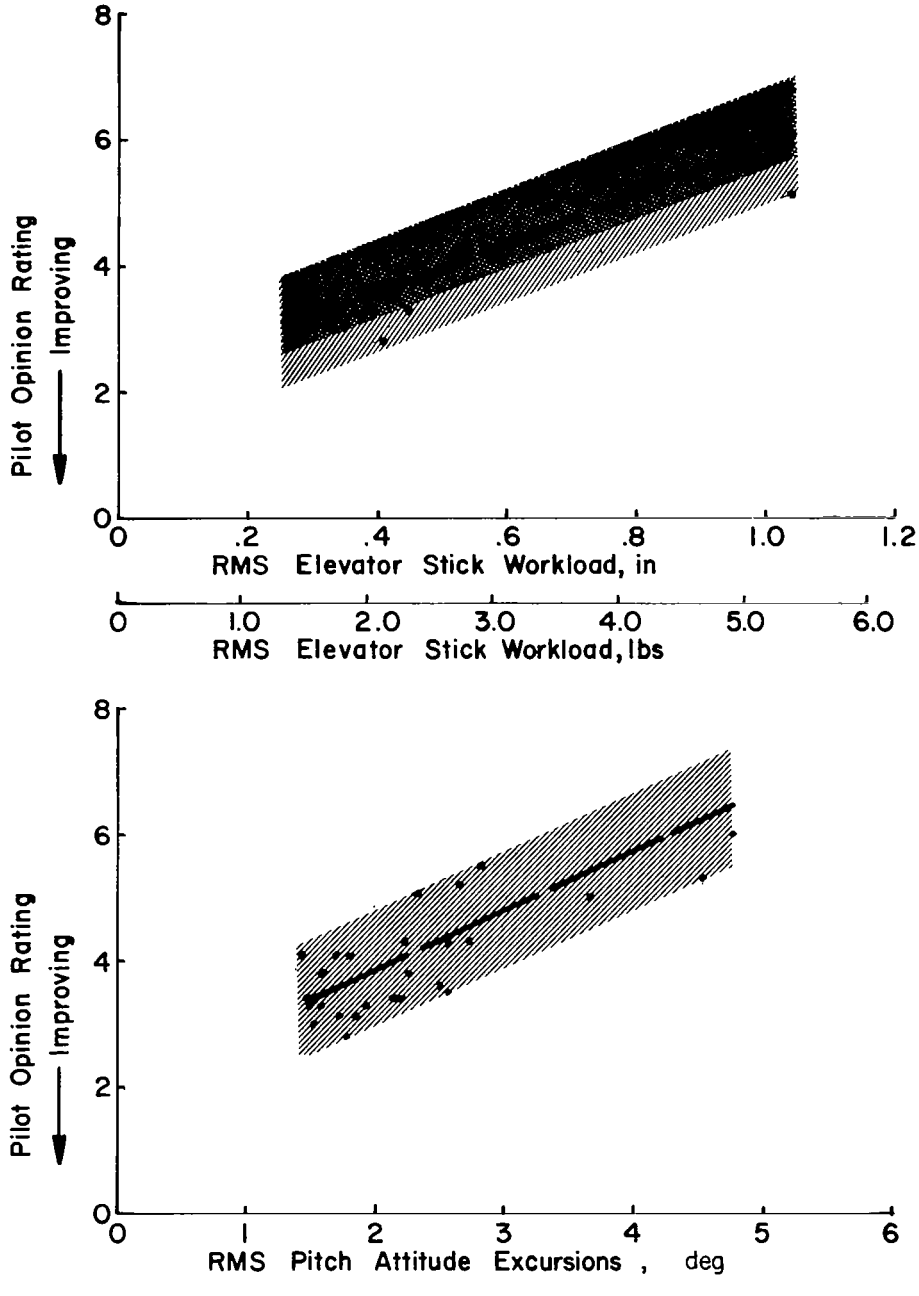

Figure 48. Trends of Pilot Rating with Elevator Workload and Pitch Attitude Performance

An objective of the analytical program was to obtain an understanding of the relationships between these measures of performance and workload and the parameters of the pilot model, the turbulence, and the longitudinal dynamics. To this end, predictions of rms pitch attitude, altitude, and stick activity have been made based on the closed loop analysis set out in the preceding pages. Rms magnitudes (σ) were defined by

$$\sigma_i^2 = \int_0^\infty \Phi_i(\omega)\, d\omega \tag{54}$$

where the integral was evaluated using the solution technique (Phillip's integrals) discussed in Reference 13. The approach described therein involves complex integration of a function of the form

$$I = \frac{1}{2\pi j} \int_{-\infty}^{\infty} \frac{c(j\omega)\, c(-j\omega)}{d(j\omega)\, d(-j\omega)}\, d(j\omega) \tag{55}$$

where $c(j\omega)/d(j\omega)$ and $c(-j\omega)/d(-j\omega)$ are the Fourier transform and its complex conjugate of the particular response whose power spectrum, Φ_i, appears in equation (54).

Raw data from this solution were first plotted to show the tradeoff between rms performance (σ_θ) and workload (σ_{δ_s}) as a function of lead compensation. Cross-plots of σ_{δ_s} and T_{L_θ} were then made assuming a constant level of σ_θ to assess the tradeoff between workload and compensation. Finally, values of the rms performance-workload measures were chosen for a particular closed loop bandwidth and lead compensation and then plotted to show the effects of variations in turbulence and dynamics. Root locus and Bode analyses are presented along with the performance-workload data to show the closed loop control characteristics of each dynamics configuration. The format of this presentation parallels that of the flight test data discussion. To reiterate, the items emphasized in that discussion were

- contributions of turbulence, considering effects of pitch and heave disturbance magnitude, bandwidth and correlation for one (good) set of dynamics,
- effects of short period frequency in combination with disturbance magnitude and bandwidth,
- effects of short period damping in combination with pitch disturbance magnitude and bandwidth, and
- effects of lift curve slope in combination with disturbance magnitude and bandwidth.

Contribution of turbulence - Configuration 1

The first consideration in the analytical study involves the effects of turbulence for the case of good longitudinal dynamics (Configuration 1). Closed loop pitch control characteristics are discussed first and then the independent influences of pitch and heave disturbance magnitude and turbulence bandwidth on predicted precision of performance and control workload are evaluated.

The favorable pitch attitude control characteristics of this configuration are evident in the root locus and Bode plots of Figure 49. The effects of varying amounts of the pilot's lead compensation may be noted. On the root locus plot, only the short period branch is shown for all three values of T_{L_θ}. The phugoid branch and the other branch of the locus on the real axis are not affected to any significant degree by lead time constant and to avoid the confusion of three overlapping loci on the real axis, only the case for $T_{L_\theta} = .25$ seconds is shown. Increasing lead compensation improves the damping of the closed loop short period roots and serves to create a K/ s type of system in the region of crossover. Adequate bandwidth and stability margin exist for low values of lead compensation. In particular, for $T_{L_\theta} = .25$ seconds the crossover frequency ($\omega_{co} = \omega_{db=0}$) is 4.0 radians/ second with a phase margin of 35 degrees and a gain margin of 6 db. Adequate low frequency gain is available for suppressing the phugoid mode and for attenuating any disturbance inputs in this frequency range.

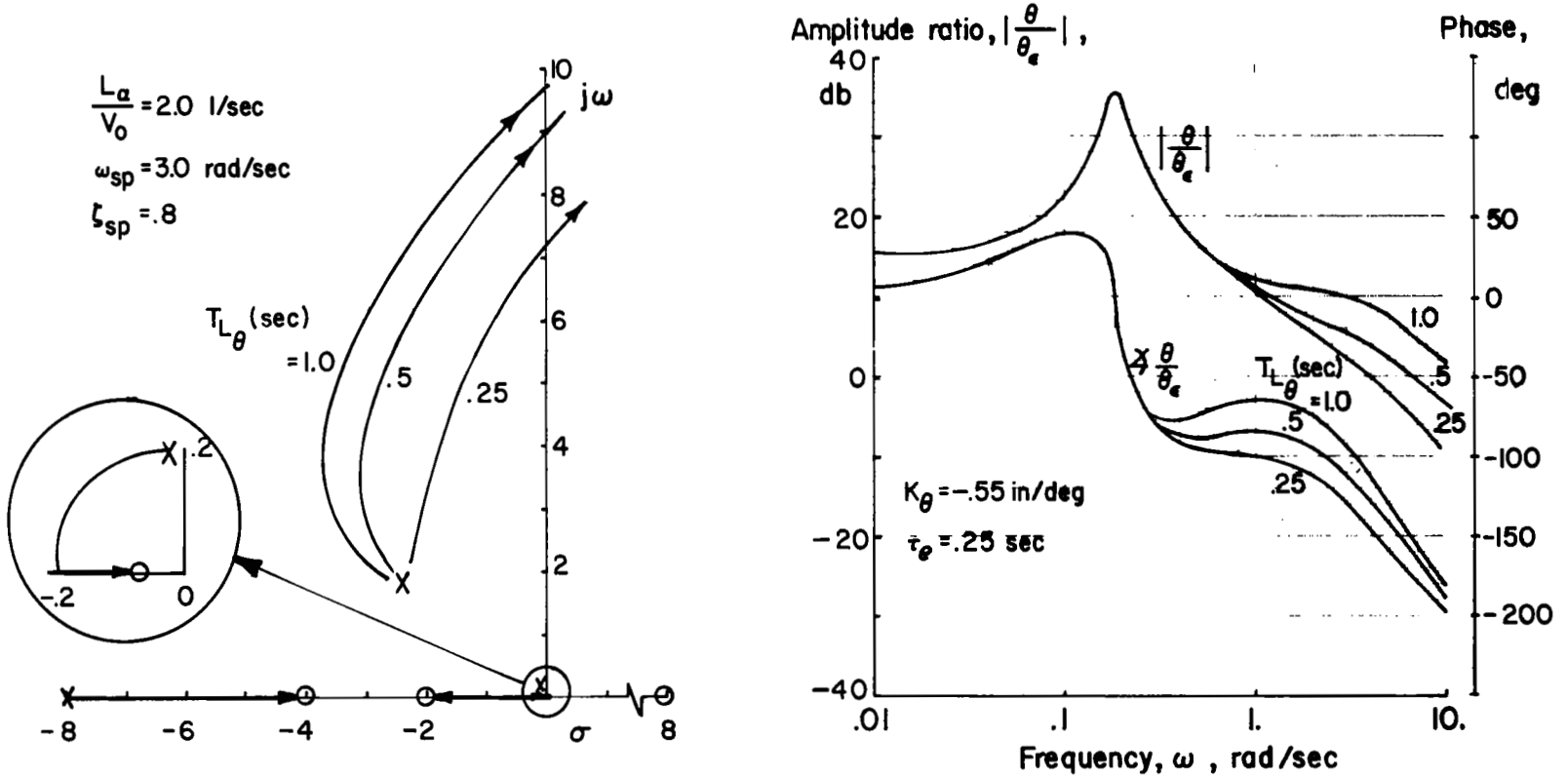

Figure 49. Pitch Attitude Control with Elevator - Configuration 1

From this root locus and Bode analysis, the choice of lead compensation is not obvious. The effects of lead are more apparent in Figure 50. The tradeoff between pitch attitude excursions due to heave turbulence and the pilot's control workload is shown in this figure for four values of T_{L_θ} for a particular set of dynamics and turbulence characteristics. As would be expected, pitch attitude precision (σ_θ) may be improved if the pilot increases his effort (σ_{δ_s}), at least up to a point approaching closed loop instability. The effect of lead compensation is indicated in the inset diagram, assuming a constant level of pitch attitude precision, σ_θ = .4 degrees. Lead compensation has no profound effect on the pilot's workload, and what influence is apparent is adverse with increasing lead compensation. It would therefore seem best to have little or no lead compensation in the pitch attitude loop for this configuration, and a value of T_{L_θ} = .25 seconds will be used hereafter for Configuration 1.

While there is evidence from fixed base simulator data to suggest a pilot gain which produces a crossover frequency on the order of 4.5 radians/second for pitch attitude control (Reference 11), other closed loop analyses seem to favor lower closed loop gains and hence lower crossover frequencies (References 6, 14, 15, and 16 among others). Crossover frequencies as low as 2.0 radians/second have been used for the inner loops ($\theta \rightarrow \delta e$, $\varphi \rightarrow \delta a$) of these analyses. An indication of the effect of closed loop bandwidth on the prediction of pitch attitude excursions and control workload is presented in Figure 51. Longitudinal dynamics again are constant. The performance-workload tradeoff is shown for varying levels of pitch disturbances while the other turbulence characteristics are again constant. The range of crossover frequencies between 2.0 and 4.5 radians/second brackets the region of the knee of the $\sigma_\theta - \sigma_{\delta_s}$ curve. It is in this region that the pilot would be expected to achieve the best return for his effort, that is, the most significant reduction in pitch excursions without an excessive workload. The tails of the tradeoff curve imply either that the pilot is taking it easy and paying an inordinate penalty in pitch attitude precision, or that he is working too hard without achieving a commensurate improvement in pitch precision. From

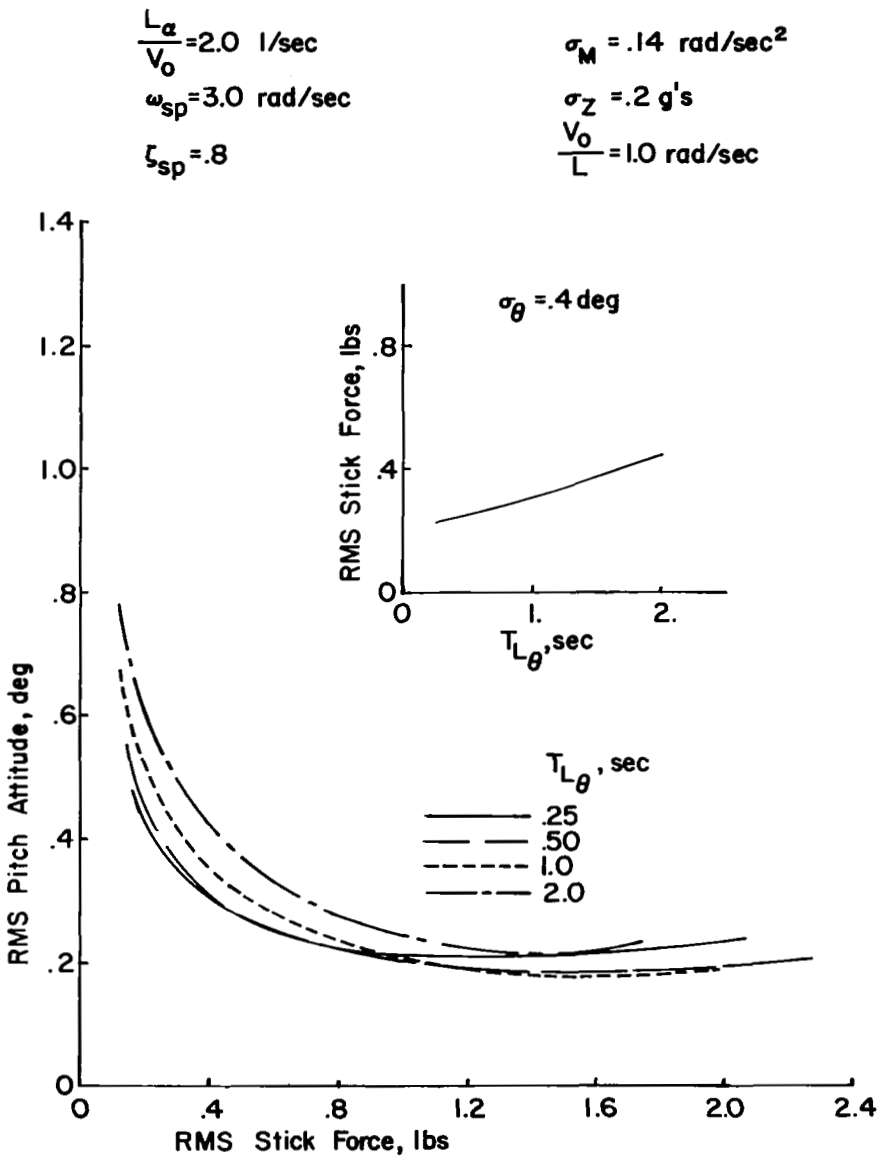

Figure 50. Tradeoff Between Pitch Attitude Precision and Stick Workload - Configuration 1

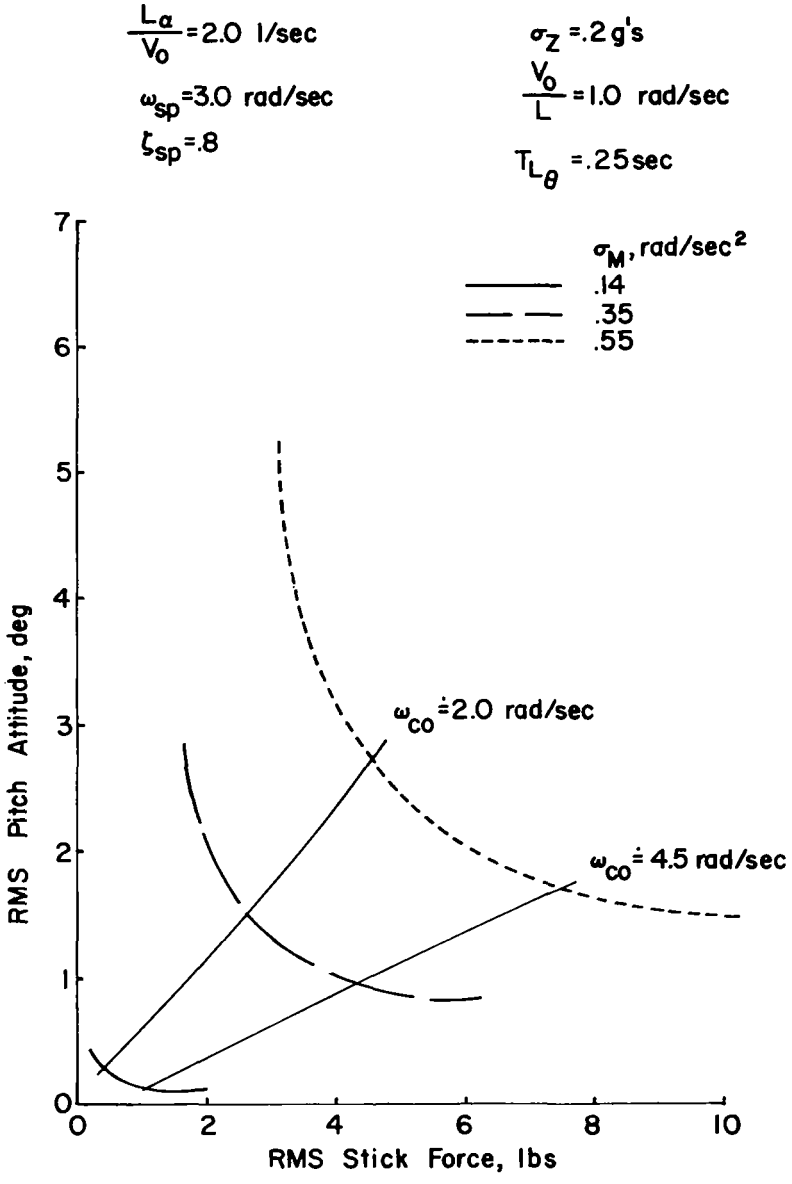

Figure 51. Effect of Crossover Frequency on Closed Loop Performance and Workload

the point of view just mentioned, it is reasonable to expect the pilot to close the pitch attitude loop at a gain corresponding to the region roughly defined by $2.0 \leq \omega_{co} \leq 4.5$ radians/second. Based on the simulator data of Reference 11, the higher value of crossover frequency, $\omega_{co} \doteq 4.5$ radians/second, will be used in the subsequent analyses of the pitch attitude loop.

Altitude control characteristics, assuming a pitch attitude inner loop as described in the foregoing discussion, are shown in Figure 52. A bandwidth corresponding to a crossover frequency from 1.0 to 2.0 radians/second with phase margins from 20 to 60 degrees is possible. Subsequent data which utilizes the altitude loop closure corresponds to a crossover frequency, $\omega_{co} =$ 1.0 radian/second.

Predictions of task performance and control workload, including rms pitch attitude and stick force for a $\theta \rightarrow \delta e$ loop alone and rms altitude and stick force for a series loop closure of $\theta \rightarrow \delta e$ and $h \rightarrow \theta_c \rightarrow \delta e$, are presented in Figures 53, 54, and 55. The effects of pitch disturbances on performance and workload are shown in Figure 53. Strong trends are predicted in rms pitch attitude, stick force, and altitude excursions with pitch disturbance magnitude. The trends are comparable to those observed in the flight test data of Figure 17. For the extreme disturbance ($\sigma_M = .55$ rad/sec^2), rms stick force predictions are higher than flight values while predicted pitch attitude excursions are lower than flight test data, which suggests that the pilot may be closing the $\theta \rightarrow \delta e$ loop at a lower gain (lower ω_{co}) than assumed in this analysis. Altitude excursions are not excessive, although the maximum excursions reached (assuming $h_{max} \doteq 4\sigma_h$) could be on the order of 30 to 40 feet. The effects of heave disturbances and spectral bandwidth are insignificant in comparison to the adverse influence of pitch disturbances on performance-workload. Heave disturbances primarily cause a degradation in altitude tracking performance, and this effect, as shown in Figure 54, is only minor. Neither pitch attitude precision nor control workload suffer from the increase in heave disturbances. Spectral bandwidth shows only a minor influence on control workload in Figure 55. Pitch attitude precision is not affected by changes in bandwidth over the range corresponding to

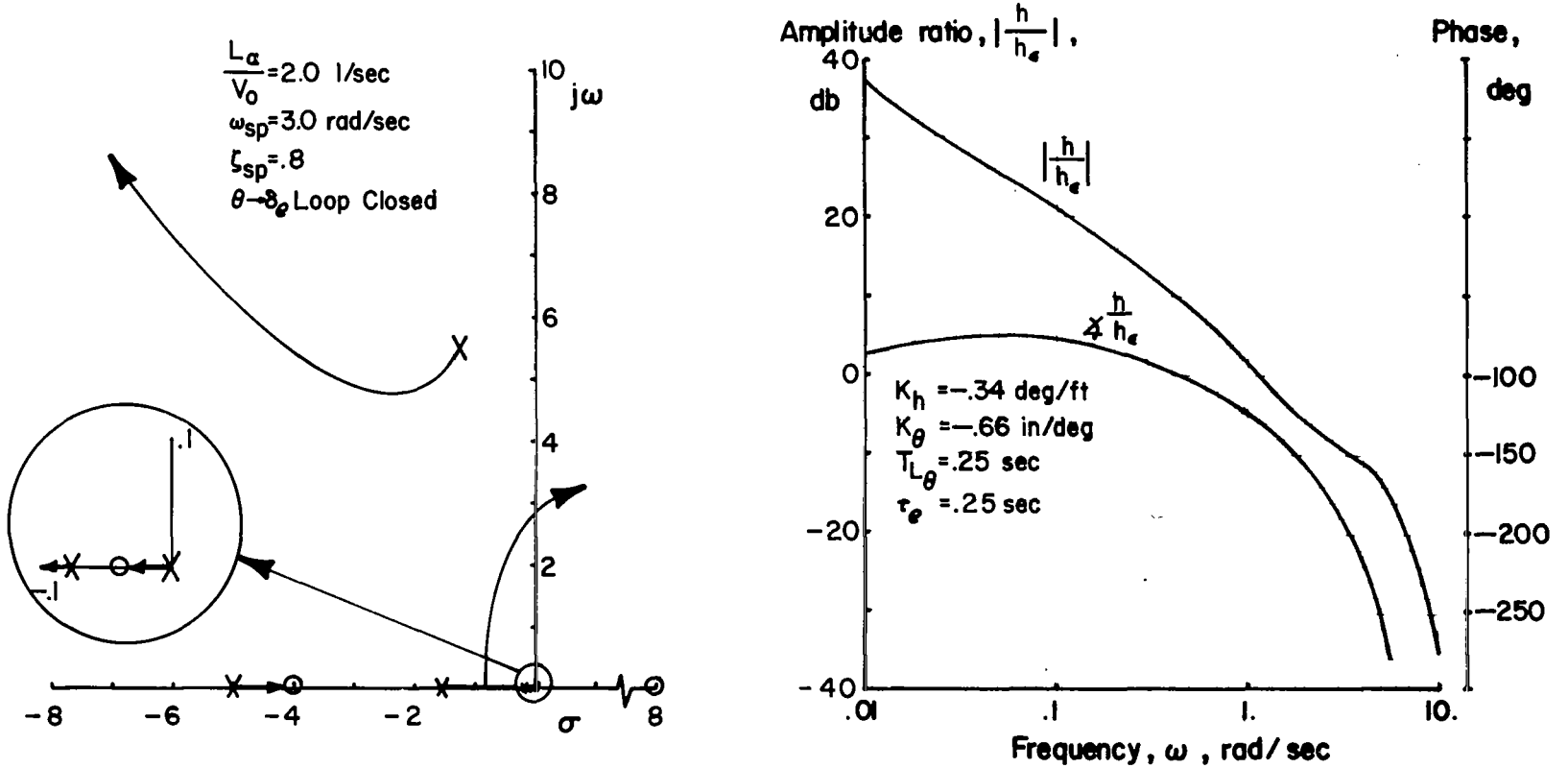

Figure 52. Altitude Control with Elevator - Configuration 1
($\theta \rightarrow \delta_e$ Loop Closed)

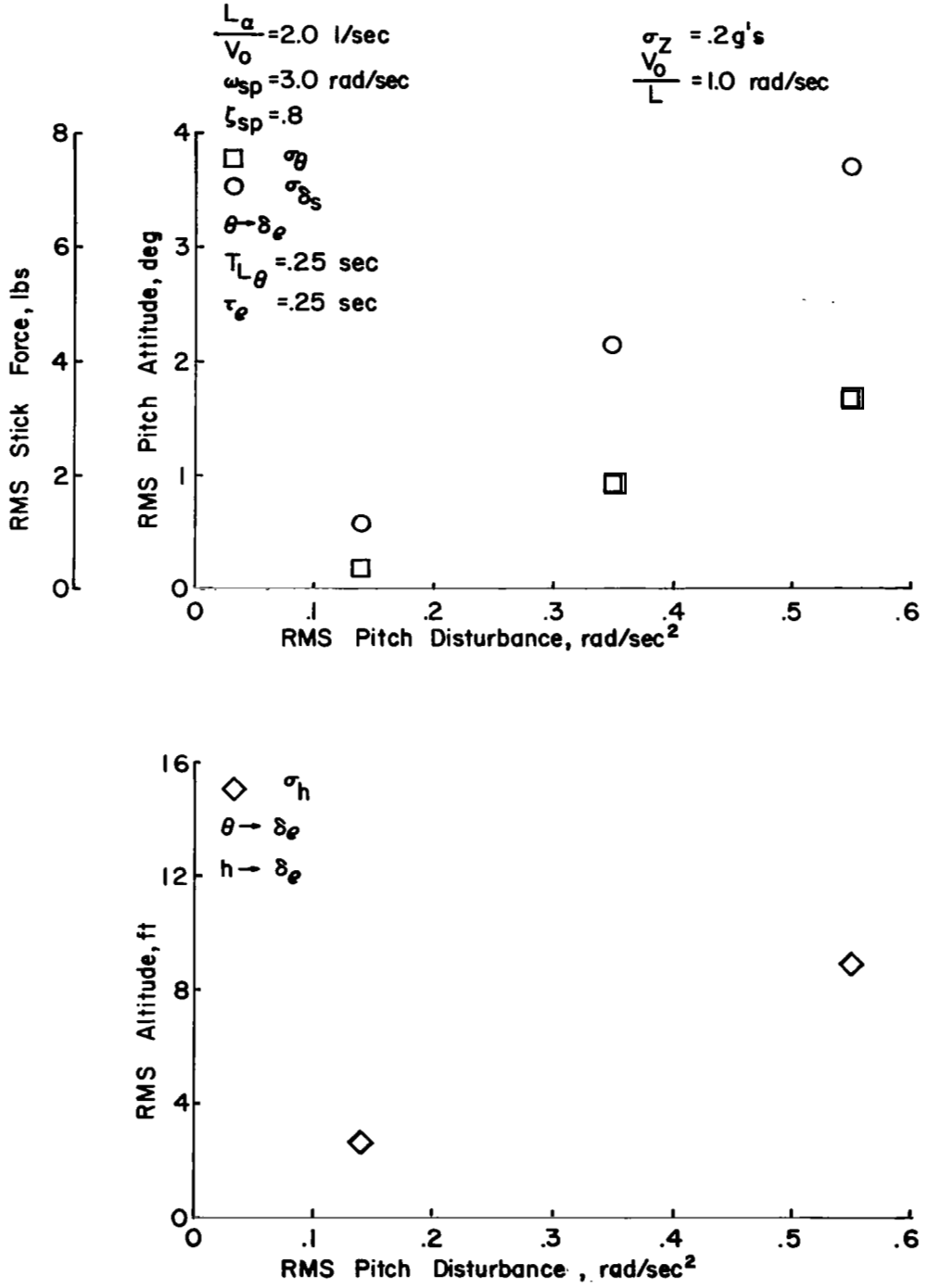

Figure 53. Predicted Effect of Pitch Disturbances on Task Performance and Control Workload - Configuration 1

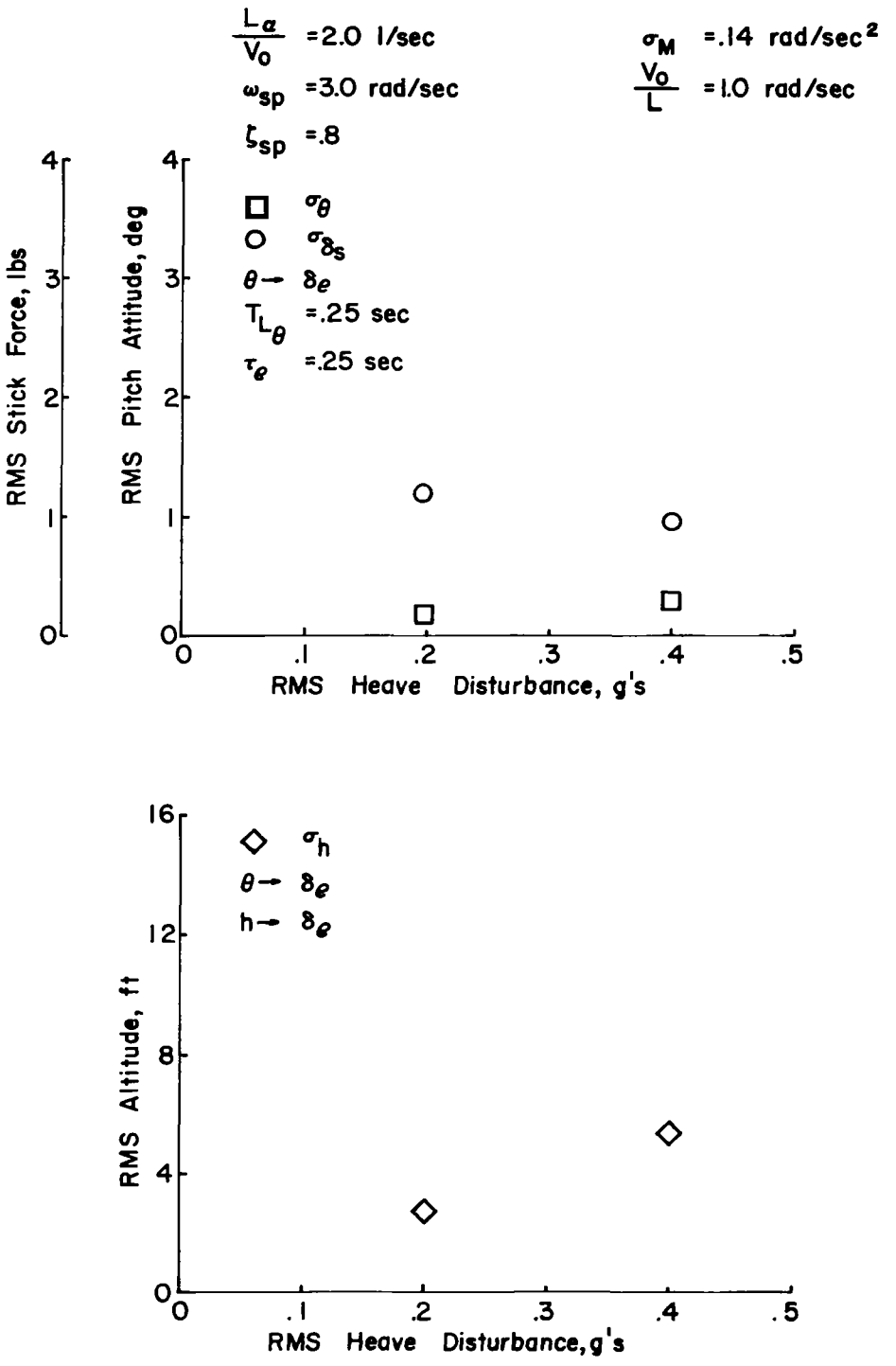

Figure 54. Predicted Effect of Heave Disturbances on Task Performance and Control Workload - Configuration 1

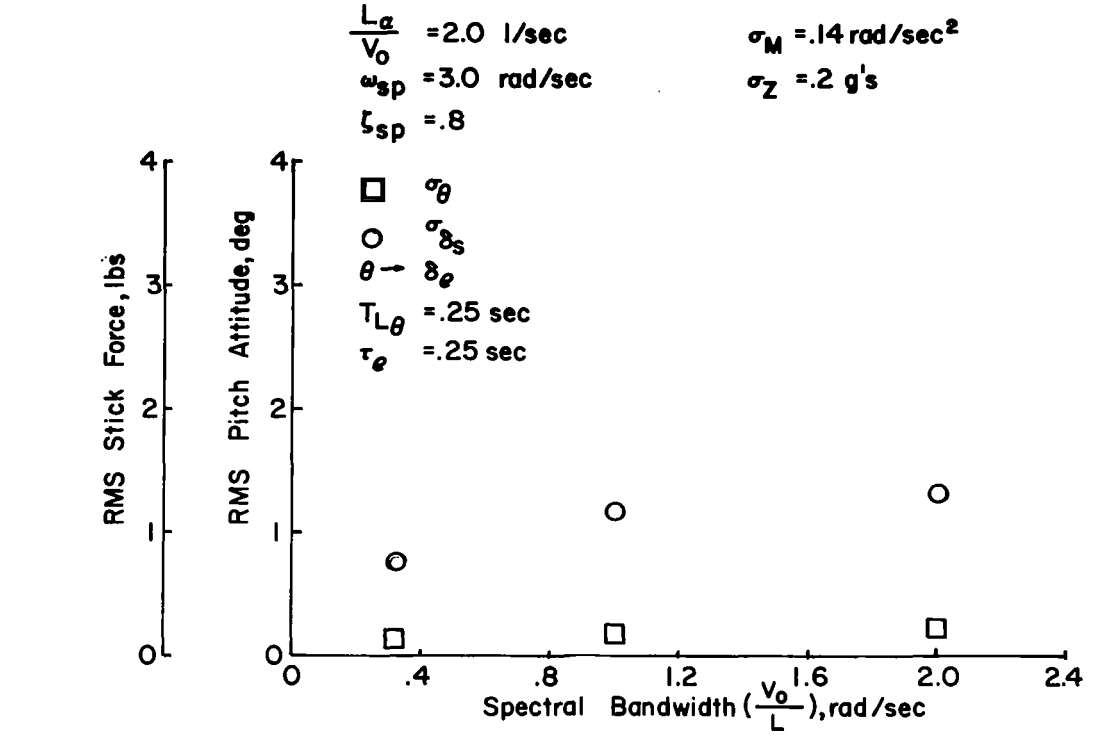

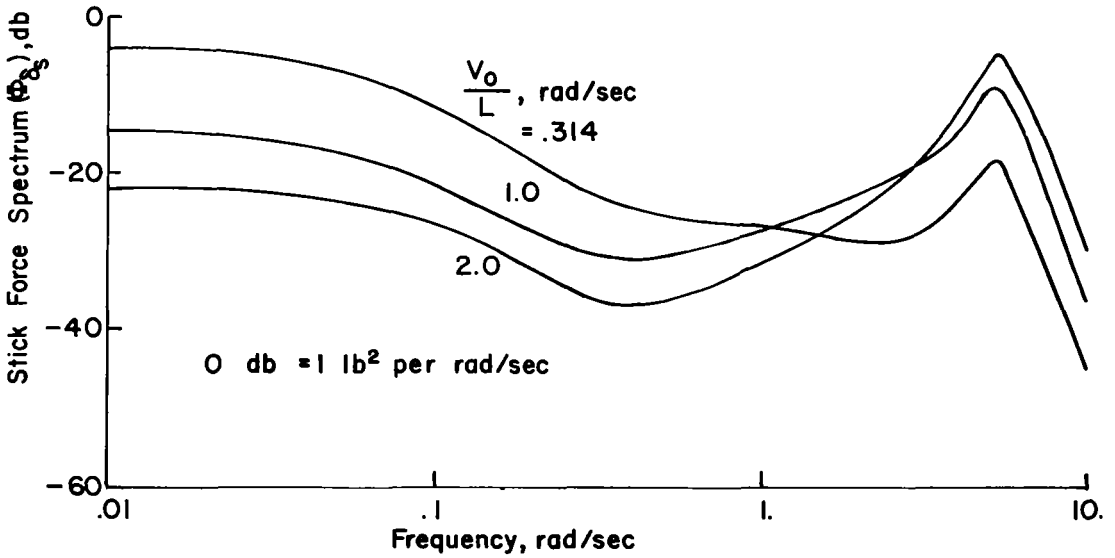

Figure 55. Predicted Effect of Spectral Bandwidth on Task Performance and Control Workload - Configuration 1

$V_o/L = .314$ to 2.0 radians/second. What little adverse effect there is from increasing bandwidth is explained by the increase in energy in the region of the peak of the power spectrum of stick force shown in the lower diagram.

To summarize the independent contributions of turbulence to longitudinal flying qualities for the ILS approach, the magnitude of pitch disturbances is the dominant influence on the pilot's evaluation of the task. Control workload increases considerably and pitch attitude precision deteriorates with increasing pitch disturbances. Pilot commentary focuses on these two factors as the reason for degraded flying qualities. The degradation is confirmed by in-flight measures of rms pitch excursions and control activity and also by predictions of σ_θ and σ_{δ_s} using closed loop pilot-airplane systems analysis. For extremely large pitch disturbances, the poor control of pitch attitude made it difficult to stay on the glide slope and to hold airspeed. Increasing heave disturbances (keeping in mind the limitation in the simulation, $\Delta Z_{max} \doteq .5$ g's) did not affect the pilot's evaluation seriously. The adverse effect of increasing heave disturbances related to a slight degradation in glide slope tracking and to the increasing distraction and discomfort associated with the increased level of normal acceleration. No deterioration in pitch attitude precision or workload is either observed in flight or predicted by the closed loop analysis.

The effect of turbulence bandwidth is much more modest than the effect of disturbance magnitude. The slight deterioration in pilot rating with increasing bandwidth for a constant rms disturbance level is attributable to an increase in high frequency pitch attitude excursions which the pilots were unable to suppress satisfactorily. When the level of the pitch disturbance was sufficient to make these pitch attitude excursions a distraction to glide slope tracking, the pilot's rating deteriorated slightly.

High frequency attenuation of the turbulence spectrum, associated with the corner frequency at $\omega_{w_2} = V_o/\sqrt{bc}$, had no influence on the pilot's evaluation of the ILS task. Pitch-heave correlation was also of little or no consequence to pilot ratings.

Contribution of short period frequency

It has been noted previously in this report that short period frequency, or equivalently angle of attack stability, affects the pilot's ability to control pitch attitude precisely. Reductions in short period frequency apparently have an adverse effect on pitch attitude control. This subsection will concentrate on the effects of short period frequency, particularly as concerns the low frequency configuration which has a slight static angle of attack instability (Configuration 2). Combined effects of turbulence and dynamics, specifically the influence of pitch disturbance magnitude and spectral bandwidth,will be considered.

A root locus and Bode diagram of the pitch attitude control loop for the low short period frequency configuration is shown in Figure 56. The static instability associated with M_{α} = + 1.0 radians/ second^2 per radian is evident in the positive real root in the vicinity of the origin. By controlling pitch attitude excursions with the elevator the pilot can easily stabilize the divergent mode. In other respects, the pitch attitude to elevator loop seems satisfactory. Adequate bandwidth and stability margin is achieved, even for low levels of lead compensation. For example, with T_{L_θ} = .25 seconds, the crossover frequency is approximately 3.5 radians/ second and the phase margin is 20 degrees. While this crossover frequency and phase margin are not as large as those of Configuration 1 for low lead compensation, they are sufficient for good pitch control. Increasing lead compensation permits higher crossover frequencies for the same phase margin or, conversely, an increase in phase margin for the same open loop bandwidth. Low frequency gain is more than adequate to provide precise pitch attitude control and suppression of disturbances in the frequency range below crossover. The difficulty associated with the longitudinal dynamics of this configuration must be attributed to the open loop instability. The unattended behavior of the airplane is objectionable since the airplane has no natural restoring tendency in the presence of disturbances. Thus the pilot is required to continually

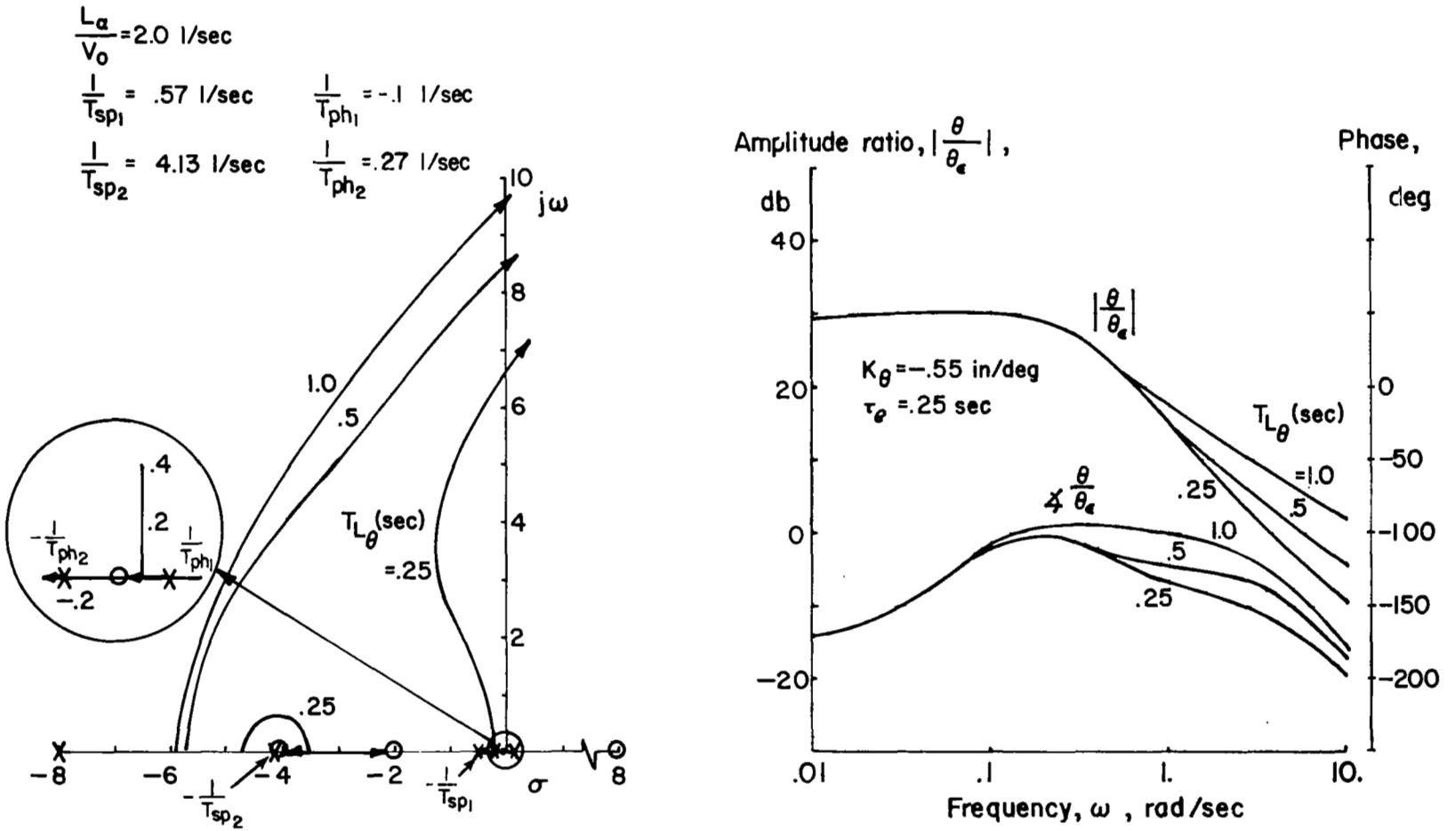

Figure 56. Pitch Attitude Control with Elevator - Configuration 2

make corrections for pitch attitude and airspeed excursions excited by turbulence. This imposes an additional workload on the pilot in the form of increased control activity and the necessity that he pay constant attention to the longitudinal control situation.

The choice of lead compensation for subsequent loop closures and for the prediction of performance and workload is made on the same basis as for Configuration 1. The effect of lead compensation on the performance-workload tradeoff is shown in Figure 57 for one set of turbulence characteristics. Somewhat of an improvement in control workload is obtained with increasing lead compensation up to approximately $T_{L_\theta} = .5$ seconds. The inset diagram shows the favorable effect of lead compensation for pitch attitude excursions held constant either at an rms value of 1.0 or 3.0 degrees. On this basis, lead compensation of $T_{L_\theta} = .5$ seconds will be used in the analyses to follow for Configuration 2.

Characteristics of altitude control with the elevator, assuming a pitch attitude to elevator inner loop, are indicated in Figure 58. The pitch attitude loop is closed for a bandwidth of 4.5 radians/second. Altitude control characteristics are as good as those shown in Figure 52 for Configuration 1. For a crossover frequency of 1.0 radian/second, the corresponding phase margin is approximately 60 degrees. Hence, so long as the pilot controls pitch attitude tightly enough to stabilize the divergent real root, good altitude control with the elevator should be possible. Subsequent predictions of altitude excursions due to turbulence will be made assuming a pitch attitude loop closure as previously described and an altitude loop with a crossover frequency of approximately 1.0 radian/second.

It was noted in pilot commentary for Configuration 2 that airspeed excursions presented some difficulty for the approach. If the airplane is left completely unattended, airspeed will obviously diverge from the trim approach speed due to the static instability of this configuration. Precise control of pitch attitude removes this instability and should improve speed stability in the approach. Should further control of speed be required, an airspeed to

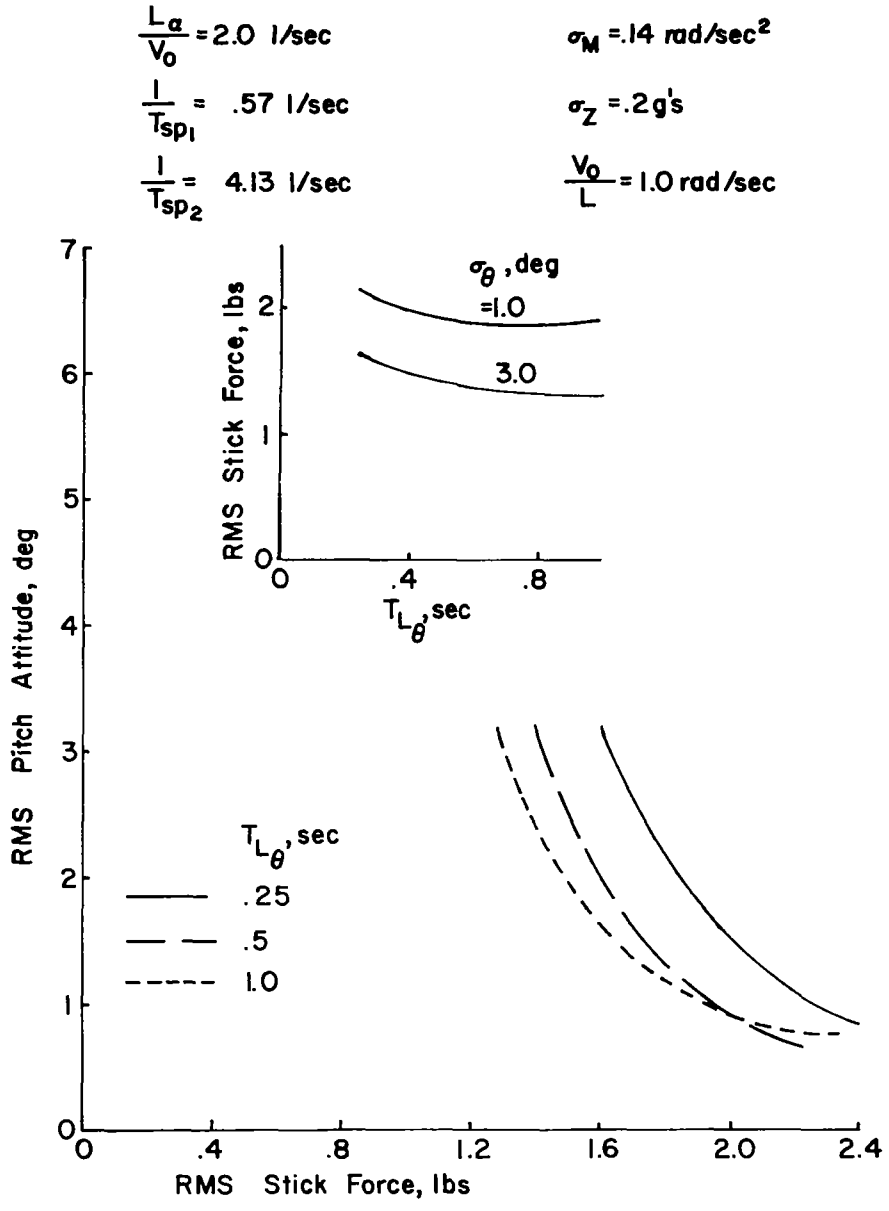

Figure 57. Tradeoff Between Pitch Attitude Precision and Stick Workload - Configuration 2

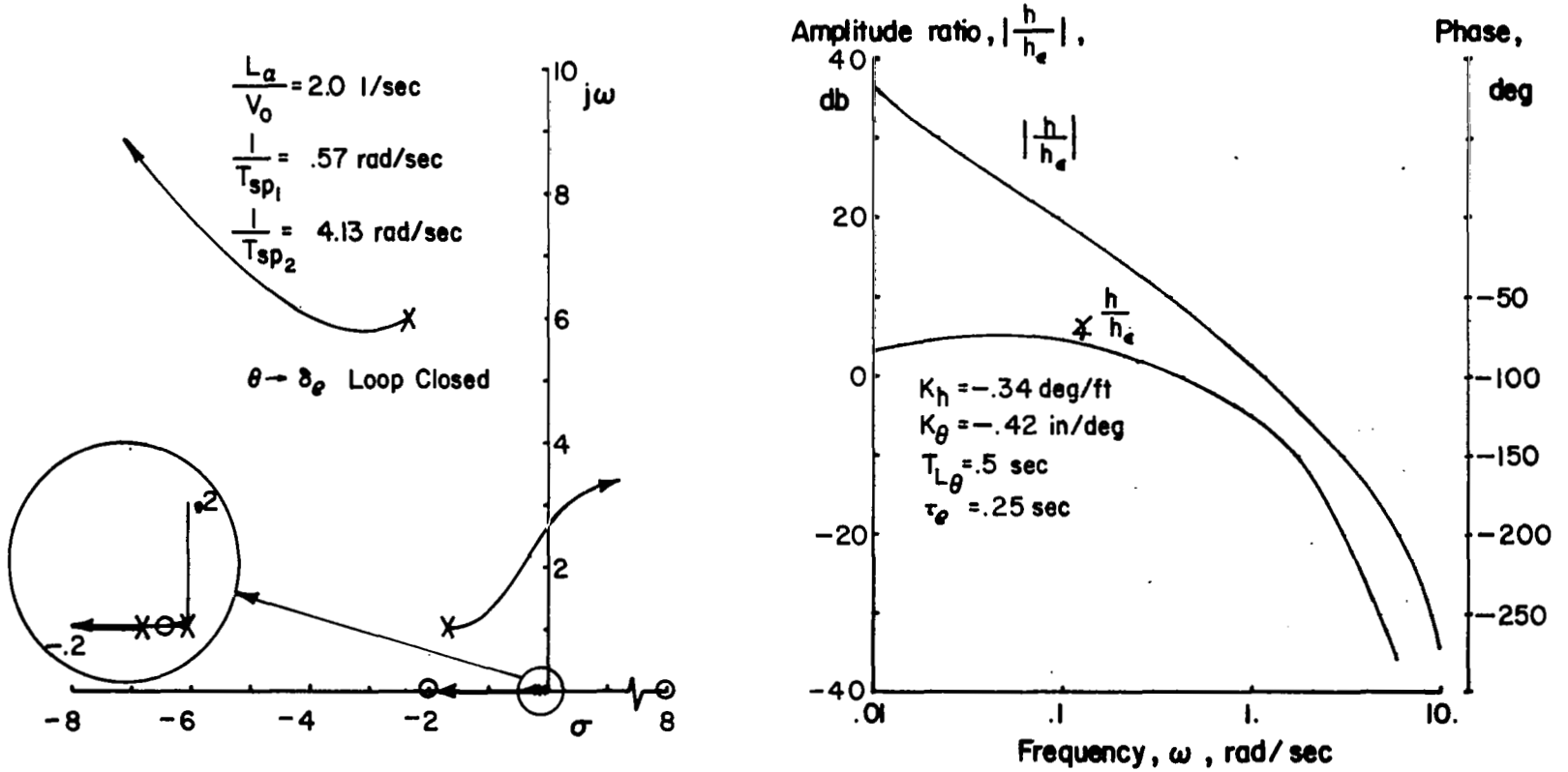

Figure 58. Altitude Control with Elevator - Configuration 2
($\theta \rightarrow \delta_e$ Loop Closed)

throttle loop provides a satisfactory control over speed excursions. In the flight test program, the pilots indicated they used power to control speed during the approach for this configuration. Effectiveness of the throttle control is evident in the root locus and Bode diagrams of Figure 59. For a pilot model corresponding to a pure gain and a time delay, i.e., $Y_{p_u} = K_T e^{-\tau_e s}$, and assuming no thrust lag to throttle inputs, the airspeed loop is quite satisfactory. High bandwidths and adequate phase margins are attainable, although it is unlikely that the pilot would ever need to control airspeed so tightly. The objection to airspeed control problems must then be attributed to the necessity of monitoring airspeed and of having to use an additional control during the approach. However, when the use of power is required, and given the rapid response of the reciprocating engine, the throttle would be expected to provide satisfactory control over airspeed.

Predictions of task performance and control workload are shown in Figures 60, 61, and 62 as functions of short period frequency, pitch disturbance magnitude, and spectral bandwidth. Rms pitch attitude excursions, stick force, and altitude excursions are shown for pitch attitude and altitude loop closures as described previously. The degradation in precision of pitch attitude and altitude control, and the increased workload which accompany the reduction in short period frequency correspond to the trends noted in the flight data. Turbulence characteristics are held constant for this comparison. In Figure 61, the combined effects of short period frequency and pitch disturbance magnitude are shown. Heave turbulence and spectral bandwidth are held constant. The increase in pitch attitude and altitude excursions with pitch disturbance magnitude is essentially the same for the low and intermediate frequency configurations (ω_{sp} = 1.5 and 3.0 rad/sec). Recall that the lead compensation used for the lower frequency configuration is greater than for the higher frequency case (T_{L_θ} = .5, ω_{sp} = 1.5 compared to T_{L_θ} = .25, ω_{sp} = 3.0). If the same lead compensation was used for both configurations (T_{L_θ} = .25), the degradation in pitch attitude precision and stick workload with increasing pitch disturbances would be greater for the low frequency airplane. At the highest

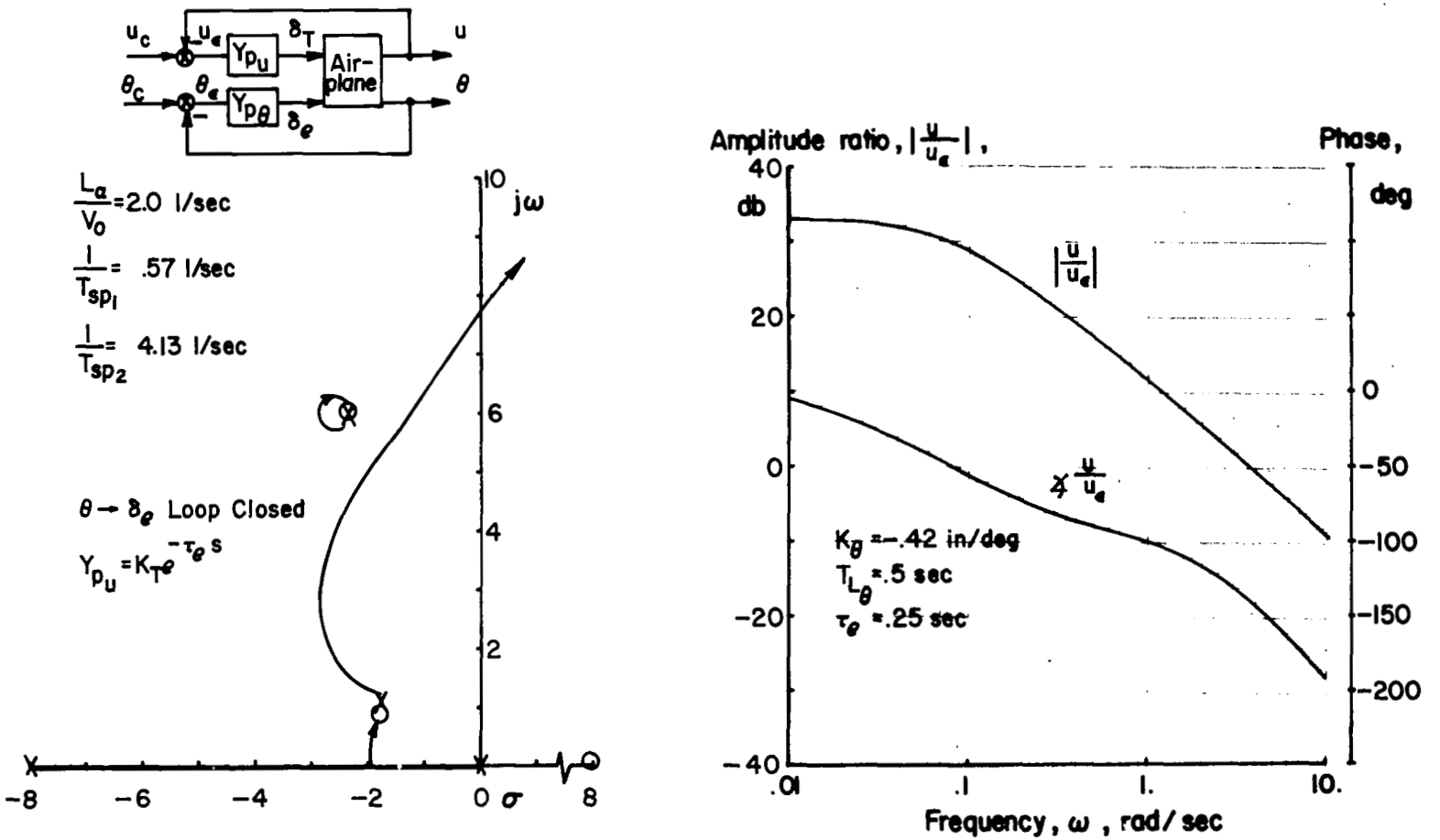

Figure 59. Airspeed Control with Throttle - Configuration 2
($\theta \rightarrow \delta_e$ Loop Closed)

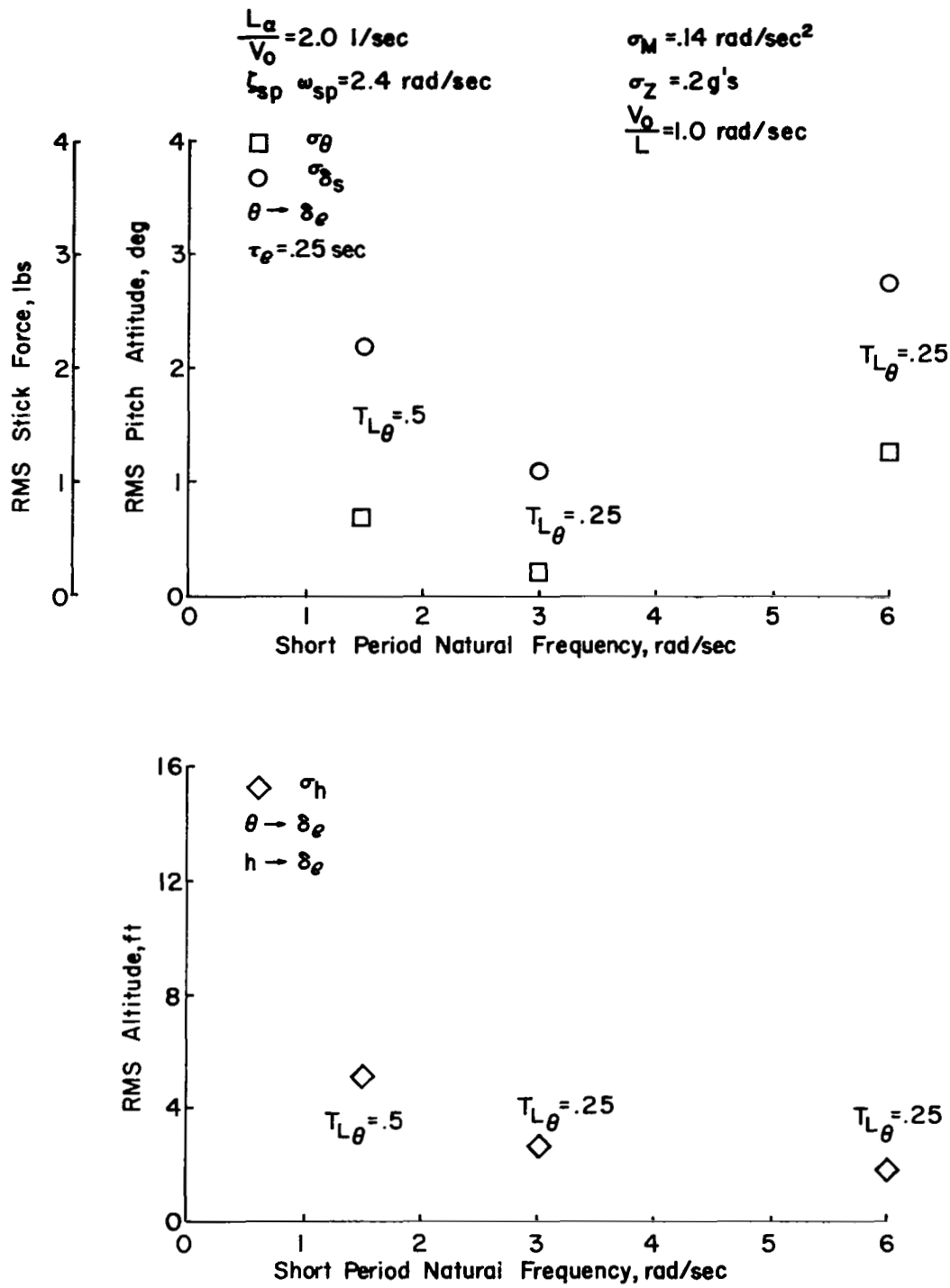

Figure 60. Predicted Effects of Short Period Frequency on Task Performance and Control Workload

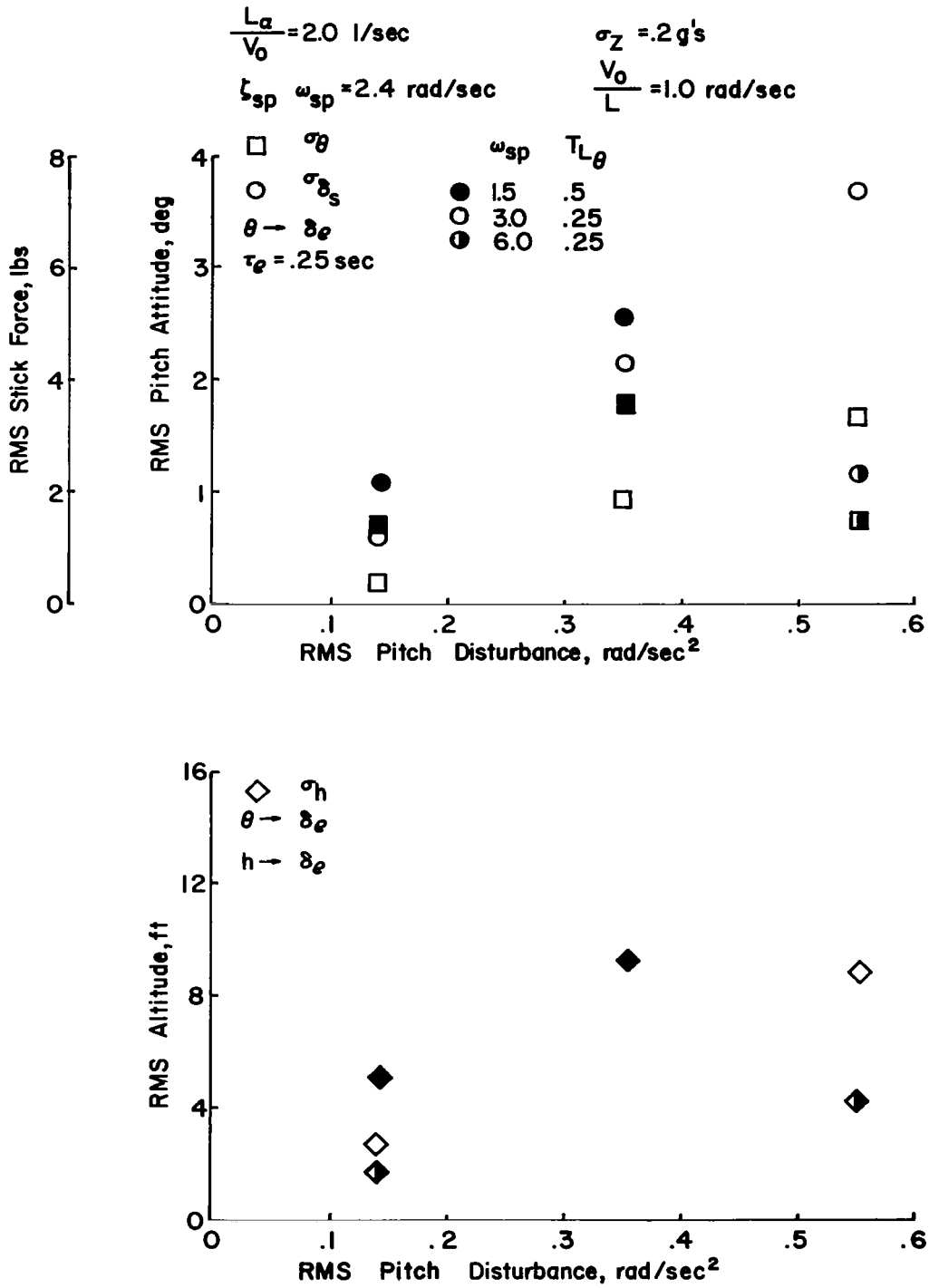

Figure 61. Combined Effects of Short Period Frequency and Pitch Disturbances on Predicted Task Performance and Control Workload

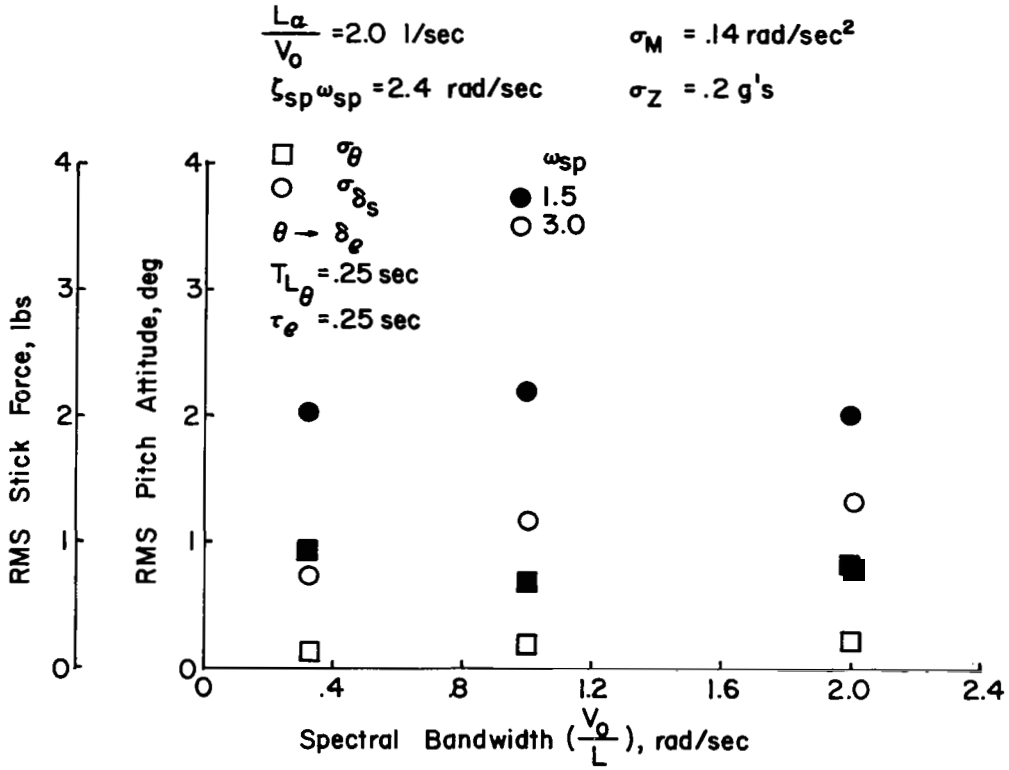

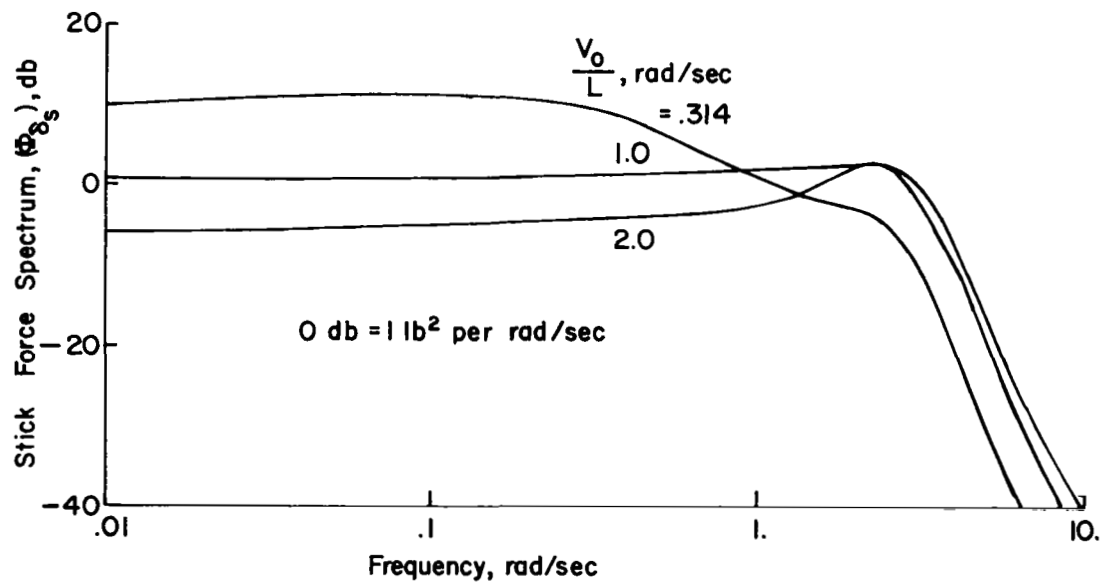

Figure 62. Combined Effects of Short Period Frequency and Spectral Bandwidth on Predicted Task Performance and Control Workload

disturbance level, note the improvement in pitch attitude precision and stick workload when the short period frequency is increased to 6.0 radians/second. Finally, it may be observed in Figure 62 that the influence of spectral bandwidth is essentially the same for either the low or high frequency airplane. This comparison is made for $T_{L_\theta} = .25$ seconds for both the low and high ω_{sp} configurations. In neither case does bandwidth affect pitch attitude precision or stick workload to any great extent. Plots of the closed loop stick force spectrum are shown in the bottom diagram for the three turbulence bandwidth cases for Configuration 2. The absence of a dominant peak at high frequency makes the control activity spectrum relatively insensitive to increases in high frequency energy of the disturbances.

Reviewing this subsection and its counterpart from the section containing flight test results, it may be concluded that reducing the short period frequency to levels approaching the condition of static angle of attack instability degrades flying qualities for the ILS approach. This degradation is caused by a deterioration in the precision of pitch attitude and airspeed control which accompanies the reduced static stability. Conversely, if the pilot is to achieve satisfactory pitch attitude control, he must devote continual attention to that objective. It may also be necessary to continuously monitor airspeed during the approach, using the throttle as the primary means of control. The end result is an increase in the pilot's workload over that required for satisfactory longitudinal configurations, e.g., Configuration 1.

Combined influences of short period frequency and pitch disturbance magnitude can best be summarized by saying that an increase in static stability is desirable when pitch disturbances are increased. The degradation in flying qualities for the approach which accompany increasing pitch disturbances is more pronounced when the short period frequency (static stability) is low, as evidenced by pilot ratings and supported by flight test measures and analytical predictions of the precision of task performance and control workload. When short period frequency and pitch disturbance magnitude are interrelated through the static angle of attack stability derivative

(i.e., $M_{\alpha_w} = M_{\alpha_{g_w}}$, $M_{\alpha_t} = M_{\alpha_{g_t}}$), the net result from changes in static stability is a degradation in flying qualities at either the low or high levels of short period frequency tested in this program. For low frequency configurations, problems with pitch attitude control override the favorable influence of the reduced pitch disturbance level. At high frequency, large pitch disturbances and annoying high frequency pitch excursions excited by turbulence or control inputs combine to make the airplane objectionable.

Finally, the influence of turbulence bandwidth is of minor importance compared to the effects of either short period frequency or pitch disturbances. Somewhat of a degradation in flying qualities occurs with increasing turbulence bandwidth, particularly if pitch disturbances are large. However, for either the low or high short period frequency configurations, the effect of turbulence bandwidth, as evident in pilot ratings or from predictions and flight test measures of performance-workload data, is of little consequence to the ILS task.

Contribution of short period damping

It was noted in the flight test program that a reduction in short period damping to a level corresponding to nearly neutral pitch damping (Configuration 5; $M_{\dot{\theta}} \doteq 0$, $\zeta_{sp} = .5$ for $\omega_{sp} = 3.0$ rad/sec) had no appreciable influence on flying qualities for the ILS approach. Referring to the root locus and Bode plots for Configuration 5 shown in Figure 63, no significant changes in pitch attitude control characteristics are apparent. Adequate crossover frequency and phase margin is available, although somewhat of an increase in lead compensation is required to obtain bandwidth and closed loop stability equivalent to Configuration 1 (Figure 49).

Control of altitude with the elevator, assuming a pitch attitude inner loop closure, also appears to be satisfactory considering the root locus and Bode diagram of Figure 64. Assuming the pitch attitude loop is closed fairly tightly ($\omega_{co} \doteq 5.0$ rad/sec, $T_{L_\theta} = 1.0$ sec), the altitude loop has adequate stability ($\varphi_m \doteq 30$ to 40 deg) for crossover frequencies in the vicinity of 1.0 radian/second. These characteristics are comparable to those of the

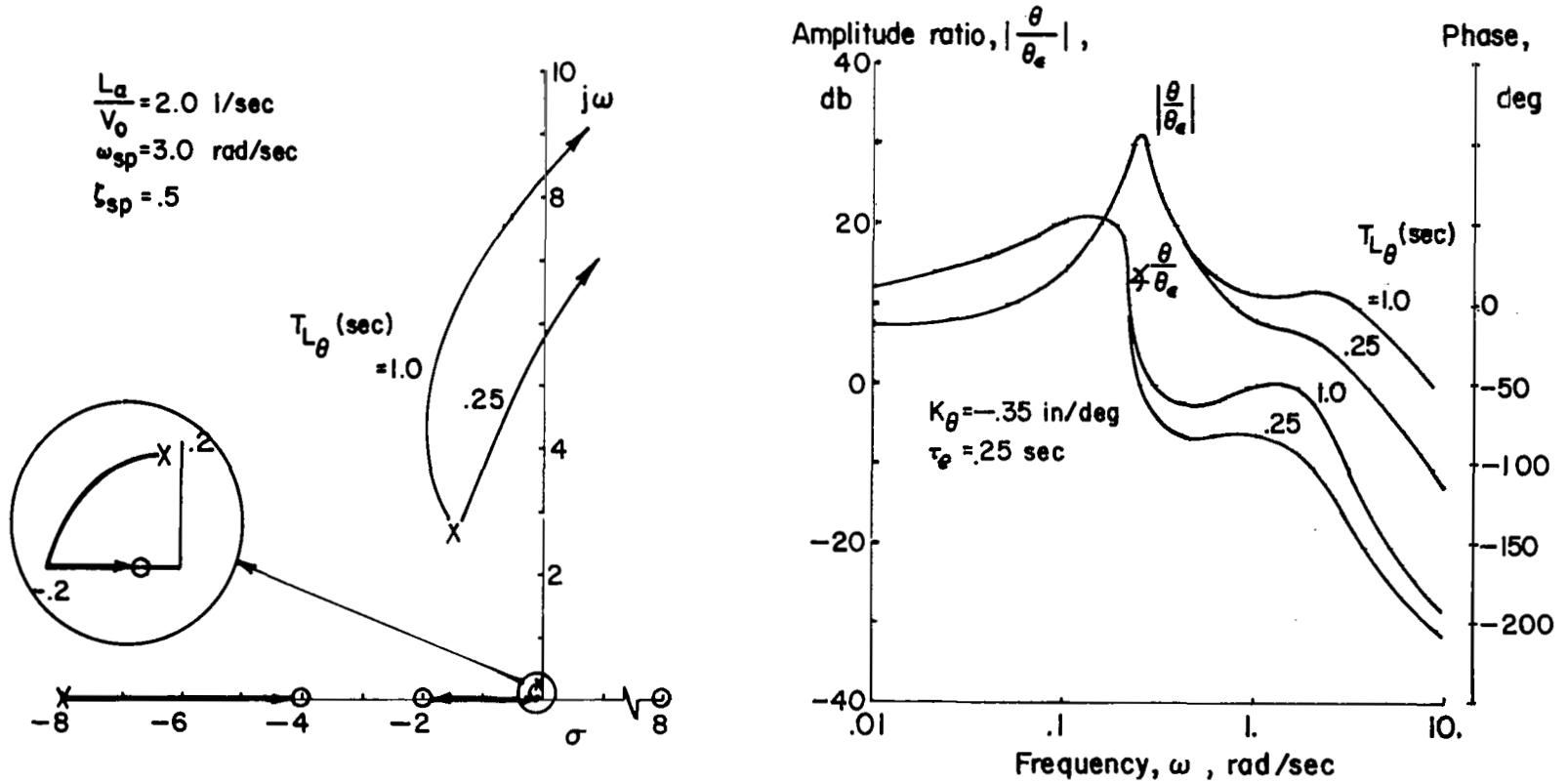

Figure 63. Pitch Attitude Control with Elevator - Configuration 5

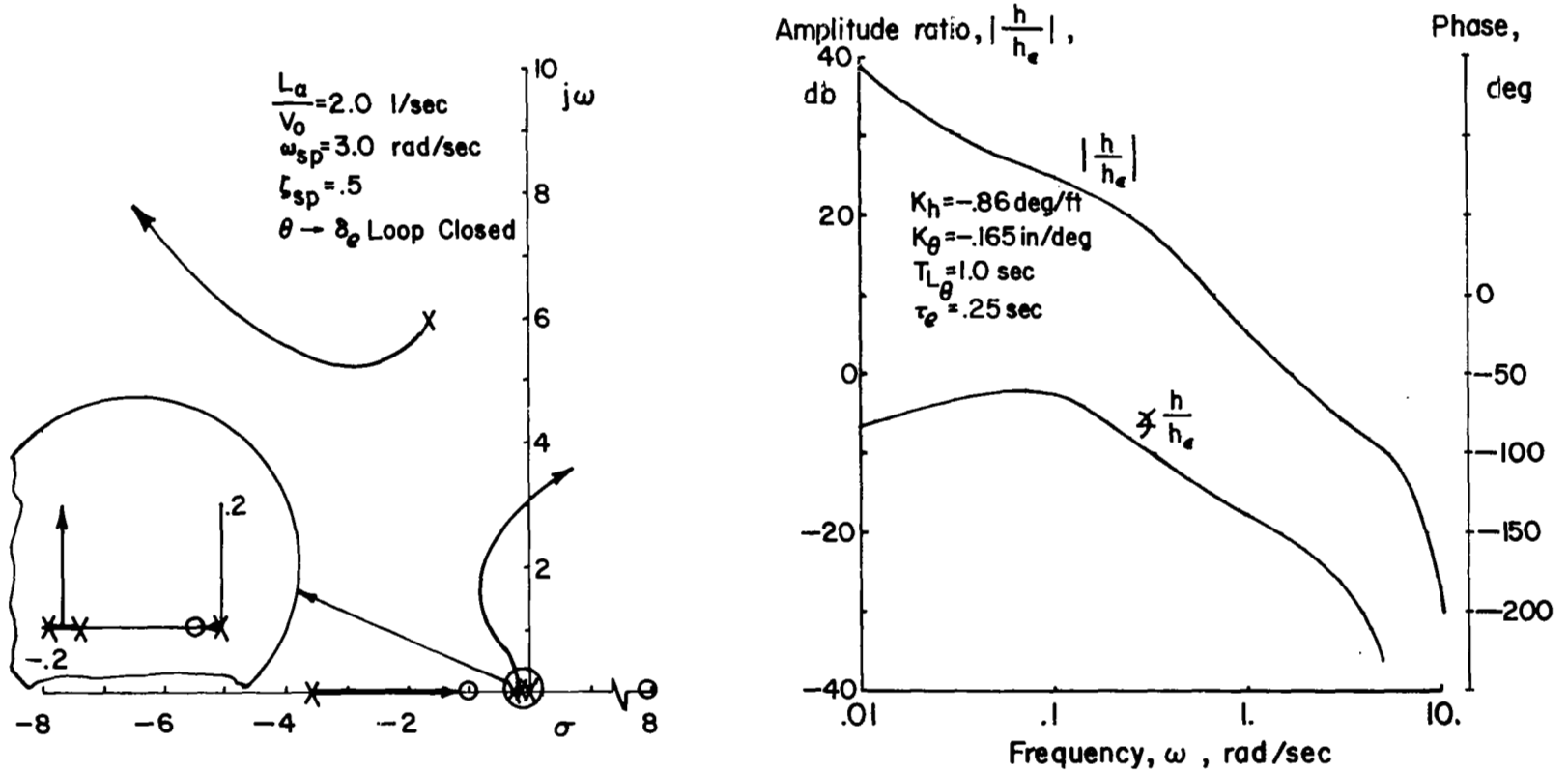

Figure 64. Altitude Control with Elevator - Configuration 5
($\theta \rightarrow \delta_e$ Loop Closed)

altitude loop for Configuration 1, even though the pitch attitude loop requires more lead compensation to make up for the reduction in pitch damping. Hence, good closed loop tracking of altitude should be anticipated for this configuration.

Predictions of the effect of short period damping on pitch attitude control precision and stick workload are shown in Figure 65. In the top diagram, the effect of a reduction in damping ratio is presented for the case of the most severe pitch disturbance. If the same low level of pilot compensation (T_{L_θ} = .25 sec) is assumed for the high and low damping cases, the reduction in damping ratio degrades pitch attitude precision while the control workload is reduced. If more lead compensation is allowed for the low damping configuration (T_{L_θ} = 1.0 sec, ζ_d = .5) the degradation in pitch attitude at low damping is reduced, but the control workload is found to increase from the level predicted for higher short period damping. In either event, the net result is a deterioration, although not serious, in pitch attitude control characteristics as the damping is reduced.

Combined influences of short period damping and pitch disturbance magnitude are shown in the lower diagram of Figure 65. These predictions would indicate a somewhat more severe degradation in pitch attitude precision and control workload for the low damping configuration as the level of pitch disturbances increase.

In summary, no dramatic effect on flying qualities for the ILS approach is evident for reductions in short period damping. The lowest limit on damping investigated in this program corresponded approximately to the $M_{\dot{\theta}} = 0$ boundary for a short period frequency of 3.0 radians/second. The pilots complained to some extent about pitch overshoots and about the persistence of pitch excursions excited by turbulence. Pitch attitude control was considered to be satisfactory. No difficulties were experienced with glide slope or airspeed control. Somewhat poorer pitch attitude precision was measured in flight when pitch damping was low compared to when the damping was high. Furthermore, increases in pitch disturbance level was found to be more detrimental to control of pitch attitude for the low level of damping. Both of these

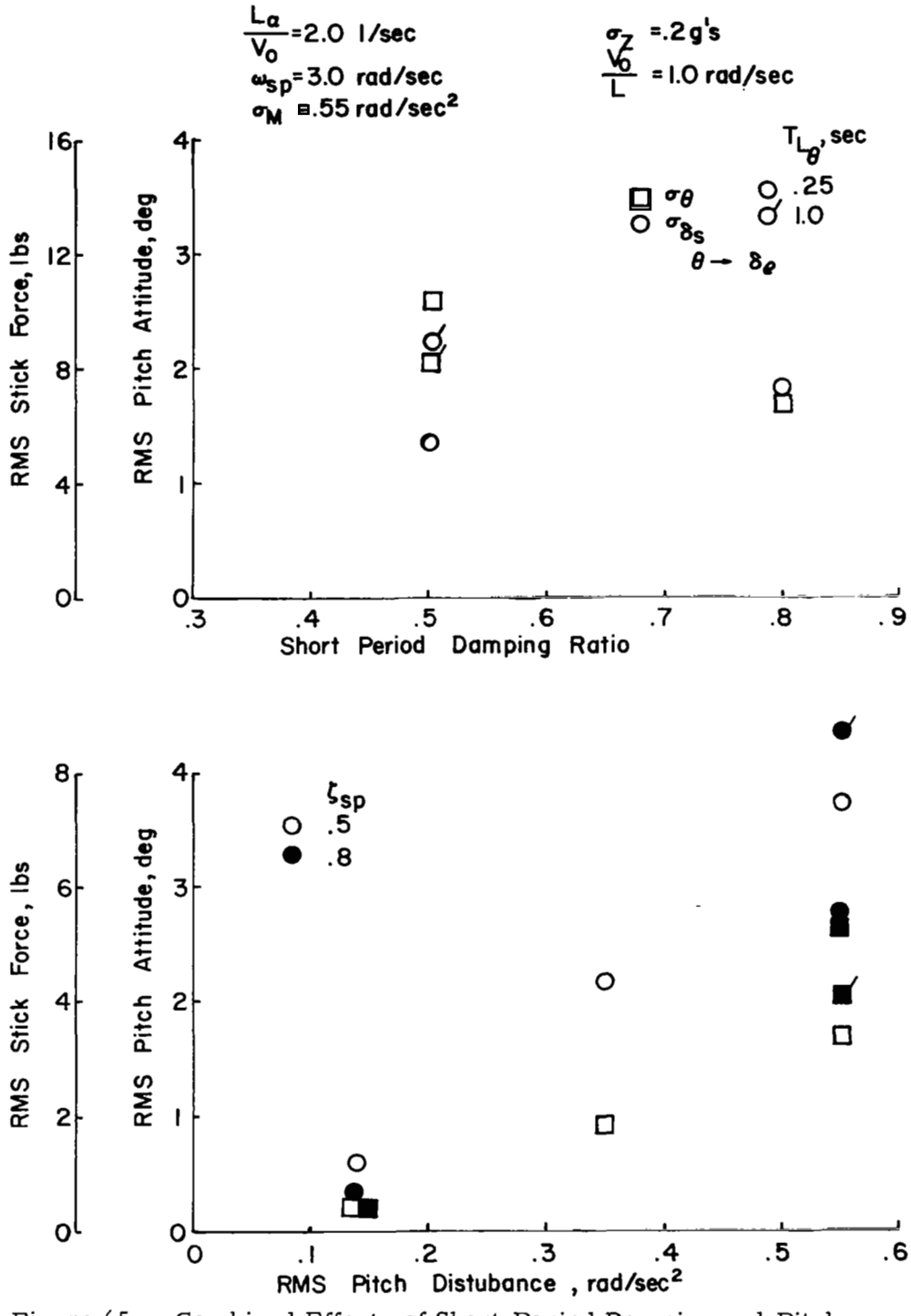

Figure 65. Combined Effects of Short Period Damping and Pitch Disturbances on Predicted Task Performance and Control Workload

trends mentioned above were substantiated by analytical predictions of pitch attitude response and control activity for the pilot-airplane system.

Contribution of lift curve slope

Reducing the airplane's lift curve slope from a value corresponding to the basic Navion ($L_\alpha / V_o = 2.0$ 1/ sec) to a value slightly half that magnitude ($L_\alpha / V_o = .9$ 1/ sec) had no apparent influence on pitch attitude control. Although the effect of L_α / V_o or $1/T_{\theta_2}$ associated with the droop of the closed loop asymptote in the vicinity of the short period mode would be aggravated by the reduction in lift curve slope, no corresponding problems with pitch attitude control were encountered. The root locus and Bode diagram of Figure 66 for the low L_α / V_o airplane (Configuration 4) support the impressions gained from pilot commentary. Open loop bandwidth and stability margin are as acceptable as those of Configuration 1 ($\omega_{co} \doteq 4.0$ rad/ sec, $\varphi_m \doteq 50$ deg). The closed loop asymptotes indicated by the heavy solid line on the Bode plot show no objectionable droop at high frequency which would compromise the precision of pitch control.

As anticipated in Reference 6, closed loop control of altitude does suffer when the lift curve slope is reduced. This effect is apparent in the root locus and Bode anslysis of Figure 67. Crossover frequencies must be reduced somewhat from the levels of Configuration 1 to maintain adequate closed loop stability. Still in all, the differences between Configurations 1 and 4 hardly seem of major consequence.

Turning to the prediction of the precision of pitch attitude and altitude performance and the control workload, data are shown in Figure 68 on the influence of lift curve slope for constant turbulence characteristics. The pitch attitude loop is closed for a bandwidth and lead compensation $\omega_{co} \doteq 4.0$ radians/ second and $T_{L_\theta} = .25$ seconds. The altitude loop is closed for a crossover frequency of approximately 1.0 radian/ second. Hardly any effect of lift curve slope can be seen on pitch control characteristics. Neither pitch attitude excursions or stick workload change appreciably when the lift

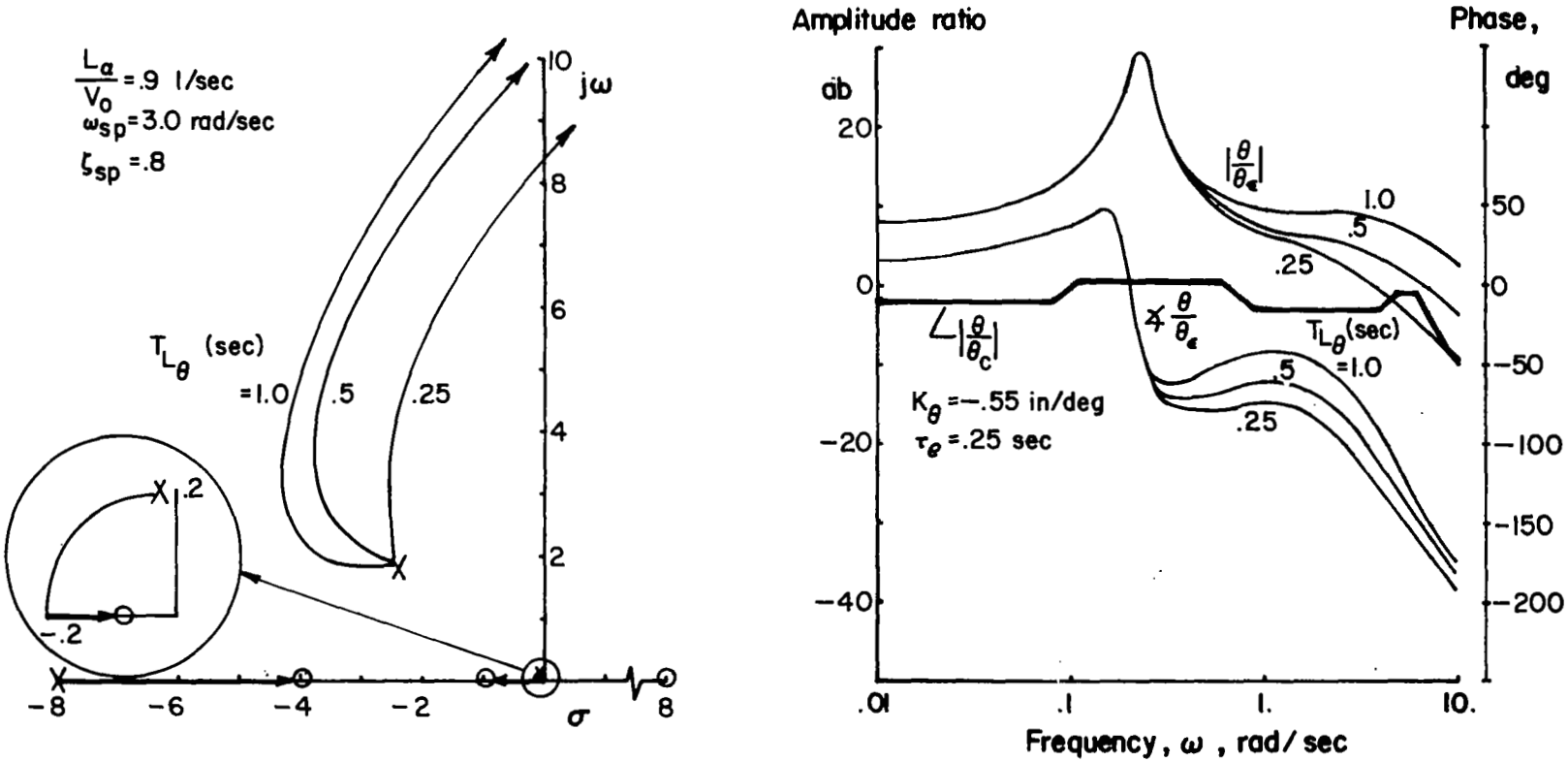

Figure 66. Pitch Attitude Control with Elevator - Configuration 4

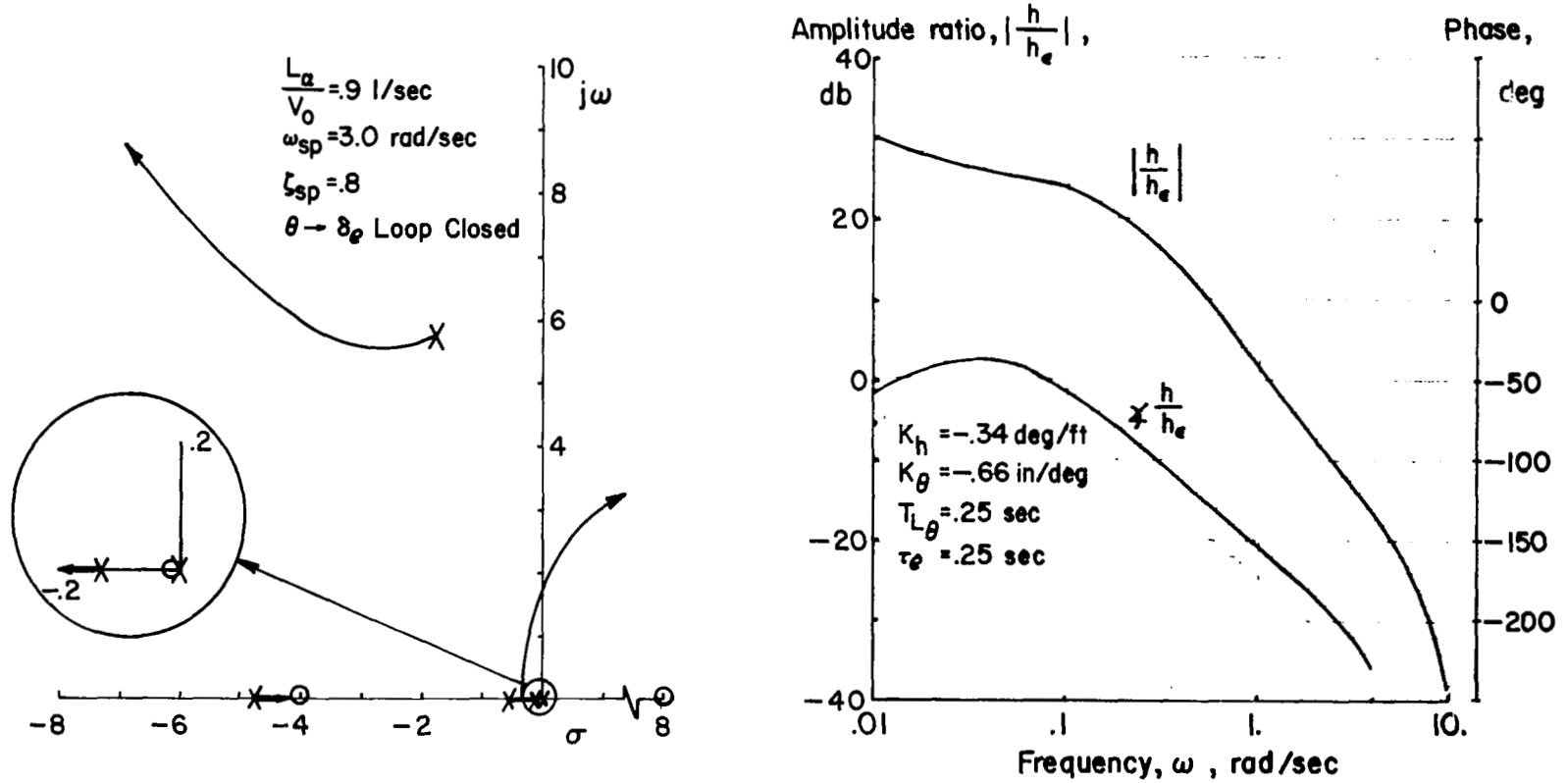

Figure 67. Altitude Control with Elevator - Configuration 4
($\theta \rightarrow \delta_e$ Loop Closed)

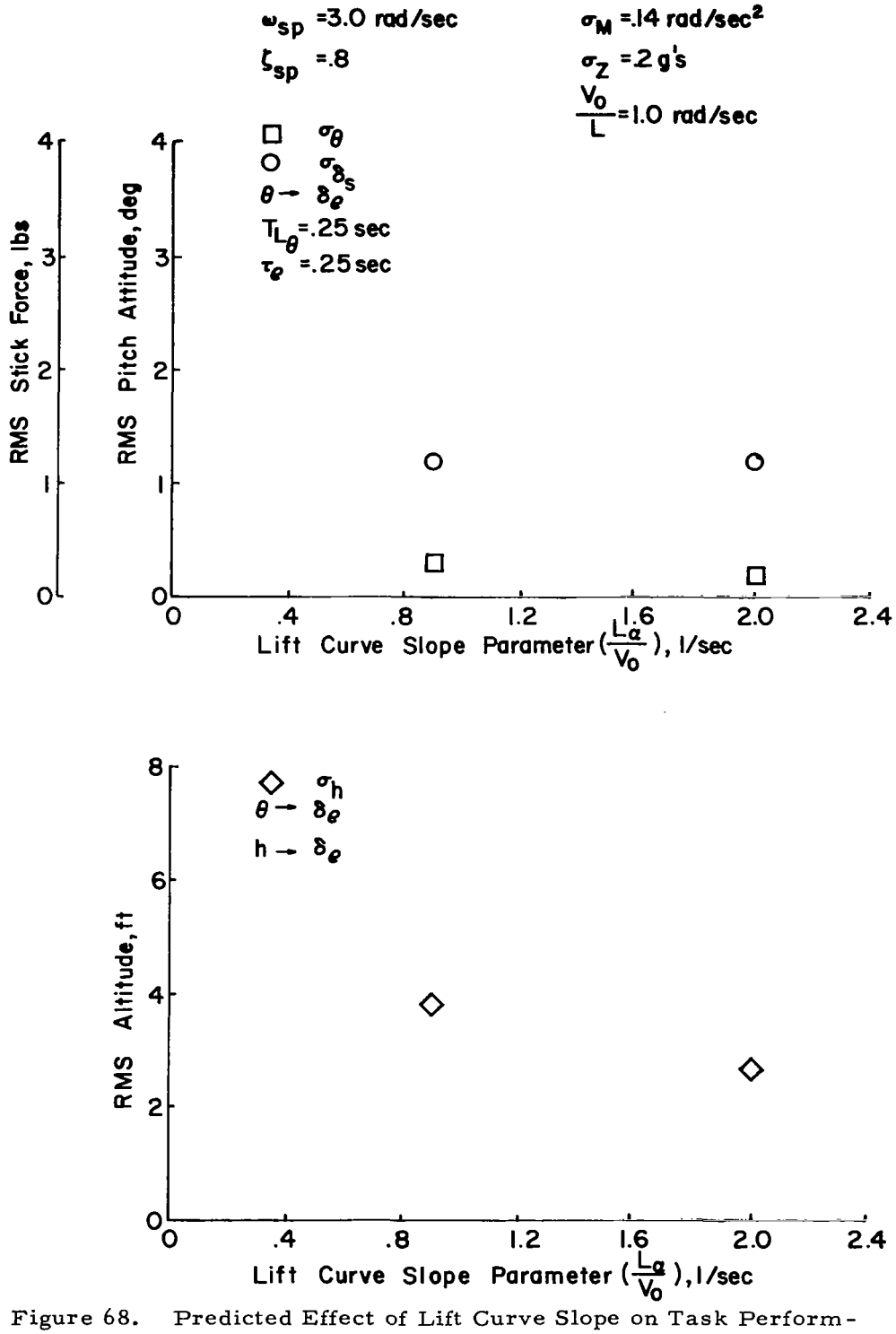

Figure 68. Predicted Effect of Lift Curve Slope on Task Performance and Control Workload

curve slope is reduced. This result would be anticipated from a comparison of closed loop pitch attitude control for the two configurations. A slight degradation in altitude tracking performance accompanies the reduction in lift curve slope; however, the incremental increase is unlikely to have an important effect on the ILS approach.

Combined effects of lift curve slope and heave disturbance magnitude are shown in Figure 69 for otherwise constant turbulence characteristics. As noted previously, pitch control characteristics (σ_θ or σ_{δ_s}) are not sensitive to the changes in lift curve slope or heave disturbances made in this program. Precision of altitude tracking may be observed to deteriorate as heave disturbances increase. This trend is essentially the same for either the low or high lift curve slope configurations.

To conclude this subsection, the influence of the slope of the lift curve on flying qualities for the approach was found to be modest. A slight degradation in flying qualities accompanies a reduction in lift curve slope with the exception of the condition of large pitch disturbances. In the latter case, a noticeable improvement in flying qualities is observed when the lift curve slope is reduced. Combined effects of lift curve slope and heave disturbance magnitude, where the two are interrelated (i.e., $Z_{\alpha_g} = Z_\alpha$), are counteracting. Reducing the lift curve slope degrades altitude control somewhat but this adverse effect is compensated by a reduction in the level of heave disturbances. The converse is true when lift curve slope is increased.

Performance-workload measures obtained from flight test or predicted using closed loop analysis agree in that neither show any significant variation with lift curve slope. Trends in these performance-workload measures with heave disturbance magnitude are similar for either the low or high lift curve slope configurations.

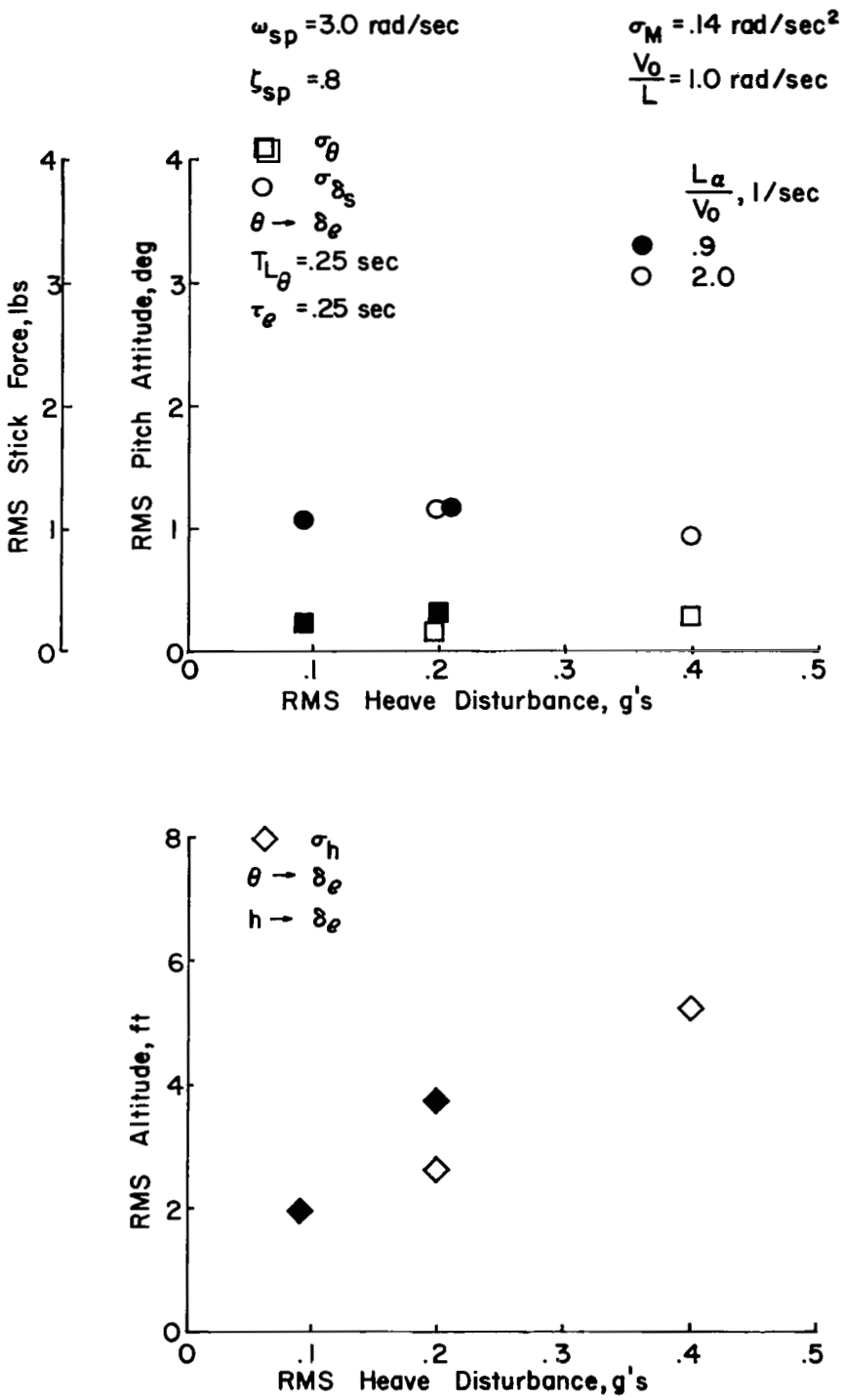

Figure 69. Combined Effects of Lift Curve Slope and Heave Disturbance on Predicted Task Performance and Control Workload

SECTION 5

CONCLUSIONS

Considering the flight test results of this program, it is apparent that the dominant influences on longitudinal flying qualities for the ILS approach are

- the pilot's control workload required to fly the ILS approach satisfactorily, and
- the precision of performance of the task as measured in terms of pitch attitude, airspeed, and glide slope or altitude excursions.

The effects of turbulence disturbances and airplane dynamics on the ILS task may be explained in terms of these performance and workload factors.

The specific influences of turbulence and dynamics on longitudinal flying qualities for the ILS which have been identified in this program may be itemized as follows.

- The dominant influence of turbulence is the rms magnitude of the aerodynamic disturbances. Pitch disturbances have a more adverse effect than heave disturbances.
- Increasing turbulence bandwidth has a mildly degrading influence on pitch attitude control. This effect is of secondary importance to the influence of disturbance magnitude. Higher frequency attenuation of the disturbance spectrum is of no consequence to the ILS task.
- Correlation between pitch and heave disturbances has no effect on the ILS task.
- Reducing short period frequency adversely affects pitch attitude, airspeed, and glide slope control when frequencies corresponding to the boundary for static angle of attack stability are reached.

- The adverse effect on pitch attitude control and ILS performance of increasing pitch disturbances is most pronounced for low short period frequencies (low static stability). When pitch disturbances are large, more static stability (higher ω_{sp}) is desired.
- Combined effects of short period frequency and pitch disturbance magnitude, where the two effects are interrelated through the aerodynamic angle of attack stability derivative (M_{α}), degrade flying qualities for either the high or low extremes of short period frequency. Little influence is noted for changes in frequency in the range from 2.0 to 5.0 radians/second.
- Reducing short period damping at intermediate short period frequencies (ω_{sp} = 3.0 rad/sec) has very little effect on the ILS. Lowest damping ratios tested corresponded to neutral pitch damping ($M_{\dot{\theta}} \doteq 0$). The only difficulty which accompanied the reduction in pitch damping was a modest degradation in pitch attitude control.
- The reduction in pitch damping has no worse effect on flying qualities when pitch disturbances are large as compared to when they are small.
- Reducing the lift curve slope has only a modest effect on the ILS task. Glide slope tracking deteriorates slightly for reductions in L_{α} / V_{o} to .9 1/seconds.
- Combined effects of lift curve slope and heave disturbance magnitude (where $Z_{\alpha_g} = Z_{\alpha}$) are counteracting. A reduction in lift curve slope with a corresponding reduction in heave disturbance magnitude does not alter flying qualities for the approach. Conversely, an increase in lift curve slope accompanied by an increase in heave disturbances also has no effect on the approach.

- The minor influence of turbulence bandwidth observed for the case of good longitudinal dynamics was not changed by variations in short period frequency or damping or lift curve slope.

Analytical interrelationships between open loop turbulence response, closed loop control characteristics, and closed loop turbulence response are discussed in the report. These interrelationships offer an understanding of the requirements for suppressing the airplane's uncontrolled pitch attitude and altitude response to turbulence. These interrelationships depend on

- the amplitude and frequency distribution of the open loop turbulence response, and
- the characteristics of the control loop closure(s) of interest, particularly regarding bandwidth and stability margin at crossover, low frequency gain, and gain and compensation required of the pilot to achieve good closed loop characteristics.

REFERENCES

1. Franklin, J. A., Turbulence and Lateral-Directional Flying Qualities, NASA CR-1718, 1971.

2. Diederich, F. W., The Response of an Airplane to Random Atmospheric Disturbances, NACA TN 3910, April 1957.

3. Diederich, F. W. and Drischler, J. A., Effect of Spanwise Variations in Gust Intensity on the Lift Due to Atmospheric Turbulence, NACA TN 3920, April 1957.

4. Drischler, J. A., Calculation and Compilation of the Unsteady-Lift Functions for a Rigid Wing Subjected to Sinusoidal Gusts and to Sinusoidal Sinking Oscillations, NACA TN 3748, October 1956.

5. Chalk, C. R., Neal, T. P., Harris, T. M., Pritchard, F. E., and Woodcock, R. J., Background Information and User Guide for MIL-F-8785 B (ASG), "Military Specification - Flying Qualities of Piloted Airplanes," AFFDL-TR-69-72, August 1969.

6. Stapleford, R. L. and Ashkenas, I. L., "Longitudinal Short-Period Handling Quality Requirements," Analysis of Several Handling Quality Topics Pertinent to Advanced Manned Aircraft: Section IV, AFFDL-TR-67-2, June 1967.

7. Chalk, C. R., Flight Evaluation of Various Phugoid Dynamics and $1/T_{h_1}$ Values for the Landing-Approach Task, AFFDL-TR-66-2, February 1966.

8. Ellis, D. R., Flying Qualities for Small General Aviation Airplanes, Part 3. The Influence of Short Period Frequency and Damping, Longitudinal Control Sensitivity, and Lift Curve Slope, Princeton University Report 949, 1971.

9. Ellis, D. R., Flying Qualities for Small General Aviation Airplanes, Part 2. The Influence of Roll Damping, Roll Control Sensitivity, Dutch-roll Excitation, and Spiral Stability, Princeton University Report No. 896, 1970.

10. Cooper, G. E. and Harper, R. P., Jr., The Use of Pilot Rating in the Evaluation of Aircraft Handling Qualities, NASA TN D-5153, April 1969.

11. McRuer, D. T., Graham, D., and Krendel, E. S.,"Manual Control of Single-Loop Systems, Part II," Journal of the Franklin Institute, Vol. 283, No. 2, Feburary 1967.

12. McRuer, D. T., Ashkenas, I. L., and Graham, D., Aircraft Dynamics and Automatic Control, Systems Technology, Inc., August 1968.

13. Newton, G. C., Jr., Gould, L. A., and Kaiser, J. F., Analytical Design of Linear Feedback Control, Wiley, New York, 1957.

14. Craig, S. J. and Campbell, A., Analysis of VTOL Handling Qualities Requirements, Part I. Longitudinal Hover and Transition, AFFDL-TR-67-179 Part I, October 1968.

15. Craig, S. J. and Campbell, A., Analysis of VTOL Handling Qualities Requirements, Part II. Lateral-Directional Hover and Transition, AFFDL-TR-67-179 Part II, February 1970.

16. Stapleford, R. L., Craig, S. J., and Tennant, J. A., Measurement of Pilot Describing Functions in Single-Controller Multiloop Tasks, NASA CR-1238, January 1969.

17. Etkin, B., Theory of the Flight of Airplanes in Isotropic Turbulence - Review and Extension, AGARD Report 372, April 1961.

APPENDIX A

SPECTRAL COMPONENT DESCRIPTION OF TURBULENCE DISTURBANCES

An approach to the definition of turbulence disturbances which has found widespread use in analyses of airplane response to turbulence is the so-called spectral component representation. This technique is discussed in detail in Reference 17. The method uses a description of the gust field by its spectral components, in other words a superposition of sinusoidal waves of varying wavelength and amplitude. This representation may be expressed in turn by a Taylor series approximation in the vicinity of the point of interest. Limiting the series approximation to first order terms simplifies the definition of gust velocities to include the local gust velocity at the point of interest and the linear spatial gradients in gust velocity along the flight path and in the spanwise direction. This simplification of the spectral component representation permits the gusts which the airplane encounters to be considered as equivalent rigid body motions (translations and rotations) of the airplane. As a result, the aerodynamic disturbances imposed on the airplane by turbulence may be approximated by products of the airplane's stability derivatives and these equivalent rigid body motions. The purpose of the following discussion is to identify the differences between the technique used in this report to define the turbulence disturbances (a modified aerodynamic strip theory) and the spectral component method.

First, considering the spectral component representation, the vertical gust field may be approximated along the airplane's flight path and in the vicinity of a point located at the center of gravity by

$$w_g \doteq w_{g_{c.g.}} + \frac{\partial w_g}{\partial x} \Delta x \qquad \text{(A1)}$$

where Δx is the spatial separation from the c.g. and where the spatial gradient term may be expressed in terms of the time rate of change of vertical gust velocity, i.e.,

$$\frac{\partial w_g}{\partial x} = \frac{\partial w_g}{\partial t} \frac{\partial t}{\partial x} = \frac{\dot{w}_g}{V_o} \tag{A2}$$

The description of vertical gust velocity used in the analysis of this report is

$$w_g = w_g (x_{c.g.} - \Delta x) \tag{A3}$$

or in the time domain

$$w_g = w_g (t - \frac{\Delta x}{V_o}) \tag{A4}$$

Hence, the only difference between the definition of vertical gusts in equations (A1) and (A2) and the definition of equations (A3) and (A4) is the value of vertical gusts at locations away from the center of gravity.

Since the predicted gust velocity at the c.g. is the same using either the spectral component or modified strip theory techniques, it follows that aerodynamic disturbances due to vertical gusts of components of the airplane near the c.g. are the same for either of these methods. This means that the contributions to vertical force and pitching moment from the wing predicted by either method should be equivalent. The previous statement is not precisely borne out because the two representations of the gust field define spanwise variations in vertical gusts differently. However, it should be appreciated from the discussion of Section 2 that spanwise variations in the gust field only affect the higher frequency components of the spectrum. Because the energy level of the spectrum is low in this frequency region, this disparity in the gust field representation is of no consequence to the problems considered in this flying qualities investigation.

The disparity between the definitions of turbulence disturbances predicted by the spectral component or modified strip theory representations is now narrowed down to the horizontal stabilizer contribution. Furthermore, the disparity lies in the pitching moment prediction, since no vertical force of any consequence is assumed to come from the stabilizer. Using the spectral component technique to predict pitching moment due to the horizontal stabilizer gives

$$M_{g_t} = M_{\alpha_t} \left(\frac{w_g}{V_o} - \frac{\dot{w}_g \, \ell_t}{V_o^2} \right) \tag{A5}$$

for $\alpha_g \doteq w_g / V_o$ and $\Delta x = - \ell_t$. This expression is perhaps more familiar when written in terms of the rotary stability derivatives $M_{\dot{\theta}}$ and $M_{\dot{\alpha}}$, i.e.,

$$M_{g_t} = M_{\alpha_t} \frac{w_g}{V_o} - (M_{\dot{\theta}} - M_{\dot{\alpha}}) \frac{\dot{w}_g}{V_o} \tag{A6}$$

with the assumptions that

$$M_{\alpha_t} \doteq Z_{\alpha_t} \ell_t \left(1 - \frac{d\epsilon}{d\alpha}\right)$$

$$M_{\dot{\theta}} \doteq Z_{\alpha_t} \frac{\ell_t^2}{V_o}$$

$$M_{\dot{\alpha}} \doteq Z_{\alpha_t} \frac{d\epsilon}{d\alpha} \frac{\ell_t^2}{V_o}$$

$$\frac{\dot{w}_g}{V_o} = - \dot{\theta}_g$$

The modified strip theory renders an approximation for the stabilizer pitching moment of the form

$$M_{g_t} = M_{\alpha_t} \frac{w_g}{V_o} \left(t - \frac{\ell_t}{V_o}\right) \tag{A7}$$

which neglects transient aerodynamic effects included in the influence function $h_{M_{g_t}}$ of equation (16). If these two expressions for pitching moment are transformed into the frequency domain, equation (A5) becomes

$$M_{g_t}(s) = M_{\alpha_t} \frac{w_g}{V_o} \left(1 - \frac{\ell_t}{V_o} s\right) \tag{A8}$$

for the spectral component approximation and equation (A7) becomes

$$M_{g_t}(s) = M_{\alpha_t} \frac{w_g}{V_o} e^{-\frac{\ell_t}{V_o} s}$$

$$\doteq M_{\alpha_t} \frac{w_g}{V_o} \left(\frac{1 - \frac{\ell_t}{2V_o} s}{1 + \frac{\ell_t}{2V_o} s} \right) \qquad \text{(A9)}$$

for the strip theory approximation, using a first order Pade representation for the transport delay.

A comparative plot of the transfer function $M_{g_t} / (M_{\alpha_t} w_g / V_o)$ for the two approximations is shown in Figure A1. The two cases diverge with respect to each other in amplitude and phase at high frequency. The spectral component representation shows increasingly higher energy levels and smaller phase lags at high frequency in comparison to the strip theory approximation. This difference between the two results is due to the over-estimation of the gust intensity at the vertical tail by the spectral technique, based on the linear gradient of the gust field at the airplane's c.g. The strip theory approximation uses the exact gust velocity in combination with a transport delay to account for the time required for the airplane to traverse the gust field a distance equivalent to the c.g. - stabilizer separation. While no amplitude error exists in the Pade approximation of the transport delay, a discrepancy from the true phase associated with $e^{-\frac{\ell_t}{V_o} s}$ is apparent at high frequency.

Differences which exist at higher frequencies between the strip theory and spectral component representations of the pitching moment disturbances are unlikely to be of any consequence in a simulation for flying qualities evaluations. Neither the amplitude or phase discrepancies should be

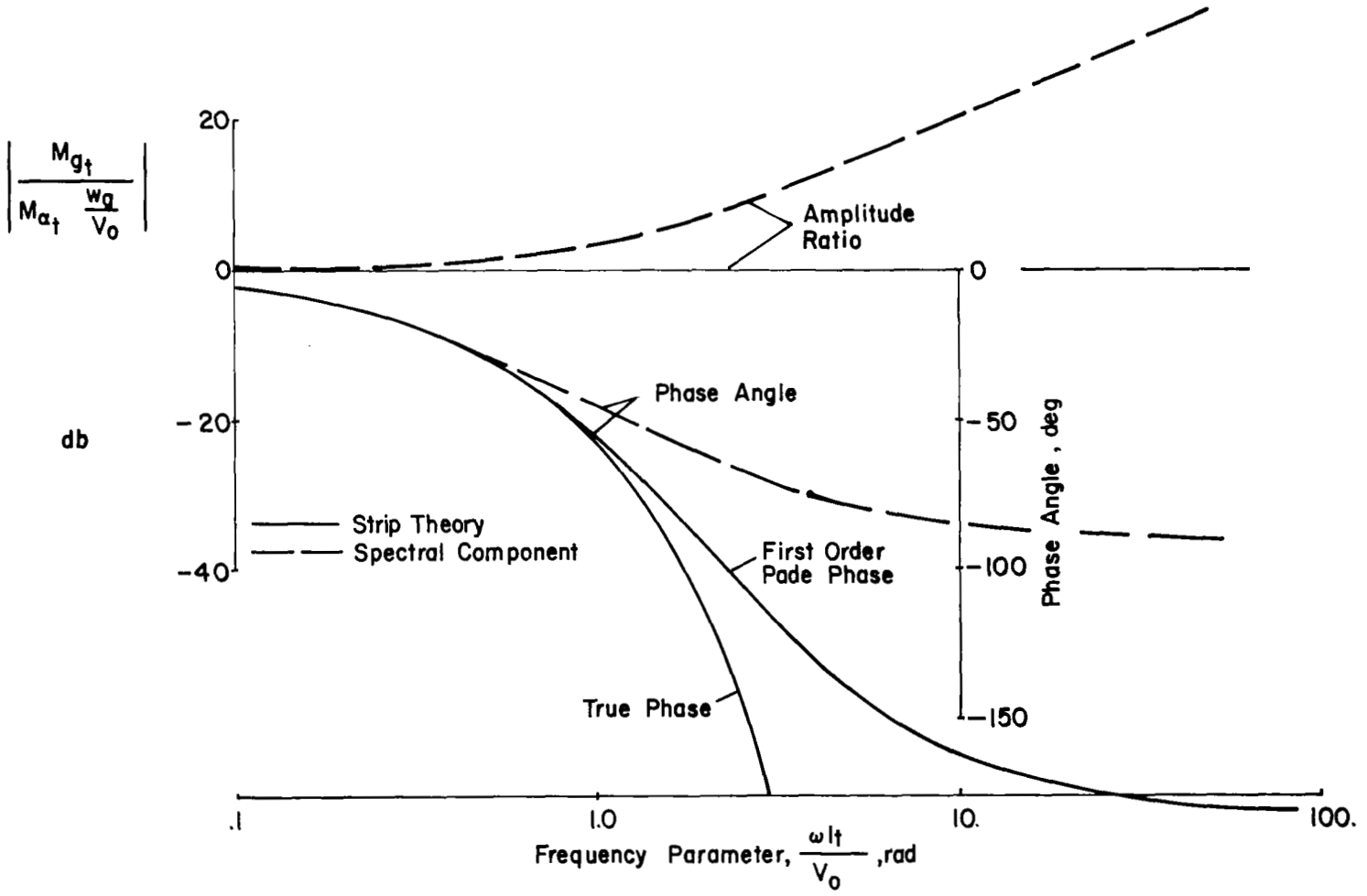

Figure A1. Comparison of Strip Theory and Spectral Component Approximation of Pitching Moment due to Vertical Gusts

apparent to the pilot at these frequencies. If it is desired to modify the characteristics of the spectral component representation at high frequencies, the stabilizer contribution to pitching moment may be attenuated by a low pass filter $(1/Ts+1)$ where the filter time constant is $T = \ell_t / V_o$.

APPENDIX B

DEFINITION OF TURBULENCE PARAMETERS

The various contributions of turbulence to longitudinal flying qualities were noted in Section 3 for the example of pitch attitude control to be

- the vertical force spectral density, $\Phi_{Z_{w_g}}$,
- the pitching moment spectral density, $\Phi_{M_{w_g}}$, and
- the cross-spectral density of pitch and heave disturbances, $\Phi_{M_g Z_g}$.

These spectral densities may be characterized by their rms energy content and the distribution of this energy as a function of frequency. From this point of view, the turbulence contributions may be represented by

- vertical force due to vertical gusts - σ_Z, ω_{w_1}, ω_{w_2},
- pitching moment due to vertical gusts - σ_M, ω_{w_1}, ω_{w_2},
- cross-correlation between pitching moment and vertical force components, ρ_{MZ}.

The derivation of rms magnitudes is based on the integral of the power spectral density over all positive frequencies

$$\sigma^2 = \int_0^\infty \Phi(\omega)\, d\omega \tag{B1}$$

Applying equation (B1) to the case of vertical force and pitching moment gives the following results

- vertical force due to vertical gusts

$$\sigma^2_{Z_{w_g}} = \int_0^\infty \Phi_{Z_{w_g}}(\omega)\, d\omega \tag{B2}$$

where with the substitution for $\Phi_{Z_{w_g}}$ from equation (28)

$$\Phi_{Z_{w_g}} = \frac{(\frac{\sigma_w}{V_o} Z_\alpha)^2 \frac{L}{\pi V_o}}{[(\frac{\omega L}{\sqrt{3} V_o})^2 + 1)(\frac{bc}{V_o^2} \omega^2 + 1)]}$$

the mean square value becomes

$$\sigma^2_{Z_{w_g}} = \frac{\pi}{2} \left[\frac{(\frac{\sigma_w}{V_o} Z_\alpha)^2 \frac{L}{\pi V_o}}{\frac{L}{\sqrt{3} V_o} + \frac{\sqrt{bc}}{V_o}}\right] \tag{B3}$$

and if $L >> \sqrt{3bc}$

$$\sigma^2_{Z_{w_g}} \doteq \frac{\sqrt{3}}{2} (\frac{\sigma_w}{V_o} Z_\alpha)^2 \tag{B4}$$

- pitching moment due to vertical gusts

$$\sigma^2_{M_{w_g}} = \int_o^\infty \Phi_{M_{w_g}} (\omega)\, d\omega \tag{B5}$$

where with the substitution for $\Phi_{M_{w_g}}$ from equation (21)

$$\Phi_{M_{w_g}} \doteq \frac{(\frac{\sigma_w}{V_o})^2 \frac{L}{\pi V_o} [M^2_{\alpha_w} + M^2_{\alpha_t} + 2 M_{\alpha_w} M_{\alpha_t} \cos \frac{\omega \ell_t}{V_o}]}{(\frac{\omega L}{\sqrt{3} V_o})^2 + 1} \tag{B6}$$

the mean square value becomes

$$\sigma^2_{M_{w_g}} \doteq \int_o^\infty \frac{L}{\pi V_o} \left(\frac{\sigma_w}{V_o}\right)^2 \frac{M^2_{\alpha_w} + M^2_{\alpha_t}}{\left(\frac{\omega L}{\sqrt{3}\, V_o}\right)^2 + 1} d\omega$$

$$+ \int_o^\infty \frac{2L}{\pi V_o} \left(\frac{\sigma_w}{V_o}\right)^2 \frac{M_{\alpha_w} M_{\alpha_t} \cos \frac{\ell_t}{V_o} \omega}{\left(\frac{\omega L}{\sqrt{3}\, V_o}\right)^2 + 1} d\omega \qquad \text{(B7)}$$

which reduces to

$$\sigma^2_{M_{w_g}} = \frac{\sqrt{3}}{2} \left(\frac{\sigma_w}{V_o}\right)^2 \left(M^2_{\alpha_w} + M^2_{\alpha_t} + 2 M_{\alpha_w} M_{\alpha_t} e^{-\sqrt{3} \frac{\ell_t}{L}}\right) \qquad \text{(B8)}$$

The normalized correlation function ρ_{MZ} may be defined by

$$\rho_{MZ} = \frac{R_{MZ}(0)}{\sigma_M \sigma_Z} \qquad \text{(B9)}$$

Neglecting transient aerodynamic influences associated with the influence function $h_{w_g}(t)$ and disregarding spanwise averaging effects for simplicity, the vertical force and pitching moment due to vertical gusts may be expressed

$$Z_{w_g} = Z_\alpha \frac{w_g(t)}{V_o} \qquad \text{(B10)}$$

$$M_{w_g} = M_{\alpha_w} \frac{w_g(t)}{V_o} + M_{\alpha_t} \frac{w_g}{V_o}\left(t - \frac{\ell_t}{V_o}\right) \qquad \text{(B11)}$$

The cross-correlation between M_{w_g} and Z_{w_g} is

$$R_{MZ}(\tau) = \frac{M_{\alpha_w} Z_\alpha}{V_o^2} R_{ww}(\tau)$$

$$+ \frac{M_{\alpha_t} Z_\alpha}{V_o^2} R_{ww}(\tau - \frac{\ell_t}{V_o}) \qquad \text{(B12)}$$

The turbulence correlation function R_{ww} is normally expressed in terms of a spatial rather than a time variable. For the time-spatial equivalence $(x - x_o) = V_o(t - t_o)$

$$R_{w_w}(r) = R_{ww}[V_o(\tau - \frac{\ell_t}{V_o})] \qquad \text{(B13)}$$

and for $\tau = 0$

$$R_{w_w}(r_o) = R_{ww}(-\ell_t)$$

The correlation function corresponding to the spectral density function for vertical gusts

$$\Phi_{ww} = \frac{\sigma_w^2 \frac{L}{\pi V_o}}{(\frac{\omega L}{\sqrt{3} V_o})^2 + 1}$$

is

$$R_{w_w}(r) = \frac{\sqrt{3}}{2} \sigma_w^2 e^{-\sqrt{3} \frac{r}{L}} \qquad \text{(B14)}$$

For the case at hand

$$R_{w_w}(\ell_t) = \frac{\sqrt{3}}{2} \sigma_w^2 e^{-\sqrt{3} \frac{\ell_t}{L}} \qquad \text{(B15)}$$

Substituting equation (B15) into (B12) and recognizing that $R_{ww}(0) = \sqrt{3}/2\ \sigma_w^2$, gives the final result for the normalized correlation function

$$\rho_{MZ} = \frac{\sqrt{3}}{2}\left(\frac{\sigma_w}{V_o}\right)^2 \left(\frac{M_{\alpha_w} Z_{\alpha} + M_{\alpha_t} Z_{\alpha}\ e^{-\sqrt{3}\frac{\ell_t}{L}}}{\sigma_M \sigma_Z}\right)$$

$$= \left(\frac{\sqrt{3}}{2}\right)^{\frac{1}{2}} \left(\frac{\sigma_w}{V_o}\right) \left(\frac{M_{\alpha_w} + M_{\alpha_t}\ e^{-\sqrt{3}\frac{\ell_t}{L}}}{\sigma_M}\right) \qquad \text{(B16)}$$

APPENDIX C

SUMMARY OF PILOT RATINGS AND COMMENTARY

Config. / Dynamics \ Turb.	Pilot	Mean Rating	No. of Ratings	Max. Deviation	Comments
1/1	A	3.5	2	0	
1/2	A (Primary)	3	11	+.5	Good pitch dynamics. Good A/S control. Mild turbulence.
	B (Secondary)	2.2	3	+.3	
	C (Secondary)	2.6	7	-1.1	
	D (Secondary)	3	2	0	
1/3	A	4.1	2	±.3	Acceptable G/S and A/S performance. Moderate compensation. Pitch upsets more obvious than heave.
	B	3	1	0	
	C	4	1	0	
	D	4.5	1	0	
1/4	A	5.2	3	+.3	θ control dominant requirement, detracts from G/S. θ control troublesome. Working hard. Large pitch upsets - turbulence moderate to heavy. Hard to track G/S close in (D).
	B	6.5	1	0	
	C	7	1	0	
	D	7	1	0	
1/5	A	2.5	2	0	G/S and A/S OK. Easy to track G/S. Light turbulence. Hardly aware of it.
	D	3.3	1	0	
1/6	A	3.9	2	±.1	G/S OK. Some rapid G/S excursions at end of approach. Not working hard. Low frequency pitch upsets.
	B	4.5	1	0	
1/7	A	5.3	3	-.8	θ objectionable. G/S not quite what I want. Workload not too bad. Poor A/S control. Heavy pitch disturbances. Hard to track G/S close in (D).
	D	8	1	0	

Config. / Dynamics / Turb.	Pilot	Mean Rating	No. of Ratings	Max. Deviation	Comments
1/8	A	3.8	3	-.3	G/S OK. Moderate compensation. Busy with scan. Moderate to heavy heave turbulence. Doesn't move airplane off G/S. Annoying.
	B	4.5	1	0	
	C	4	3	+1.5	
	D	4.5	3	± .5	
1/9	A	4.5	2	0	Pushed off G/S. Moderate compensation. Mostly heave turbulence. Annoying.
	B	3.5	1	0	
	C	4	1	0	
1/10	A	5.5	3	± .5	Poor A/S and G/S. Large θ excursions. Reluctant to make nose up corrections when speed is low (B). Considerable compensation tracking θ. Large pitch and heave upsets.
	B	7	1	0	
	C	4	1	0	
1/11	A	3.1	3	+ .4	Good θ control. G/S corrections not as quick as desired. Workload acceptable. Heave annoying.
	C	2.8	3	-1.3	
1/12	A	3.3	2	± .3	Nominal workload. A few large upsets.
1/13	A	5	2	0	Considerable trouble with θ. Pushed off G/S. Trouble with A/S. Considerable compensation. Can only stop low frequency upsets with gross δ_s motion.
	C	7.5	1	0	
1/14	A	2.8	2	± .3	Mildly unpleasant. Turbulence not apparent.
1/15	A	3.8	2	± .3	θ excursions larger than I like. Not much trouble with G/S and A/S. Moderate compensation.

Config. / Dynamics / Turb.	Pilot	Mean Rating	No. of Ratings	Max. Deviation	Comments
1/16	A	3.1	3	+ .4	G/S OK. Not much effort required. Low amplitude high frequency upsets.
	C	2	1	0	
1/17	A	3.9	2	± .1	Annoying ride. Moderate compensation. Heave upsets seemed high frequency.
1/18	A	6	3	0	Couldn't get adequate performance. Poor G/S. θ excursions $\pm 10^{\circ}$. Working hard on θ. Gross pitch upsets. Frequency high enough. I have difficulty tracking it.
	C	8	1	0	
1/19	A	3	1	0	Nothing wrong. Light turbulence.
1/20	A	4.5	1	0	Some difficulty with G/S and A/S.
1/21	A	3.7	2	± .4	A little uncomfortable. Heave moves airplane off G/S. Heave turbulence large and sharp.
1/22	A	2.5	2	± .5	Nominal task.
1/23	A	3.7	2	± .2	Uncomfortable ride. Not that hard. Moderate compensation.
1/24	A	3.6	2	± .3	Nominal task. Moderate to high frequency heave turbulence.
1/25	A	3.9	2	± .1	Appreciable heave and pitch. θ requires a little attention.
1/26	A	3.4	2	± .1	A/S and G/S OK. Had to work a little on θ.

Config. / Dynamics / Turb.	Pilot	Mean Rating	No. of Ratings	Max. Deviation	Comments
1/27	A	3.3	2	± .3	Good G/S. Pitch upsets noticeable.
1/28	A	5.4	2	± .1	Objectionable. θ larger than I'm used to. Considerable compensation. Large pitch and heave.
2/1	A B C D	4.1 5 5.9 5.8	6 2 4 1	+ .4 0 -1.4 0	Low static stability. θ and A/S control difficult. Had to pay close attention to A/S. Difficulty with G/S. High workload.
2/2	A C	4.1 4.5	2 1	● .3 0	θ and A/S control problems. θ sloppy. Low M_α. Turbulence emphasizes the problem. Moderate compensation.
2/3	A C	5.1 7	3 1	+ .4 0	θ excited by turbulence. Moderately large disturbances. Large θ excursions. Requires considerable attention and compensation.
2/4	A	9-10	1		Control can be lost. Ran out of control. Couldn't perform task.
2/5	A	4	2	0	A/S problems due to low $M_{\dot{\alpha}}$. A little work required for θ control. Not much heave turbulence. Some pitch.
2/8	A	4.3	3	+ .7	No bad θ problems. Held A/S pretty well. Heave turbulence annoying.
2/11	A C	4.1 4	4 1	+ .9 0	Lot of θ motion. A/S control difficult. Some trouble with G/S. Moderate to high workload. Sluggish θ response.

Config. / Dynamics / Turb.	Pilot	Mean Rating	No. of Ratings	Max. Deviation	Comments
2/16	A C	4.3 4	3 1	- .3 0	Difficulty with θ. Quite a bit of work. Used δ_T on A/S. Heave turbulence upsetting. High frequency.
3/2	A C	3.3 3.5	3 1	- .3 0	High static stability. Rapid θ response. Good A/S control. Annoying θ bobble. Can't contend with it. High frequency pitch disturbances.
3/3	A C	3.6 4	2 1	± .3 0	A lot of θ bobbing. Doesn't degrade G/S. No A/S problems. Ignore high frequencies.
3/4	A C	3.8 5	4 3	- .3 0	Large M_α. No A/S problem. Airplane doesn't go far. Large pitch and heave turbulence.
3/7	A	3.5	1	0	Large M_α. High frequency θ bobbing. Minimal compensation.
3/10	A	4.8	1	0	Large θ excursions. Working hard. Large heave upsets. Uncomfortable.
3/11	A	3.5	1	0	Annoying θ bobbing. A/S control not bad.
3/13	A	3.3	2	± .3	Stiff airplane in pitch. Nominal turbulence.
3/16	A	3.5	1	0	No θ problem. Very little compensation.
3/18	A C	3.8 5	2 1	0 0	Can't do much about θ bobble. Ignore high frequencies. Annoying ride. No trouble with G/S. Moderate heave and pitch disturbances. High frequency.

Config. / Dynamics / Turb.	Pilot	Mean Rating	No. of Ratings	Max. Deviation	Comments
4/2	A D	3.3 4.3	5 1	+ .7 0	Low L_α apparent. Not much θ problem. Good A/S control. Just a little dissatisfied with G/S. Long time to make G/S corrections. Heave turbulence pushes airplane off G/S.
4/5	A D	2.8 4.2	4 3	- .3 - .2	Low L_α. Not a bad airplane. Difficult to correct G/S. Requires attention.
4/6	A	2.9	2	± .1	A little work on G/S. Very little turbulence.
4/7	A D	3.3 6	3 1	- .3 0	Just a little objectionable. Didn't track rapid θ bobbing. Seems to do a better job damping itself. Would have to work pretty hard to improve performance. $\delta_s \rightarrow \theta$, $\delta_T \rightarrow$ G/S. Pitch upsets dominant.
4/11	A	3.4	3	+ .6	Heave upsets move airplane off G/S. Low frequency heave. Not immediately aware of G/S error. G/S corrections difficult.
4/14	A	2.8	1	0	Nice airplane. Low L_α. Minimal turbulence.
4/16	A	3.4	3	± .4	Didn't get far off G/S. Moderate workload. Higher frequency upsets.
4/19	A	2.8	1	0	Very little problem.
5/1	A	4	1	0	Some θ excursions due to low damping. Moderate compensation for θ control. Moderate heave upsets.

Config. / Dynamics / Turb.	Pilot	Mean Rating	No. of Ratings	Max. Deviation	Comments
5/2	A C	3.5 2.7	4 3	± .5 + .3	Low damping apparent. Some θ bobble. θ overshoots. Nothing wrong with G/S performance. No need to work hard.
5/3	A C	4.6 4	3 1	-1.1 0	Large θ excursions. Working hard on θ. Large pitch turbulence makes it unsatisfactory.
5/4	A C	6 7.5	2 1	0 0	Can't stop θ excursions. Can't get desired θ performance. A/S excursions 8-9 kts. Uncomfortable g's. Extensive compensation. Extremely large pitch upsets.
5/5	A	3	1	0	Some θ excursions. G/S and A/S OK. Low damping - more preferred.
5/8	A	4.3	3	+ .5	Moderately objectionable. Poor ride. G/S not bad. θ control degraded. Workload not bad. Strong heave upsets.
5/11	A	3.4	2	± .1	
5/12	A	3.3	1	0	Not much to do. Low energy turbulence.
5/16	A	3.6	3	+ .2	No θ problems. Heave upsets apparent.
5/17	A	3.8	1	0	Working a little harder than desired. Heave upsets more noticeable than pitch.
6/2	A	3.8	2	● .3	Low static stability, low damping. Some θ overshoot. θ response touchy. A/S control not bad.

Config. / Dynamics / Turb.	Pilot	Mean Rating	No. of Ratings	Max. Deviation	Comments
6/3	A	5.3	2	± .3	θ objectionable. A/S and G/S difficulties. Extensive compensation. θ reinforced g's getting to me.
6/8	A	4.8	3	+1.2	Don't trust the airplane. Never as bad as I expect. G/S performance not good. A/S off 9-10 kts occasionally. Moderate compensation, $\theta \rightarrow \delta_S$, $u \rightarrow \delta_T$.
6/16	A	3.8	2	0	Heave is some problem. Don't like low static stability and damping. Don't dare divert attention.